

**UNIVERSIDADE DE SÃO PAULO
CENTRO DE ENERGIA NUCLEAR NA AGRICULTURA**

GEOVANI TADEU COSTA JUNIOR

Foliar uptake of CuO and CeO₂ nanoparticles by soybean (*Glycine max* L.)

Piracicaba

2020

GEOVANI TADEU COSTA JUNIOR

Foliar uptake of CuO and CeO₂ nanoparticles by soybean (*Glycine max* L.)

Revised version according Resolution CoPGr 6018 de 2011

**Thesis presented to Center for Nuclear Energy in
Agriculture of the University of São Paulo as a
requisite to the Doctoral Degree in Sciences**

**Concentration Area: Chemistry in Agriculture
and Environment**

**Advisor: Prof. Dr. Hudson Wallace Pereira de
Carvalho**

Co-Advisor: Prof. Dr. José Lavres Júnior

Piracicaba

2020

AUTORIZO A DIVULGAÇÃO TOTAL OU PARCIAL DESTE TRABALHO, POR QUALQUER MEIO CONVENCIONAL OU ELETRÔNICO, PARA FINS DE ESTUDO E PESQUISA, DESDE QUE CITADA A FONTE.

Dados Internacionais de Catalogação na Publicação (CIP)
Seção Técnica de Biblioteca - CENA/USP

Costa Junior, G. T.

Absorção foliar de nanopartículas de CuO e CeO₂ em soja (*Glycine max* L.) / Foliar uptake of CuO and CeO₂ nanoparticles by soybean (*Glycine max* L.) / Geovani Tadeu Costa Junior; orientador Hudson Wallace Pereira de Carvalho; co-orientador José Lavres Junior. - - Revised version according Resolution CoPGr 6018 de 2011. - - Piracicaba, 2020.

92 p. : il.

Tese (Doutorado – Programa de Pós-Graduação em Ciências. Área de Concentração: Química na Agricultura e no Ambiente) – Centro de Energia Nuclear na Agricultura da Universidade de São Paulo, Piracicaba, 2020.

1. Absorção 2. Cério 3. Cobre 4. Espectrometria de massas 5. Impactos ambientais 6. Nanopartículas 7. Nutrição vegetal 8. Raios X 9. Soja I. Título

CDU 620.3 : (631.811 + 633.34)

Elaborada por:

Marília Ribeiro Garcia Henyei

CRB-8/3631

Resolução CFB N° 184 de 29 de setembro de 2017

*To my son Pedro Henrique Moraes Costa,
to my parents Maria Isabel Correa Costa and Geovani Tadeu Costa,
and to my brother Matheus Correa Costa.*

ACKNOWLEDGMENTS

First of all, to God, for all the strength and support during the hard moments I have been through in this journey during my PhD and in my life.

To my son Pedro Henrique Moraes Costa, thank you for the companionship, for understanding many times that I could not have been with you and for teaching me how to be a better person. I love you with all my strength.

To my parents Maria Isabel Correa Costa and Geovani Tadeu Costa for all the love, support, for being my ground at any time and my brother Matheus Correa Costa, who has always been a reference in my life. You are the most valuable people in my life.

To all my relatives, my grandparents Alza Luzia Costa, José Maria Costa (*in memorian*), Amélia Santana Correa (*in memorian*) and Antônio Francisco Correa (*in memorian*), my aunts, uncles and cousins.

To the Professor Hudson Wallace Pereira de Carvalho (CENA) for the confidence, patience and specially teachings.

To the group of the Nuclear Instrumentation Laboratory (LIN) for all the moments we have spent together, for all the help, laughter, conversations and all the support. Thank you Susi, Eduardo, Joyce, Nádia, Tati, Rafael, Bianca, Marcos, Gabriel and Sara.

To the friends I have made and I will have you in my heart no matter what, Débora Grandino, Eduardo Santos, Susi Savassa, Victor Botteon and Thiago Bompadre. You are a gift from God to my life.

To my very special friend Lidiane Cristina Nunes, I have no words to thank you for all you have done for me. Thank you for the friendship, companionship, laughter, great moments we spent together and support in my personal life, and also for all the knowledge and tips you have given me to conclude this study.

To the technicians Dr. Eduardo de Almeida for all the patience, tips and specially for sharing your knowledge, Cleusa Pereira Cabral for helping me during the greenhouse experiment and Aparecida Fátima and Liz Mary for helping me in the ICP OES analysis. Thank you.

To the University of São Paulo (USP), the Center for Nuclear Energy in Agriculture (CENA) and its Postgraduate Science Program for the opportunity and structure to develop this work.

This study was financed in part by the Coordenação de Aperfeiçoamento de Pessoal de Nível Superior – Brasil (CAPES) – Finance Code 001.

ABSTRACT

COSTA JUNIOR, G. T. **Foliar uptake of CuO and CeO₂ nanoparticles by soybean (*Glycine max* L.)**. 2020. 92 p. Tese (Doutorado em Ciências) - Centro de Energia Nuclear na Agricultura, Universidade de São Paulo, Piracicaba, 2020.

Nanotechnology presents a huge potential for plant nutrition. In this sense, foliar application of fertilizers has the advantages of delivering nutrients, reducing the environmental impact in relation to soil application. This study has investigated the effects of foliar application of CuO and CeO₂ nanoparticles on soybean plants. Copper was chosen due to its importance as a nutrient for higher plants and all the processes the element participates. Cerium is the most abundant rare earth element in the Earth's crust and its abundance is not that different compared with Zn and Cu, which are much more involved in environmental investigations than Ce. During the study, it was attempted to develop an X-ray spectrometric method to trace the uptake and redistribution of nanoparticles in living plants. Even though this was not possible, such method allowed to access the nutritional status of soybean under vivo conditions. The deposition of copper sources on leaves, such as nano and micro CuO and copper sulphate, caused damages, inducing to absence or scarce presence of platelets crystals. Shoot dry mass of plants was positively affected by the treatments, especially by the 40 nm nCuO. Copper speciation showed that the element undergoes redox reactions from Cu¹⁺ to Cu²⁺ after 14 days of application. The nanoparticles were able to supply Cu and Ce to soybean since these elements were found in other plant tissues that were not directly exposed to the nanoparticles. However, it is not clear whether the particles are dissolved outside the leaves or taken up entirely. The use of cerium nanoparticles did not interfere in agronomic parameters such as biomass production and number of pods.

Keywords: *Glycine max* (L.) Merrill. Mineral nutrition. CuO nanoparticles. CeO₂ nanoparticles. X-ray absorption. ICP OES. ICP-MS.

RESUMO

COSTA JUNIOR, G. T. **Absorção foliar de nanopartículas de CuO e CeO₂ em soja (*Glycine max* L.)**. 2020. 92 p. Tese (Doutorado em Ciências) - Centro de Energia Nuclear na Agricultura, Universidade de São Paulo, Piracicaba, 2020.

A nanotecnologia possui potencial aplicação à nutrição mineral de plantas. A aplicação foliar de fertilizantes tem como uma de suas principais vantagens a aplicação específica do nutriente, reduzindo assim o impacto ambiental em relação à aplicação no solo. Este estudo investigou os efeitos da aplicação foliar de nanopartículas de CuO e CeO₂ em plantas de soja. O cobre foi escolhido devido à sua importância como nutriente e por todos os processos metabólicos que o elemento participa. O cério é o elemento terra rara mais abundante na crosta terrestre, e é sujeito de várias investigações ambientais, mas sua essencialidade no metabolismo ainda não foi demonstrada. Durante este estudo, tentou-se desenvolver um método de espectrometria de raios X para rastrear a absorção e redistribuição de nanopartículas em plantas vivas. Mesmo não sendo possível, tal método permitiu acessar o estado nutricional de plantas de soja sob condições *in vivo*. A deposição de fontes de cobre, como nano e micro CuO e sulfato de cobre, nas folhas causou danos, induzindo a ausência ou presença escassa de cristais. Massa seca da parte aérea foi afetada positivamente pelos tratamentos, especialmente pela nanopartícula de óxido de cobre de 40 nm. A especiação de cobre mostrou que o ele é transformado de Cu¹⁺ em Cu²⁺ após 14 dias de exposição. As nanopartículas foram capazes de fornecer Cu e Ce à soja, uma vez que esses elementos foram encontrados em outros tecidos vegetais que não foram diretamente expostos às nanopartículas. No entanto, não está claro se as partículas são dissolvidas fora das folhas ou absorvidas inteiramente. O uso de nanopartículas de cério não interferiu em parâmetros agrônômicos como produção de biomassa e número de vagens.

Palavras-chave: *Glycine max* (L.) Merrill. Nutrição mineral. Nanopartículas de CuO. Nanopartículas de CeO₂. Absorção de raios X. ICP OES. ICP-MS

SUMMARY

1 INTRODUCTION	13
1.1 Hypotheses	17
1.2 Objectives	17
1.3 Structure of the thesis	18
References	18
2 DIRECT DETERMINATION OF MINERAL NUTRIENTS IN SOYBEAN LEAVES UNDER <i>VIVO</i> CONDITIONS BY PORTABLE X-RAY FLUORESCENCE SPECTROSCOPY ¹	21
Abstract.....	21
2.1 Introduction	21
2.2 Materials and Methods	23
2.2.1 Soybean cultivation	23
2.2.2 Portable XRF analysis	24
2.2.3 Elemental Sensitivity.....	25
2.2.4 Signal-to-noise ratio	26
2.2.5 Emission-transmission (ET) method	26
2.2.6 pXRF validation	29
2.2.7 Microprobe XRF analysis.....	29
2.2.8 Comparative method (ICP OES)	30
2.2.9 Limits of Detection.....	30
2.3 Results and Discussion	31
2.3.1 Optimization of experimental parameters	31
2.3.2 Determination of elements in soybean leaves	35
References	41
3 FOLIAR UPTAKE OF NANO COPPER OXIDE IN SOYBEAN PLANTS	45
Abstract.....	45
3.1 Introduction	45
3.2 Materials and Methods	47
3.2.1 Nanomaterials characterization. Purity.....	47
3.2.2 Structural characterization.....	47
3.2.3 Physicochemical features of dispersions	48
3.2.4 Nano CuO morphology.	48
3.2.5 Soybean cultivation.	49
3.2.6 Copper solutions.....	50
3.2.7 ICP OES analysis.	51

3.2.8 Chemical speciation analysis.	51
3.2.9 Scanning electron microscopy (SEM).	52
3.2.10 Experimental design and statistical analysis.	52
3.3 Results and Discussion.	53
3.3.1 Nanomaterials characterization.	53
3.3.2 Effect of CuO nanoparticles on the soybean leaf.	56
3.3.3 Effects of nCuO on plant biometrics and Cu translocation	58
3.3.4 Characterization of CuO NPs deposited on the leaf surface.	62
3.4 Conclusions.	63
References.	64
4 FOLIAR UPTAKE OF NANO CERIUM OXIDE IN SOYBEAN PLANTS.	67
Abstract.	67
4.1 Introduction.	67
4.2 Materials and Methods.	72
4.2.1 Nanomaterials characterization. Purity.	72
4.2.2 Structural characterization	72
4.2.3 Physicochemical features of dispersions.	72
4.2.4 Nano CeO ₂ morphology.	72
4.2.5 Soybean cultivation.	73
4.2.6 Cerium solutions.	73
4.2.7 Analytical blank test.	74
4.2.8 ICP-MS analysis	74
4.2.9 Experimental Design and statistical analysis.	74
4.3 Results and Discussion.	74
4.3.1 Nanomaterials characterization.	75
4.3.2 Analytical blank test.	77
4.3.3 Effects of nCeO ₂ on plant biometrics and Ce translocation.	77
4.3 Conclusions.	83
References.	83
5 GENERAL CONCLUSIONS.	87
ANNEX.	87

1 INTRODUCTION

There are several definitions for nanomaterials depending on the scientific community that addresses the subject. According to the IUPAC glossary, nanoparticles are those with dimensions of approximately 1 to 100 nm (IUPAC, 2018). Some researchers, however, consider that a material can only be labeled "nano" if, due to its size, the material has different properties from those so-called bulk form, i.e., excitation, emission, chemical reactivity and stability, which are size-dependent properties (KOLAHALAM et al., 2019).

While increasing the surface-to-volume ratio, i.e., decreasing size, gives rise to new properties with technological potential, on the other hand, studies also show that undesirable characteristics such as toxicity may arise. In general, the reactivity of nanomaterials depends on size and shape (SANTEN, 2009).

According to the inventory maintained by the Nanotech Project, around 1,600 commercial products containing nanomaterials are currently available on the market. Table 1 highlights some applications of nanomaterials in agriculture and the food industry.

Table 1. Some examples of commercial products containing nanomaterials used in the food industry and agriculture. Data extracted from Mukhopadhyay (2014)

Product	Application	Institution
Nanocides	Pesticides encapsulated in nanoparticles for controlled release nanoemulsions for greater efficiency	BASF
Buckyball fertilizer	Ammonia from buckyballs	Kyoto University
Food packaging	Airtight plastic packaging with silicate nanoparticles	Bayer AG
Use of agricultural waste	Nanofibers from cotton waste for improved strength of clothing	Cornell University
Nanosensors	Contamination of packaged food	Nestle, Kraft
Precision farming	Nanosensors linked to a global positioning system tracking unit for real-time monitoring of soil conditions and crop growth	US Department of Agriculture

The potential application of nanotechnology in agriculture encompasses gene transfer methods as well as fertilizer and chemical pesticide technology. The oldest and most comprehensive application of nanotechnology is the size reduction of previously existing pesticide emulsions (GREEN; BEESTMAN, 2007).

Except for the nanosuspension and nanodispersion formulations, the use of nanomaterials in agriculture is indeed still modest. However, the possibilities are enormous, and scientific production in this area increases each year. We can highlight the implantation of carbon nanotubes in chloroplasts, leading to a significant increase in electron transport and, consequently, an improvement in photosynthesis yield (GIRALDO et al., 2014); and the treatment of seeds or seedlings with carbon nanotubes that result respectively in increased germination rate and root elongation (HAGHIGHI; SILVA, 2014; TRIPATHI; SONKAR; SARKAR, 2011).

Over the past decade, there has been a fierce debate in the literature about the effects of nanomaterials on living beings. Despite the possible benefits mentioned above, many studies report that nanomaterials can cause alterations in DNA (CUI et al., 2014; GHOSH et al., 2010; RICO et al., 2011; KUMARI; MUKHERJEE; CHANDRASEKARAN, 2009; KUMARI et al., 2011), decreased chlorophyll content (SADIQ et al., 2017) and inhibition of root growth (TAYLOR et al., 2014; DIMKPA et al., 2013; MA et al., 2011; ZHANG et al., 2012; CASTIGLIONE et al., 2011; ASLI; NEUMANN, 2009; LEE et al., 2010).

Leaf absorption of minerals was first confirmed in the 19th century. Since then, foliar application of minerals has been studied in various agricultural crops. One of the main advantages of foliar absorption is the specific application of the mineral, which reduces the environmental impact in relation to soil application. Moreover, the use of foliar fertilization has been increasing in different regions. Factors inherent to the leaf, nutrients, applied solution and external parameters influence the nutrient absorption by the leaves.

Nutrient uptake depends on structure (number of stomata, thin cuticles, hairiness), chemical composition (quality and quantity of wax) and leaf age (as new leaves absorb much more nutrients than adult ones) (EICHERT; FERNANDEZ, 2011). Other factors inherent to the leaf are cuticle moisture and internal ionic concentration (MALAVOLTA, 2006).

Regarding nutrients, leaf absorption of nutrients is regulated by ion mobility and its metabolization, solubility, ion diameter and hydration. Table 2 shows the classification of nutrients as to their mobility in phloem (mobility as redistribution). Mobile ions are rapidly absorbed and transported to other parts of the leaf and redistributed from the residence organ to other parts of the plant.

Table 2. Nutrients classification regarding their mobility in plants (WHITE, 2011)

Mobility		
High	Intermediate	Low
Potassium	Iron	Calcium
Magnesium	Zinc	Manganese
Phosphorus	Copper	Boron*
Sulfur	Boron*	
Nitrogen	Molybdenum	
Chlorine		

*Boron mobility varies depending on the species.

Nutrient application by foliar spraying should be done in uniform sprays and in tiny droplets, and the solutions should be sprayed on the most absorbed leaf face. The excess causes dripping or dripping of the solution to the lower leaves and the soil, causing poor distribution of the solution on the leaves, waste of nutrients that will not be used by the foliage, and washing, which removes nutrients from the leaves. However, the results are often varied and not reproducible due to the lack of knowledge of various factors that affect the absorption process (FERNANDEZ; EICHERT, 2009).

Copper (Cu) is an essential element for plants, participating in a series of enzymatic processes such as prosthetic group. Cu gets in contact with the root predominantly by mass flow, with Cu^{2+} being the form readily available for absorption (MALAVOLTA, 2006). Chelating agents, such as citric, tartaric, malic, oxalic acids and phenols, may also help copper absorption (MALAVOLTA, 2006).

The absorption process occurs in a metabolically active manner (membrane transporters). Zn^{2+} inhibits the process competitively, which is reduced by respiratory inhibitors and by H_2PO_4^- , K^+ , Ca^{2+} and NH_4^+ . Root and leaf absorption processes occur by similar mechanisms (MALAVOLTA, 2006).

Cu has high affinity for sulfhydryl, peptide, carboxylic and phenolic groups and, therefore, 98% of the copper found in the cytoplasm is complexed and the free Cu^{2+} and Cu^+ contents are very low (BROADLEY et al., 2011a). Redistribution occurs via phloem, with copper bound to organic compounds such as amino acids. In case of deficiency, copper has low mobility for organ drains, and therefore, deficiency symptoms appear primarily in younger leaves (strong drains) (MALAVOLTA, 2006).

Malavolta (2006) and Broadley et al. (2011a) report that the main functions of copper in plants are:

- (i) Participate in the structure of proteins such as azurine, stercyanin, umecianin, glycoproteins
- (ii) Constituent of enzymes such as ascorbate oxidase, polyphenol oxidase, laccase, plastocyanine, diamine oxidase, cytochrome oxidase, ribulose diphosphate carboxylase
- iii) Participates in physiological processes such as electron flux in the light phase and the activation of ribulose diphosphate carboxylase in the dark phase of photosynthesis, respiration, hormonal regulation, indirect effect of biological nitrogen fixation and metabolism of secondary compounds.

In addition to these functions, Cu plays an important role in disease resistance, which may be due to the fungistatic role of the element or its function in lignin synthesis, pollen grain structure and uniform grain maturation, thus aiding the harvest process (MALAVOLTA, 2006; BROADLEY et al., 2011a).

Cerium (Ce) is one of the elements known as rare earth elements (REE). This name was given due to the supposed scarcity of these elements in the earth's crust, however it is already known that certain REEs are more abundant than some metals, such as silver (ENGHAG, 2004). Among the REEs, cerium is the most abundant and the 25th most abundant element in the earth's crust (ROCIO et al., 2012).

Although abundant, these elements are difficult to extract from the rocks. Modern techniques of cation exchange, fractional crystallization and liquid-liquid extraction are used, which makes production more expensive (ROCIO et al., 2012).

The most relevant applications of cerium include oxidizing agent, polishing powder, glass and ceramic dyes, catalysts in self-cleaning furnaces and oil refinery fluids (ROCIO et al., 2012). In 2012, the estimated annual production of cerium oxide nanoparticles ($n\text{CeO}_2$) was 1,000 tons (PICCINNO et al., 2012). China, which has the largest natural deposit of these elements (37%) (ROCIO et al., 2012), was the first to use this and other REEs as fertilizers in their crops (HU et al., 2002).

The study of the effects of REE is still incipient in the literature. An example of this is that the book Marschner's Mineral Nutrition of Higher Plants, Broadley et al. (2011b) devote only one paragraph to the use of cerium in agriculture.

Even though there are controversies about the biological effects of REEs, it is a fact that traces of these elements are found in phosphate fertilizers marketed in Brazil and in low concentrations they may be beneficial depending on the species. However, studies with cerium applications in Brazilian crops, including soybean, are still few.

The first idea of this study was to develop a method to detect the nanoparticles in plants under *in vivo* conditions. Such method was not able for this purpose but it was possible to achieve the plant nutritional status for some plant nutrients. Methods of direct analysis of solids diminish the number of steps in the analytical sequence and minimize or even eliminate the generation of chemical waste. In this context, X-ray fluorescence spectroscopy (XRF) arises as an alternative and promising technique for foliar diagnosis, presenting attractive features such as multielemental and simultaneous capabilities, non-destructive analysis, minimal or no sample preparation and equipment portability.

1.1 Hypotheses

This study has tested the following hypotheses:

- i) Cu and Ce elements from nanoparticulate sources may be absorbed by soybean leaves.
- ii) The plant transports these elements as complexes or chelates instead of oxides.
- iii) The element applied to the leaf is redistributed to other parts of the plant.
- iv) The application of nanoparticulate Cu and Ce influence soybean agronomic parameters such as shoot mass gain and number of pods.

1.2 Objectives

This study aimed at investigating the absorption, effects on the plant and the assimilation of nanomaterials absorbed by the leaves of plants. To this end, it was used CuO and CeO₂ nanoparticles as materials, and *Glycine max* (L.) Merrill as a model organism.

Specifically, it was investigated:

- i) What were the effects of nanomaterials applications on plant development.
- ii) If Cu and Ce elements present in nanomaterials were absorbed by the leaves.
- iii) If absorbed by the leaves, were they redistributed to different leaves/organs.

It was also aimed at developing a spectrometric method to monitor the movement of the foliar applied nutrients under *in vivo* conditions.

1.3 Structure of the thesis

In addition to the introductory text, this thesis contains more three chapters:

Chapter 2: Direct determination of mineral nutrients in soybean leaves under vivo conditions by portable X-ray fluorescence spectroscopy. This chapter was issued from our attempts to develop a method to detect the redistribution of Cu after foliar application. However, it did not work since the amount of Cu redistributed was below the limits of detection of the technique. On the other hand, the method allowed assessing the concentration of several nutrients in the plant tissue. Thus, due to its novelty and importance to assess the nutritional status of soybean plants the results were included in this thesis. The data was published in the *Journal X-Ray Spectrometry* in 2019. DOI: 10.1002/xrs.3111.

Chapter 3: Foliar uptake of nano copper oxide in soybean plants. [This chapter will be sent to publication]. In this chapter it was carried out a chemical, physiological and morphological study in order to evaluate if Cu nanoparticles can improve copper uptake and possible conjugation with organic acids comparing to soluble sources, such as CuSO₄

Chapter 4: Foliar uptake of nano cerium oxide in soybean plants. [This chapter will be sent to publication]. This chapter regards the study about the effects of a rare earth element on soybean plants. Although Ce is not considered essential to plants, some studies have shown that in a proper concentration Ce can improve plant growth and development, increase yields and alleviate environmental stresses.

References

ASLI, S.; NEUMANN, P. M. Colloidal suspensions of clay or titanium dioxide nanoparticles can inhibit leaf growth and transpiration via physical effects on root water transport. **Plant, Cell and Environment**, v. 32, p. 577–584, 2009.

BROADLEY, M. et al. Beneficial Elements. In: MARSCHNER, P. (Ed.). **Marschner's Mineral Nutrition of Higher Plants**. 3.ed. New York: Academic Press, 2011b. p. 249–269.

BROADLEY, M. et al. Function of nutrients: Micronutrients. In: MARSCHNER, P. (Ed.). **Marschner's Mineral Nutrition of Higher Plants**. 3.ed. New York: Academic Press, 2011a. p. 206–211.

CASTIGLIONE, M. R. et al. The effects of nano-TiO₂ on seed germination, development and mitosis of root tip cells of *Vicia narbonensis* L. and *Zea mays* L. **Journal of Nanoparticle Research**, v. 13, p. 2443–2449, 2011.

CUI, D. et al. Effect of cerium oxide nanoparticles on asparagus lettuce cultured in an agar medium. **Environmental Science. Nano**, v. 1, p. 459–465, 2014.

DIMKPA, C. O. et al. Fate of CuO and ZnO nano- and microparticles in the plant environment. **Environmental Science and Technology**, v. 47, p. 4734–4742, 2013.

EICHERT, T.; FERNÁNDEZ, V. Uptake and Release of Elements by Leaves and Other Aerial Plant Parts. In: MARSCHNER, P. (Ed.). **Marschner's Mineral Nutrition of Higher Plants**. 3.ed. New York: Academic Press, 2011. p. 71–84.

ENGHAG, P. Scandium, Yttrium, Lanthanum and the 14 Lanthanides – Rare Earth Metals (REMs). In: **Encyclopedia of the Elements: Technical Data – History --Processing – Applications**. Weinheim, GE: Wiley Verlag, 2004. p. 373–492.

FERNANDEZ, V.; EICHERT, T. Uptake of hydrophilic solutes through plant leaves: Current state of knowledge and perspectives of foliar fertilization. **CRC Critical Reviews in Plant Sciences**, v. 28, p. 36–68, 2009.

GHOSH, M.; BANDYOPADHYAY, M.; MUKHERJEE, A. Genotoxicity of titanium dioxide (TiO₂) nanoparticles at two trophic levels: plant and human lymphocytes. **Chemosphere**, v. 81, p. 1253–1262, 2010.

GIRALDO, J. P. et al. Plant nanobionics approach to augment photosynthesis and biochemical sensing. **Nature Materials**, v. 13, p. 400–408, 2014.

GREEN, J. M.; BEESTMAN, G. B. Recently patented and commercialized formulation and adjuvant technology. **Crop Protection**, v. 26, p. 320–327, 2007.

HAGHIGHI, M.; SILVA, J. A. T. The effect of carbon nanotubes on the seed germination and seedling growth of four vegetable species. **Journal of Crop Science and Biotechnology**, v. 17, p. 201–208, 2014.

HU, X. et al. Bioaccumulation of lanthanum and cerium and their effects on the growth of wheat (*Triticum aestivum* L.) seedlings. **Chemosphere**, v. 48, p. 621–629, 2002.

IUPAC. **Compendium of Chemical Terminology**. The Gold Book: Nanogel. 2. ed. Research Triangle Park, 2018. Available at: <https://doi.org/10.1351/goldbook.NT07521>. Accessed: 27th Mar. 2018.

KOLAHALAM, L. A. et al. Review in nanomaterials: synthesis and applications. **Materials today: Proceedings**, v. 18, p. 2182-2190, 2019.

KUMARI, M. et al. Cytogenetic and genotoxic effects of zinc oxide nanoparticles on root cells of *Allium cepa*. **Journal of Hazardous Materials**, v. 190, p. 613–621, 2011.

KUMARI, M.; MUKHERJEE, A.; CHANDRASEKARAN, N. Genotoxicity of silver nanoparticles in *Allium cepa*. **Science of the Total Environment**, v. 407, p. 5243–5246, 2009.

LEE, C. W. et al. Developmental phytotoxicity of metal oxide nanoparticles to *Arabidopsis thaliana*. **Environmental Toxicology and Chemistry**, v. 29, p. 669–675, 2010.

MA, Y. et al. Phytotoxicity and biotransformation of La₂O₃ nanoparticles in a terrestrial plant cucumber (*Cucumis sativus*). **Nanotoxicology**, v. 5, p. 743–753, 2011.

MALAVOLTA, E. Funções dos macro e micronutrientes. In: MALAVOLTA, E. (Ed.). **Manual de nutrição mineral de plantas**. São Paulo: Agronômica Ceres, 2006. p. 336–347.

MUKHOPADHYAY, S. S. Nanotechnology in agriculture: prospects and constraints. **Nanotechnology, Science and Applications**, v. 7, p. 63–71, 2014.

PICCINNO, F. et al. Industrial production quantities and uses of ten engineered nanomaterials in Europe and the world. **Journal of Nanoparticle Research**, v. 14, p. 1109-1119, 2012.

RICO, C. M. et al. Interaction of nanoparticles with edible plants and their possible implications in the food chain. **Journal of Agricultural and Food Chemistry**, v. 59, p. 3485–3498, 2011.

ROCIO, M. A. R. et al. Terras-raras: situação atual e perspectivas. **BNDES Setorial**, n. 35, p. 369-420, 2012. Disponível em: <https://web.bndes.gov.br/bib/jspui/handle/1408/1527>.

SADIQ, I. M. et al. Corrigendum: ‘Ecotoxicity study of titania (TiO₂) NPs on two microalgae species: *Scenedesmus* sp. and *Chlorella* sp.’ [Ecotoxicol. Environ. Saf. 74/5 (2011) 1180–1187], (S0147651311000728), (10.1016/j.ecoenv.2011.03.006). **Ecotoxicology and Environmental Safety**, v. 142, p. 597, 2017.

SANTEN, R. A. van. Insensitive Catalytic Relationships. **Accounts of Chemical Research**, v. 42, p. 57-66, 2009.

TAYLOR, A. F. et al. Nanoparticle Formation and Genetic Response of Plants to Gold. **PLoS One**, v. 9, e93793, 2014.

TRIPATHI, S.; SONKAR, S. K.; SARKAR, S. Growth stimulation of gram (*Cicer arietinum*) plant by water soluble carbon nanotubes. **Nanoscale**, v. 3, p. 1176-1181, 2011.

WHITE, P. J. Long-distance Transport in the Xylem and Phloem. In: MARSCHNER, P. (Ed.). **Marschner’s Mineral Nutrition of Higher Plants**. 3.ed. New York: Academic Press, 2011. p. 49–70.

ZHANG, P. et al. Comparative toxicity of nanoparticulate/bulk Yb₂O₃ and YbCl₃ to cucumber (*Cucumis sativus*). **Environmental Science and Technology**, v. 46, p. 1834–1841, 2012.

2 DIRECT DETERMINATION OF MINERAL NUTRIENTS IN SOYBEAN LEAVES UNDER *VIVO* CONDITIONS BY PORTABLE X-RAY FLUORESCENCE SPECTROSCOPY¹

Abstract

A portable energy dispersive X-ray fluorescence spectrometer furnished with a Rh X-ray tube was evaluated for the determination of macro and micronutrients in soybean leaves (*Glycine max* (L.) Merrill). XRF instrumental parameters were optimized in a univariate way and emission intensities were measured for 60 s and under vacuum for macronutrients, and during 180 s, under air and 305 Al + 25.1 μm Ti filter, for micronutrients. Fresh and dried leaves were irradiated and it was possible to identify P, K, Ca, S, Mn, Fe, Cu and Zn $K\alpha$ emission lines. For comparative purpose, the samples were also microwave-assisted digested and analyzed by ICP OES. In general, linear correlations between K, Ca, Mn, Fe, Cu and Zn mass fractions in the tested samples and the corresponding pXRF intensities were obtained. The linear determination coefficients (R^2) ranged from 0.42 to 0.86. In addition, the limits of detection were suitable for plant nutrient diagnosis. It is demonstrated that pXRF is a simple and powerful tool for analysis of plant materials.

Keywords: foliar diagnosis, mineral nutrition, soybean leaves, portable X-Ray fluorescence spectrometry

2.1 Introduction

Foliar diagnosis has been used for a long time (LUNDEGARDH, 1943; THOMAS, 1937) to evaluate plant nutritional status and still is a matter of study nowadays, partly due to promising recent advances in analytical techniques allowing multielemental (GUERRA et al., 2015; 2018; OLIVEIRA; RAPOSO; GOMES NETO, 2009), direct (GUERRA et al., 2015; 2018) and non-destructive (GUERRA et al., 2018) analysis.

Usually, essential elements determination in most routine laboratories requires sample pre-treatments. The samples are washed, dried and grinded with further wet acid decomposition in open or closed systems (GUERRA et al., 2015; TREVISAN et al., 2008). Finally, the solution can be analyzed using spectroscopic techniques such as visible spectrophotometry

¹ This chapter has already been published as a scientific paper in the Wiley *X-ray spectrometry*. Costa Junior et al. Direct determination of mineral nutrients in soybean leaves under *vivo* conditions by portable x-ray fluorescence spectroscopy. **X-ray Spectrometry**. (2019). DOI: 10.1002/xrs.3111.

for B, P and S, atomic absorption spectrometry for K, Ca, Mg, Fe, Cu, Mn, Zn and Na, or inductively coupled plasma optical emission spectrometry (ICP OES) for multielemental and simultaneous P, K, Ca, Mg and S as well as Mn, Fe, Cu, Zn, Mo and B determinations. Some of the main drawbacks faced by this approach regard the great number of steps involved in the process and the time elapsed from all analytical procedures, i.e. collecting the samples, and getting the results may take in practice from one to two weeks.

Precision agriculture presents potential to increase crop yield. Hence, efforts have been made towards the development of quick, precise and accurate methods that allow assessing the plant and soil (GEBBERS; SCHIRRMANN, 2015; MCLAREN et al., 2012) nutritional status in field. This analytical strategy will permit the readily correction of nutritional deficiency. Methods of direct analysis of solids diminish the number of steps in the analytical sequence and minimize or even eliminate the generation of chemical waste. In this context, X-ray fluorescence spectroscopy (XRF) arises as an alternative and promising technique for foliar diagnosis, presenting attractive features such as multielemental and simultaneous capabilities, non-destructive analysis, minimal or no sample preparation and equipment portability. The samples can be analysed as powders, pellets or even under *vivo* conditions (DURAN et al., 2017; TOWETT; SHEPHERD; LEE, 2016).

XRF is available in wavelength or energy dispersive detection modes (JENKINS, 1999). It includes millimeter range and micro-focused excitation beam benchtop units, total reflection geometry and last but not least, the portable devices. The main differences between these variants regard the lateral resolution, limits of detection and portability (WEST et al., 2017). Portable XRF (pXRF) equipment can be manipulated in field and in principle; it may be even boarded to agricultural machinery. In addition to faster results, in field XRF measurements might become a tool for precision agriculture, allowing farmers to improve the sampling grid and therefore, leading to site-specific nutrient management.

Laser-induced breakdown spectroscopy (LIBS) is another complementary tool that presents promising features aiming at the direct analysis of solid samples. It is fast, multielemental, allows simultaneous determinations and the instruments are also available as portable devices (GUERRA et al., 2015; CAMPOS et al., 2015; CARVALHO et al., 2015a; 2015b; GOMES et al., 2013; GUERRA et al., 2013; 2014; SOUZA et al., 2013).

LIBS (GUERRA et al., 2015; CARVALHO et al., 2015b; AWASTHI et al., 2017; EL-DEFTAR et al., 2015; GONDAL et al., 2016) and XRF (GUERRA et al., 2018; ABEROUMAND, 2009; BLONSKI et al., 2007; CHUPARINA; AISUEVA, 2011; DALY; FENELON, 2018; DEMIR et al., 2010; KHRAMOVA et al., 2012; KHUDER et al., 2009; MCLAREN; GUPPY; TIGHE, 2012; NAYAK et al., 2011) have been employed for the determination of macro and micronutrients in different plant leaves, e.g., sugarcane (GUERRA et al., 2015; CARVALHO et al., 2015b; MELQUIADES et al., 2012), *cannabis* (EL-DEFTAR et al., 2015), black tea (GONDAL et al., 2016), tomato (CARVALHO et al., 2015b; DEMIR et al., 2010), medicinal plants (ABEROUMAND, 2009; CHUPARINA; AISUEVA, 2011; KHUDER et al., 2009), orange (BLONSKI et al., 2007), lemon (BLONSKI et al., 2007), wheat (MCLAREN; GUPPY; TIGHE, 2012), soybean (MCLAREN; GUPPY; TIGHE, 2012), cotton (MCLAREN; GUPPY; TIGHE, 2012), maize (MCLAREN; GUPPY; TIGHE, 2012) and grass (DALY; FENELON, 2018). However, in all the above-mentioned studies, prior to analysis, the leaves were either detached from the plants (GUERRA et al., 2018) or pelletized after washing, drying and grinding (ABEROUMAND, 2009; BLONSKI et al., 2007; CHUPARINA; AISUEVA, 2011; DEMIR et al., 2010; KHRAMOVA et al., 2012; KHUDER et al., 2009; NAYAK et al., 2011).

In view of the analytical capabilities of XRF, the present study aims at demonstrating the feasibility and challenges of portable XRF to assess the nutritional status of soybean leaves under *vivo* and dried conditions. For this purpose, we used a commercial portable energy dispersive X-ray fluorescence spectrometer. The elements of agricultural importance focused in this study were P, S, K, Ca, Mn, Fe, Cu and Zn.

2.2 Materials and Methods

2.2.1 Soybean cultivation

Four seeds of soybean (*Glycine max* (L.) Merrill), cultivar KWS RK 7214 IPRO, were sown in pots containing sand, watered exclusively with deionized water, for two weeks. After, they were transferred to 2.2 L pots containing Hoagland & Arnon's hydroponic solution (HOAGLAND; ARNON, 1950) at 20% until reaching the V3 phenological stage. The plants were finally transferred to regular Hoagland & Arnon's solution for three days. All cultivation assay was carried out in a light room at 24° C and 50% humidity. After this period, the second leaf (all three leaflets) was selected in each plant for direct analysis by using the pXRF.

For comparative purpose, the same leaves were removed from each plant and oven-dried at 65° C until constant weight (~48 hours) and further analysed by pXRF. Subsequently, the leaves were ground in a MA 048 model knife mill (Marconi, Piracicaba, Brazil) and the elemental concentrations were determined by ICP OES after microwave-assisted acidic digestion as described in detail below.

Afterwards, the same sample plants were placed in a Hoagland & Arnon's hydroponic solution at a concentration 10 times higher than a normal one for 3 days. Then, a subsequent superior leaf (third one) was analysed following the same procedures as above mentioned.

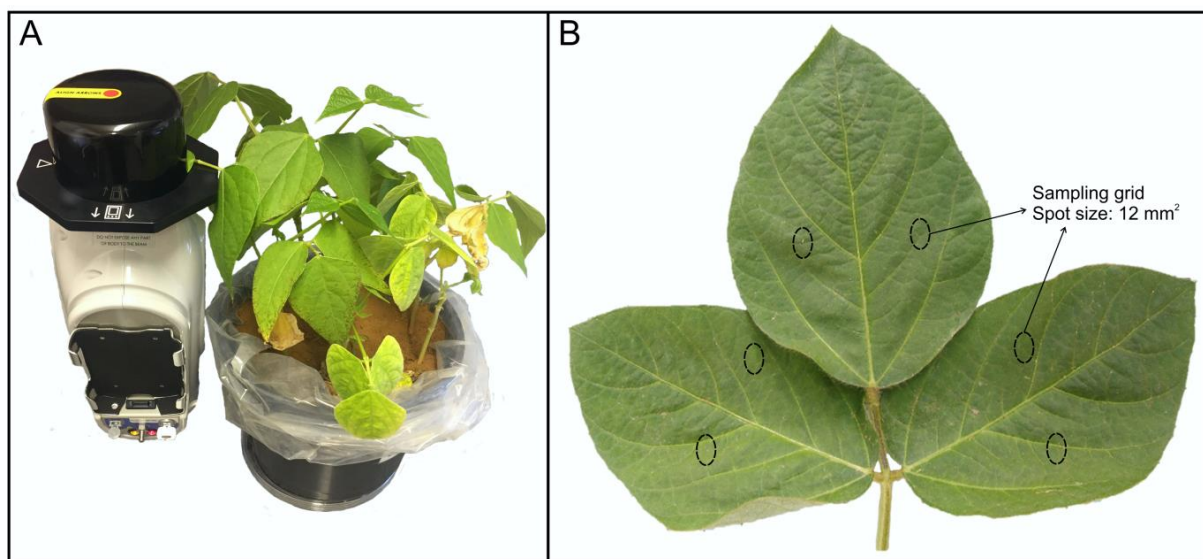
2.2.2 Portable XRF analysis

The measurements were carried out using a portable X-ray fluorescence spectrometer, Tracer III – SD model (Bruker, USA), equipped with a 4 W Rh X-ray tube and 10 mm² X-Flash[®] Peltier-cooled Silicon Drift detector (SDD), operated at 30 µA and 40 kV.

The development of a pXRF method for multi-elemental analysis involved the optimization of dwell time (30, 60, 120, 150, 180 and 300 s), number of spots per leaf (2 to 6), analysis under vacuum or air and the use of primary filters (305 µm Al/25.4 µm Ti and 25.4 µm Ti). These filters are the ones readily available for the portable Bruker Tracer III-SD equipment. These parameters were optimized to yield higher signal-to-noise ratio and lower coefficient of variation (CV) for P, S, K, Ca, Mn, Fe, Cu and Zn.

A schematic overview of the proposed protocol analysis of soybean leaves is shown in Figure 1. It is important to highlight that the leaves were not detached from the petiole, as shown in Figure 1A. The abaxial face of each trefoil was directly analysed (n=2) at one spot per side of the blade by using the pXRF spectrometer (Figure 1B).

Figure 1. (A) *In vivo* analysis of a plant by pXRF equipment; (B) Sampling grid showing the 6 spots for the direct analysis of soybean leaves



All data were acquired using the software Bruker S1PXRF[®]. The data were obtained through the deconvolution process using the Artax[®]. For each plant the same spot was analysed in triplicate.

2.2.3 Elemental Sensitivity

The elemental sensitivities were determined separately using a set of thin film calibration standards purchased from Micromatter Co (Vancouver, BC, Canada), ranging from silicon ($Z=14$) to strontium ($Z=38$). It is shown in Table 1 the superficial concentration ($\mu\text{g cm}^{-2}$) of Si, P, S, K, Ca, Sc, Ti, Mn, Fe, Cu, Zn, Se and Sr thin film standards.

Table 1. Concentration of thin film X-ray calibration standard (MicroMatter, Canada)

Serial number	Composition	Element	Superficial concentration ($\mu\text{g cm}^{-2}$)
6321	SiO	Si	32.18
6322	GaP	P	14.00
6323	CuS _x	S	12.00
6324	KCl	K	26.69
6325	CaF ₂	Ca	30.90
6326	ScF ₃	Sc	21.87
6327	Ti	Ti	43.30
30111	Mn	Mn	60.00
6329	Fe	Fe	49.40
6323	CuS _x	Cu	42.30
6330	ZnTe	Zn	16.16
30112	Se	Se	49.50
30113	SrF ₂	Sr	32.70

2.2.4 Signal-to-noise ratio

For the pXRF method optimization, the signal-to-noise ratios were evaluated. It was determined by dividing the characteristic X-ray net intensities by the background square root (GUERRA et al., 2014; BACHIEGA et al., 2019).

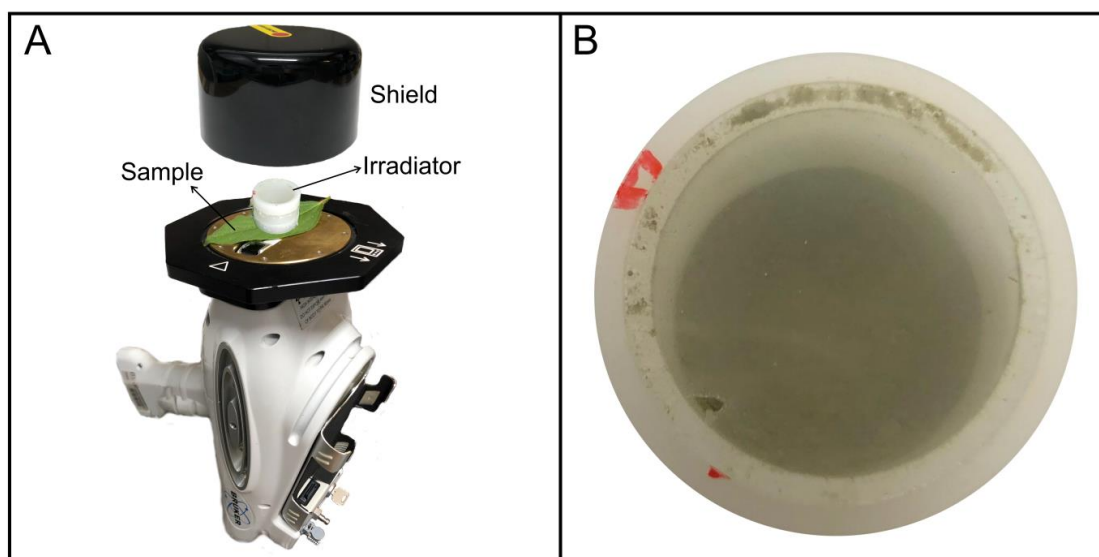
2.2.5 Emission-transmission (ET) method

For quantitative determination of elements, the ET method was chosen (BLONSKI et al., 2007; LEROUX; MAHMUD, 1966). An irradiator was prepared using a set of P.A. salts containing macro (P, S, K and Ca) and micronutrients (Mn, Fe, Cu and Zn). The salts were dried at 60°C for 24 h and ground in an agate mortar. Subsequently, 2 g of the irradiator was added in X-ray cup (Chemplex, n°. 1530), sealed with a 5 μm -polypropylene thin film (Spex, n°. 3520) on both sides of the sample cup. The irradiator was manually pressed with an acrylic piston. The irradiator composition is shown in Table 2 and the ET method scheme and irradiator cup in Figure 2.

Table 2. Composition (%) of the irradiator used in emission-transmission quantitative method

Salt	Concentration (%)
Na_3PO_4	22.70
$\text{Zn}(\text{PO}_4)_2$	9.10
K_3PO_4	18.20
$\text{CuSO}_4 \cdot 5\text{H}_2\text{O}$	9.10
$\text{MnSO}_4 \cdot 4\text{H}_2\text{O}$	13.60
FeSO_4	9.10
CaNO_3	18.20

Figure 2. (A) Emission-transmission method scheme; (B) Irradiator sample cup



Equation 1 was used to determine the element concentration in wet basis (C_w):

$$C_w = \frac{I^{sam}}{A \cdot S \cdot d} \quad \text{Equation 1}$$

where:

C_w : concentration of the element in the wet basis (mg kg^{-1})

I^{sam} : characteristic X-ray net intensity of the element i in the sample (cps)

A : absorption factor (unitless)

S : sensitivity ($\text{cps} \cdot \text{cm}^2 \cdot \mu\text{g}^{-1}$)

d : surface density of the sample (g cm^{-2})

The sensitivity (S) was calculated using Equation 2 and the values are presented in Figure 3:

$$S = \frac{I^{elem}}{C_s} \quad \text{Equation 2}$$

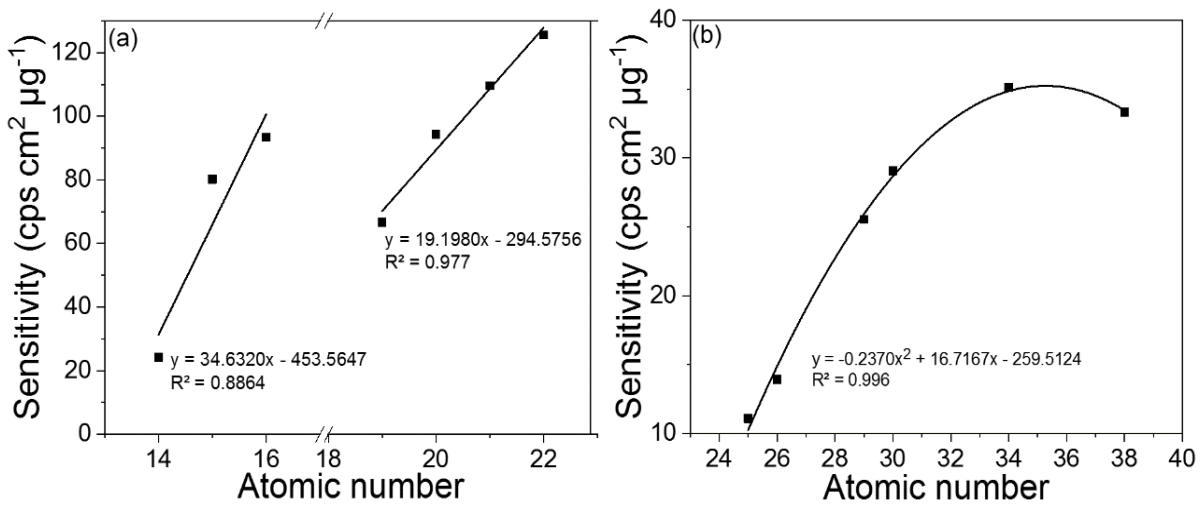
where:

S: sensitivity ($\text{cps}\cdot\text{cm}^2 \mu\text{g}^{-1}$)

I^{elem} : characteristic X-ray net intensity of the element i in the thin film calibration standards from Micromatter Co (cps)

C_s : superficial concentration of the element i in the thin film calibration standards from Micromatter Co ($\mu\text{g cm}^{-2}$)

Figure 3. Dependence of elemental sensitivity ($\text{cps cm}^2 \mu\text{g}^{-1}$) on atomic number. (a) from 14 to 22. Conditions of analysis: 60 seconds, under vacuum and no filter; (b) from 25 to 38. Conditions of analysis: 180 seconds, under air and filter composed by $305 \mu\text{m Al}/25.4 \mu\text{m Ti}$



For intermediate thickness samples, the dimensionless absorption factor (A) was determined through the Equation 3:

$$A = \frac{1-H}{-\ln(H)} \quad \text{Equation 3}$$

with:

$$H = \left(\frac{I_{\text{irrad+sam}} - I_{\text{sam}}}{I_{\text{irrad}}} \right)$$

where:

I^{irrad} : characteristic X-ray intensity of the element i in the irradiator (cps)

$I^{\text{irrad+sam}}$: characteristic X-ray intensities of the element of interest i in the irradiator transmitted by the sample plus the element i in the sample (cps)

I^{sam} : characteristic X-ray intensity of the element i in the sample (cps)

To convert the concentration found in wet basis to the most used dry basis (C_d), Equation 4 was used:

$$C_d = \frac{C_w TM}{DM} \quad \text{Equation 4}$$

where:

C_d : concentration of the element i in the dry basis (mg kg^{-1})

C_w : concentration of the element i in the wet basis (mg kg^{-1})

TM: total (wet) mass of the sample (g)

DM: dry mass of the sample (g)

2.2.6 pXRF validation

For validation of the proposed pXRF method, a pellet of NIST SRM 1547 (Peach leaves) standard reference material (SRM) was prepared by transferring 50 mg of the powdered material to a 15 mm die set and applying 8.0 t cm^{-2} for 5 minutes.

2.2.7 Microprobe XRF analysis

The dried leaves, previously analysed by the pXRF, were analysed by a microprobe XRF spectrometer (Orbis PC EDAX, USA). In this device, the excitation X-ray beam was provided by a Rh anode operating at 45 kV and 900 μA , using a 1 mm collimator and dwell time of 5 s. The X-ray fluorescence photons were detected by a 30 mm^2 silicon drift detector (SDD) with a dead time smaller than 7 %. To improve the sensitivity towards light elements the measurements were carried out under vacuum. The maps were collected using a matrix of 32 x 25 points.

2.2.8 Comparative method (ICP OES)

After XRF analysis, the dried leaves were ground in a knife mill and weighed (n=3 leaflets per plant). The samples were submitted to microwave-assisted acidic digested in closed TFM[®] vessels (Provecto Analitica DGT 100 plus) according to the following procedure: 70 to 100 mg were accurately weighed in the TFM[®] vessels and then 6.0 mL of 20% v v⁻¹ HNO₃ and 2.0 mL of 30% w w⁻¹ H₂O₂ were added. The microwave heating program consisted of 4 steps: a) 7 minutes at 400 W; b) 15 minutes at 850 W; c) 7 minutes at 320 W and; d) 2 minutes at 0 W. After cooling, the residual solutions were transferred to 25 ml volumetric flasks, and the volume made up with high-purity de-ionized water (resistivity < 18.2 MΩ cm). The resulting solutions were analysed by ICP OES, with a dual view (iCap 7400 Duo optical emission spectrometer, Thermo Scientific, Waltham, MA, USA). The analysis conditions of the ICP OES are presented in Table 3. SRM NIST1547 (Peach leaves) was used for quality control in the ICP OES analysis.

Table 3. Characteristics and operational conditions of the analysis carried out in ICP OES (iCap 7400 Duo optical emission spectrometer, Thermo Scientific, USA)

Characteristics	Operational Conditions
View	Radial
Detector	Wavelength range: 166-847 nm
<i>Operational parameters</i>	
Exposure time	10 s
RF power	1.2kW
Plasma gas-flow rate	12 L min ⁻¹
Auxiliary gas-flow rate	0.5 L min ⁻¹
Nebulizer gas-flow rate	0.6 L min ⁻¹
Emission lines	Ca 422.673 nm Cu 324.754 nm Fe 259.940 nm K 766.490 nm Mn 257.610 nm Zn 213.856 nm

2.2.9 Limits of Detection

The limits of detection (LODs) for ICP OES analysis were estimated based on the IUPAC recommendation (CURRIE, 1968):

$$LOD = \frac{3.3s}{b}$$

where:

s: estimated standard deviation of the blank signal measurement

b: slope of the calibration curve

LODs for XRF analysis were estimate as:

$$LOD = \frac{3\sqrt{(BG/t)}}{A \cdot S \cdot d}$$

where:

BG: Element background (cps)

t: acquisition time (s)

A: absorption factor (unitless)

S: sensitivity (cps·cm² μg⁻¹)

d: surface density of the sample (g cm⁻²)

Background (BG) data for K, Ca, Mn, Fe, Cu and Zn K α net intensities were calculated from the spectra obtained by 4 randomly chosen measurements of a leaf. This procedure yielded coefficients of variation below 5% for the elements.

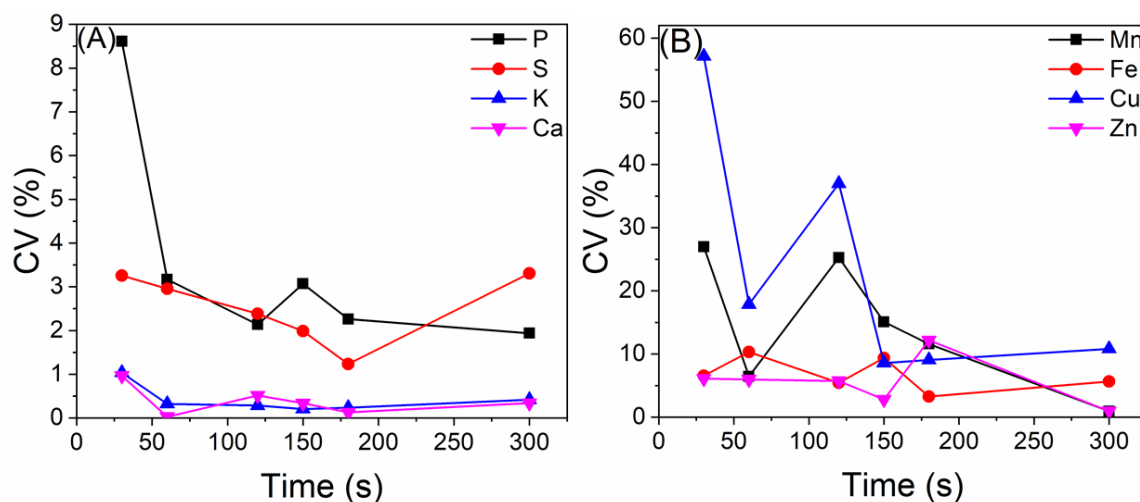
2.3 Results and Discussion

2.3.1 Optimization of experimental parameters

XRF operational parameters, such as time of analysis, number of spots, measurements under vacuum or air and the use of filters were defined by univariate optimization using a fresh leaf. For this purpose, the voltage and current were fixed at 40 kV and 30 μA, respectively. The improvement of results was based on the values of CV for 3 measurements and signal-to-noise ratios (SNRs).

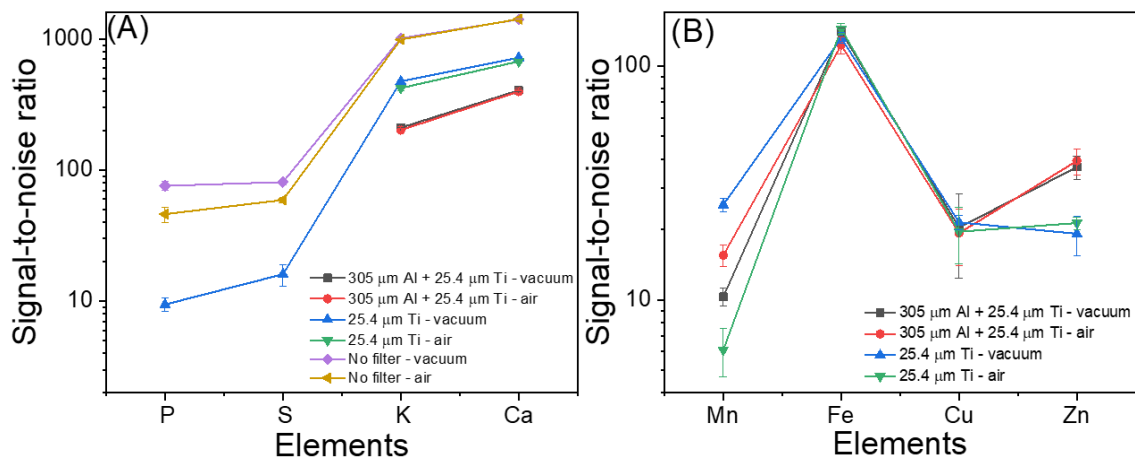
Dwell times from 30 to 300 s were evaluated and the CVs varied from 0.03 to 8.60% for macronutrients and from 0.95 to 57.00% for micronutrients (Figure 4). The shortest dwell times that resulted in the lowest CVs, for most elements, were 60 and 180 seconds for macro (< 5%) and micronutrients (< 15%), respectively.

Figure 4. Evaluation of coefficient of variation (CV) as function of time for macro and micronutrients in soybean leaves. (A): macronutrients; (B): micronutrients



The effects of vacuum and filters on the signal-to-noise ratios (SNRs) for macronutrients (P, S, K and Ca) are shown in Figure 5A and for micronutrients (Mn, Fe, Cu and Zn) in Figure 5B. For macronutrients, the vacuum improved the SNR for phosphorus and sulphur; on the other hand, its effect on the results for K and Ca was negligible. This happens because the air attenuation of low energy characteristics X-rays emitted by P and S are higher than those for K and Ca. In Figure 5B, the higher value for Fe can be explained by its high concentration in plant tissue.

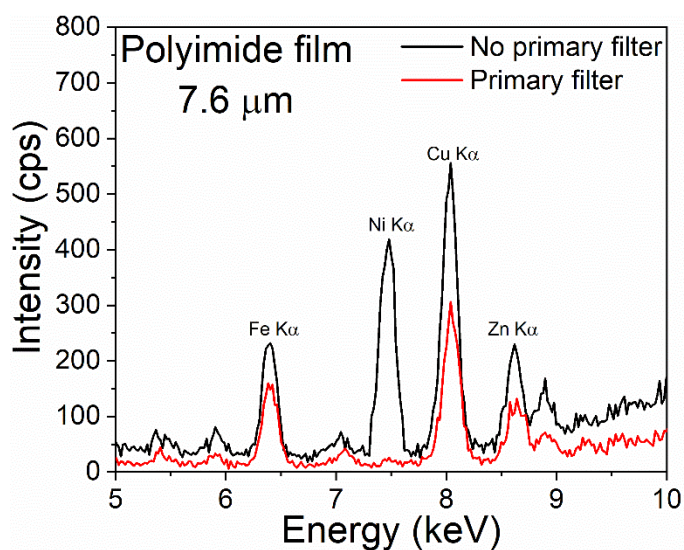
Figure 5. Evaluation of signal-to-noise ratio (SNR) for macronutrients (A) and micronutrients (B) using different filters (no filter, 305 μm Al/25.4 μm Ti and 25.4 μm Ti) and under vacuum and air condition. Time of analysis: 300 s



The filters strongly absorbed the Rh $L_{\alpha 1}$ (2.697 keV) and Rh $L_{\beta 1}$ (2.834 keV) lines from the X-ray tube. Such lines are highly effective for P and S excitation, whose corresponding absorption K edges are at 2.146 and 2.472 keV. In general, the results indicated that SNRs increased with analysis under vacuum and no filter. This condition was selected for further macronutrient determinations.

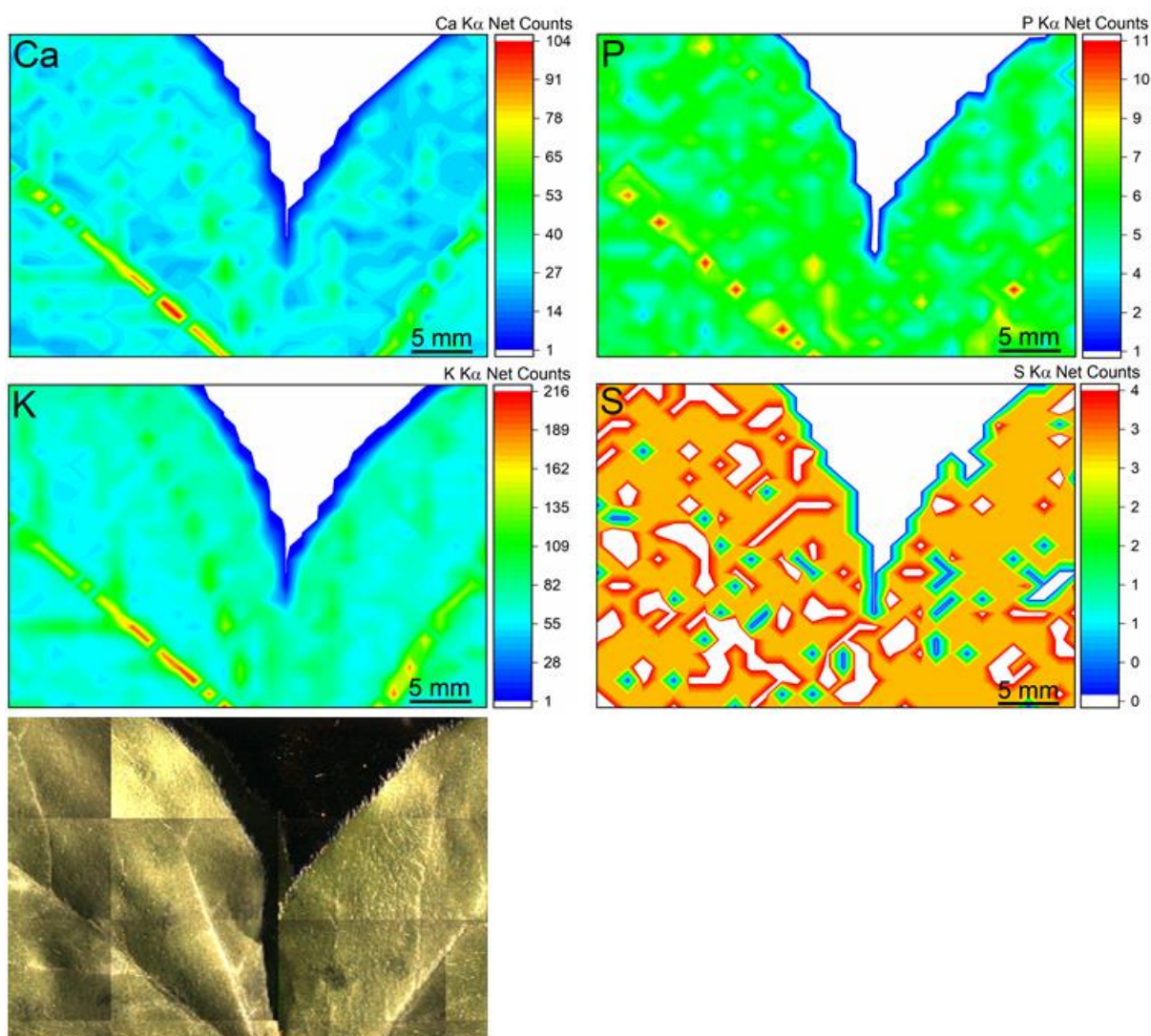
Figure 6 presents the scattered bremsstrahlung produced by the X-ray tube with and without a primary film in the micronutrients X-ray emission energy range. One can notice that the equipment contains spurious signals of Fe, Ni, Cu and Zn (without primary film), but the intensities of these elements are reduced or extinguished (Ni) due to the use of the filter. This background allied to the low content of these micronutrients rendered difficult to perform their quantitative analysis, particularly for Cu. In this case, the filter composed by 305 μm Al/ 25.4 μm Ti (under air) was chosen based on the higher SNRs of Mn and Zn, compared to the 25.4 μm Ti filter. For Fe and Cu, both filters, in the under air condition, had similar SNRs.

Figure 6. Kapton film analysed by the portable equipment. XRF analysis without primary filter



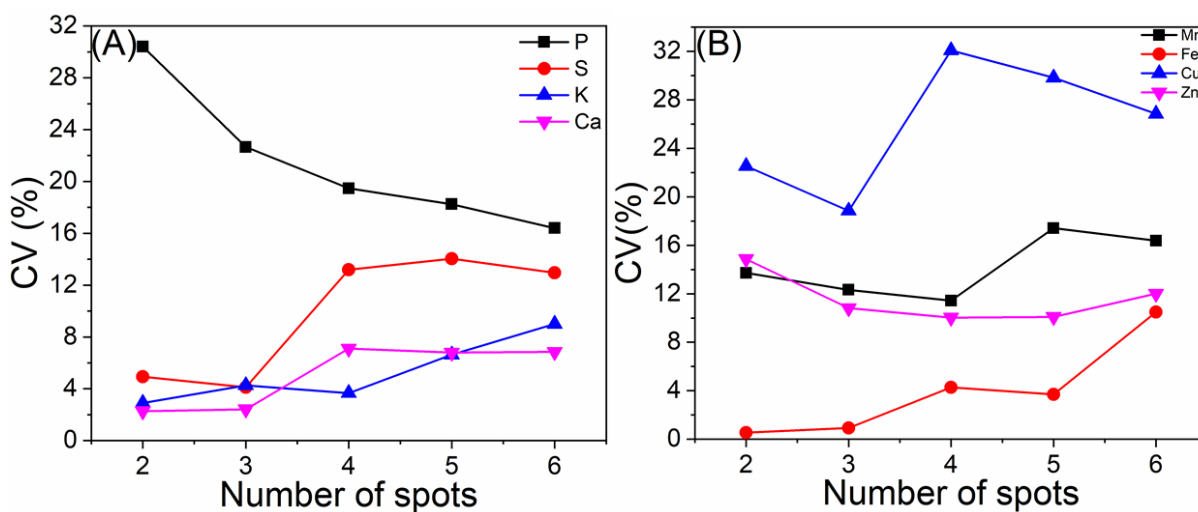
In order to define the minimum number of spots that represent the whole leaf, the influence of number of spots on the CV (%) was verified. The sampling representativeness was based on the micro chemical maps of P, S, K and Ca in 25 mm x 32 mm leaf fragment area for assessing the spatial distribution of the analytes (Figure 7). A heterogeneous elemental distribution over the diagnostic leaf is observed.

Figure 7. Distribution of P, S, K and Ca on soybean leaf revealed by microprobe X-ray fluorescence



The influence of number of spots for macronutrients determination is shown in Figure 8A. The CV (%) decreased for P and increased for K, as we increased the number of spots analysed. S and Ca had a similar pattern in which the variance increased from 2 to 4 spots, and then the variance remained stable. For micronutrients, Zn was the least influenced by the number of points, while the variance for Mn and Fe increased from 4 to 6 spots (Figure 8B). The disparity in the coefficient of variation of elements can be attributed to the heterogeneity of the sample and/or to the low concentration of the elements. The latter feature presented was critical for Mn, Fe, Cu and Zn.

Figure 8. Evaluation of number of spots in leaves of soybean for the determination of (A) macronutrients and (B) micronutrients. Spot size: 12 mm²

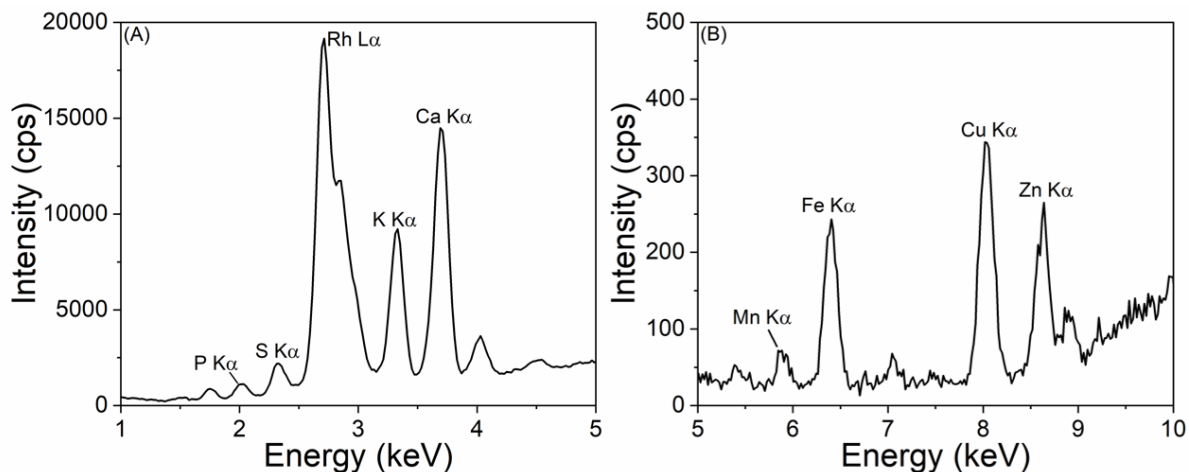


The optimization experiments suggested that two distinct instrumental conditions were necessary to determine macro and micronutrients. Aiming at the simultaneous determination of macronutrients (P, S, K and Ca) in soybean leaves, further experiments were carried out with 60 s dwell time, under vacuum and without primary filter. For micronutrients determination (Mn, Fe, Cu and Zn) samples were irradiated for 180 s, under air and using the 305 μm Al/25.4 μm Ti filter. These experimental conditions were employed in the quantitative assessment of the elements in the soybean leaves.

2.3.2 Determination of elements in soybean leaves

Figure 9 presents typical XRF spectra recorded at soybean leaves during the study. It was possible to identify the following X-ray emission lines in the spectrum obtained in the diagnostic leaf: P K α 2.01 keV, S K α 2.31 keV, K K α 3.31 keV, Ca K α 3.69 keV, Mn K α 5.90 keV, Fe K α 6.40 keV, Cu K α 8.04 keV and Zn K α 8.63 keV.

Figure 9. Fragments of pXRF spectra obtained from the fresh soybean leaf. (A) Sample analysed for 60 seconds, under vacuum, no filter; (B) Sample analysed for 180 seconds, under air and filter composed by 305 μm Al/25.4 μm Ti



Due to the low energy of P and S characteristic X-rays, the emission from the irradiator was more than 90% attenuated by the leaf itself, i.e. the leaf is considered infinitely thick for these two elements. Therefore, the emission-transmission method was applicable only to K, Ca, Mn, Fe, Cu and Zn.

The trueness checking of the pXRF ET method and conventional ICP OES were accomplished through the analysis of the NIST SRM 1547. No significant differences between Mn, Fe, and Zn certified concentrations and the results obtained by pXRF were found by applying the Student's t-test at 95% confidence level. For pXRF, it was not possible to check the method for K and Ca because the pellet, even using a mass of just 50 mg, is considered as infinitely thick sample for these two elements.

Figure 10 compares the quantitative results obtained by pXRF against those from ICP OES. Figure 10A shows the pXRF measured concentrations for leaves under *vivo* conditions and 10B for dried leaves of plants fed with regular nutrient solution. Figure 10C presents the data for leaves under *vivo* conditions and 10D for dried leaves treated with 10-fold strengthen nutrient solution. Except to Figure 10D, the highest correlation coefficients were found for macronutrients.

Figure 10. Comparison of the K, Ca, Mn, Fe, Cu and Zn content in soybean leaves by portable XRF equipment and ICP OES. (A) Fresh leaves analysed directly by portable XRF under regular concentration of Hoagland's nutritive solution. (B) Dried leaves analysed directly by portable XRF under regular concentration of Hoagland's nutritive solution. (C) Fresh leaves analysed directly by portable XRF under 10-fold strengthen concentration of Hoagland's nutritive solution. (D) Dried leaves analysed directly by portable XRF under 10-fold strengthen concentration of Hoagland's nutritive solution

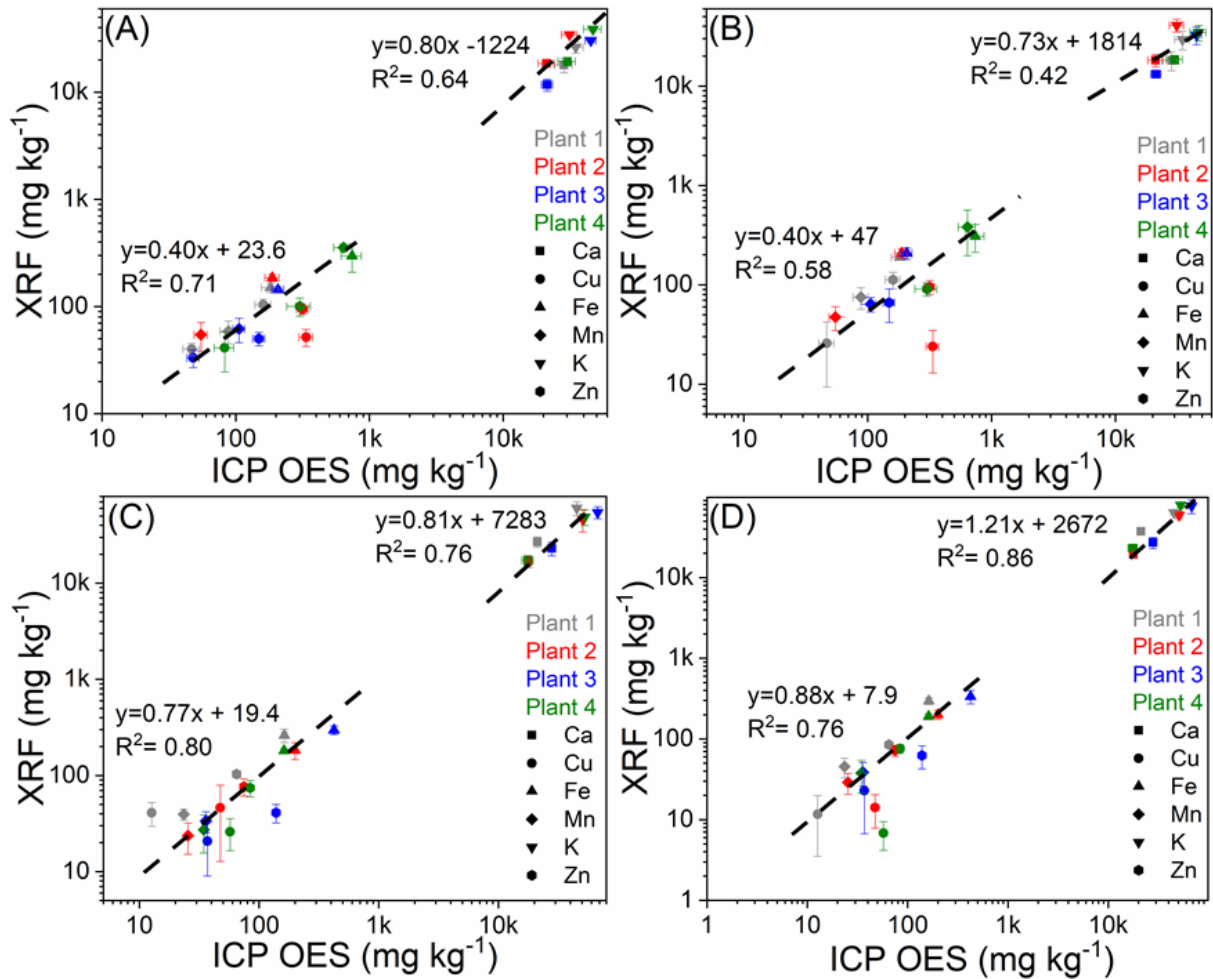


Figure 10 also shows that plants exposed to the 10-fold strengthen Hoagland solution presented higher correlation coefficients between concentration determined by pXRF and ICP OES. The higher concentration of the elements in the plant tissue facilitated the detection by pXRF and improved the correlation with ICP OES.

Another observed trend regards the curve slopes presented in Figure 10. Since the slopes are below 1, the method developed for pXRF underestimated the values of the elements compared to ICP OES. Nevertheless, the values are in the same order of magnitude. This offset might have been caused by the heterogeneity in the distribution of the elements along the leaves. Figure 7 showed that nutrient concentration was not homogenous. The highest spots were found in the leaf veins, especially in the central one. The pXRF sampling (shown in Figure 1B) did not probe these hotspots. On the other hand, the concentration determined by the ICP OES represents an average of the whole trefoil. For the sake of clarity, the data used to plot Figure 10 are also presented in Tables 4-7.

Table 4. Concentration of K, Ca, Mn, Fe, Cu and Zn in soybean leaves by pXRF equipment and ICP OES. Soybean plants cultivated under normal concentration of Hoagland's nutritive solution. Fresh leaves analysed directly by the pXRF

Sample	Technique	Element					
		K	Ca	Mn	Fe	Cu	Zn
		g kg ⁻¹		mg kg ⁻¹			
Plant 1	pXRF	26 ± 3	18 ± 3	59 ± 14	150 ± 15	40 ± 5	104 ± 13
	ICP OES	35 ± 5	28 ± 4	88 ± 12	180 ± 30	47 ± 7	160 ± 20
Plant 2	pXRF	34.3 ± 1.6	18.6 ± 1.6	55 ± 16	186 ± 14	52 ± 9	95 ± 10
	ICP OES	31 ± 4	21 ± 3	55 ± 6	190 ± 20	340 ± 40	316 ± 30
Plant 3	pXRF	30.4 ± 1.4	11.7 ± 1.5	62 ± 16	144 ± 8	33 ± 6	50 ± 7
	ICP OES	45 ± 4	21 ± 2	106 ± 11	210 ± 20	48 ± 5	149 ± 15
Plant 4	pXRF	38.7 ± 1.8	19.3 ± 1.7	350 ± 30	300 ± 90	41 ± 17	101 ± 20
	ICP OES	47 ± 7	30 ± 4	640 ± 100	740 ± 130	83 ± 14	301 ± 60

Table 5. Concentration of K, Ca, Mn, Fe, Cu and Zn in soybean leaves by pXRF equipment and ICP OES. Soybean plants cultivated under normal concentration of Hoagland's nutritive solution. Dried leaves analysed directly by the pXRF

Sample	Technique	Element					
		K	Ca	Mn	Fe	Cu	Zn
		g kg ⁻¹		mg kg ⁻¹			
Plant 1	pXRF	29 ± 6	18 ± 4	75 ± 19	189 ± 13	26 ± 16	110 ± 20
	ICP OES	35 ± 5	28 ± 4	88 ± 12	180 ± 30	47 ± 7	160 ± 20
Plant 2	pXRF	41 ± 6	18 ± 3	47 ± 13	210 ± 20	24 ± 11	95 ± 16
	ICP OES	31 ± 4	21 ± 3	55 ± 6	190 ± 20	340 ± 40	320 ± 30
Plant 3	pXRF	33 ± 7	13.2 ± 0.7	64 ± 11	210 ± 30	-----	70 ± 20
	ICP OES	45 ± 4	21 ± 2	106 ± 11	210 ± 20	48 ± 5	149 ± 15
Plant 4	pXRF	35 ± 6	18.5 ± 1.8	380 ± 180	310 ± 100	-----	90 ± 14
	ICP OES	47 ± 7	30 ± 4	640 ± 100	740 ± 130	83 ± 14	300 ± 60

Table 6. Concentration of K, Ca, Mn, Fe, Cu and Zn in soybean leaves by pXRF equipment and ICP OES. Soybean plants cultivated under a concentration 10x higher of Hoagland's nutritive solution. Fresh leaves analysed directly by the pXRF

Sample	Technique	Element					
		K	Ca	Mn	Fe	Cu	Zn
		g kg ⁻¹		mg kg ⁻¹			
Plant 1	pXRF	60 ± 10	27 ± 4	39 ± 5	260 ± 40	41 ± 11	104 ± 9
	ICP OES	45.2 ± 0.3	21.17 ± 0.08	23.5 ± 0.5	163 ± 9	12.7 ± 0.6	65.1 ± 0.8
Plant 2	pXRF	46 ± 12	17 ± 2	24 ± 9	180 ± 40	50 ± 30	77 ± 16
	ICP OES	50.8 ± 0.8	17.8 ± 0.2	25.5 ± 0.7	200 ± 9	47.4 ± 1.1	74.9 ± 1.2
Plant 3	pXRF	55 ± 8	23 ± 4	34 ± 8	300 ± 30	21 ± 12	41 ± 9
	ICP OES	67.6 ± 0.5	27.93 ± 0.09	36.0 ± 0.5	423 ± 10	37.0 ± 0.6	138.9 ± 0.9
Plant 4	pXRF	49 ± 9	17 ± 2	27 ± 12	181 ± 9	26 ± 9	74 ± 14
	ICP OES	53.82 ± 0.19	18 ± 2	34.6 ± 0.5	162 ± 6	57.4 ± 0.6	84.1 ± 0.8

Table 7. Concentration of K, Ca, Mn, Fe, Cu and Zn in soybean leaves by pXRF equipment and ICP OES. Soybean plants cultivated under a concentration 10x higher of Hoagland's nutritive solution. Dried leaves analysed directly by the pXRF

Sample	Technique	Element					
		K	Ca	Mn	Fe	Cu	Zn
		g kg ⁻¹		mg kg ⁻¹			
Plant 1	pXRF	64 ± 4	37 ± 3	45 ± 12	300 ± 30	12 ± 8	85 ± 8
	ICP OES	45.3 ± 0.3	21.17 ± 0.08	23.5 ± 0.5	163 ± 9	12.7 ± 0.6	65.1 ± 0.7
Plant 2	pXRF	59 ± 6	19.4 ± 1.1	29 ± 8	200 ± 30	14 ± 6	72 ± 11
	ICP OES	50.8 ± 0.8	17.8 ± 0.2	25.5 ± 0.7	200 ± 9	47.4 ± 1.1	74.9 ± 1.2
Plant 3	pXRF	77 ± 15	27 ± 4	39 ± 13	340 ± 60	23 ± 16	62 ± 20
	ICP OES	67.6 ± 0.5	27.93 ± 0.09	36.0 ± 0.5	423 ± 10	37.0 ± 0.6	138.9 ± 0.9
Plant 4	pXRF	79 ± 6	23 ± 2	38 ± 17	191 ± 15	7 ± 3	76 ± 10
	ICP OES	52.83 ± 0.19	18 ± 2	34.6 ± 0.5	162 ± 6	57.4 ± 0.6	84.1 ± 0.8

The challenges imposed by the leaf heterogeneity were faced by Guerra et al. (2015) during the analysis of dried sugar cane leaves. In this study the authors have concluded that it is necessary a minimum number of 15 leaf fragments (37.5% of the whole leaf) to make it representative to the whole sample. Likewise, Santos Junior et al. (2012) presented a review regarding the use of LIBS dedicated to analyse plant materials in the form of pressed pellets and they state that even after sampling washing, grinding and homogenizing, it might present differences in the results duo to the heterogeneity of the samples. Such elemental heterogeneity, which is compensated in case of pressed pellets, also explains the standard deviation for the quantitative XRF data expressed in Tables 4-7.

Table 8 presents the limits of detection (LOD) and quantification (LOQ) for ICP OES and portable XRF measurements. As expected, the values found for portable XRF were higher than those for ICP OES. On the other hand, the optimized pXRF instrumental conditions reported in the present study yielded better limits of detection than those previously reported elsewhere (GUERRA et al., 2014). One may notice that the LOD for XRF in fresh leaves was *ca.* 4.5x better than in dried leaves. It is important to highlight that the LOD, considering just the superficial concentration ($\mu\text{g cm}^{-2}$), is better in dried leaves, but when we divide it by the density of the sample, which is *ca.* 7x higher in fresh leaves, the LOD in these samples becomes lower.

Table 8. Limits of detection and quantification by ICP OES and pXRF equipment.

Element	Unit	ICP OES		XRF Fresh leaves		XRF Dried leaves	
		LOD	LOQ	LOD	LOQ	LOD	LOQ
K	g kg ⁻¹	0.02	0.07	0.02	0.08	0.08	0.27
Ca		0.01	0.0138	0.02	0.05	0.06	0.21
Mn	mg kg ⁻¹	0.03	0.08	3.5	12	17	56
Fe		1.1	3.3	2.7	9.0	14	46
Cu		0.14	0.42	1.7	5.7	8.4	28
Zn		0.42	1.3	1.8	6.0	9.1	30

Fertilization recommendation is carried out based on tables that state if the vegetal tissue presents low, adequate or high concentration of a nutrient (Table 9). For example, both pXRF and ICP OES show that the plants demonstrated in Figure 10A and Table 4 present high K, Ca, Fe Cu and Zn and adequate Mn. Therefore, from the fertilization standpoint both techniques are suitable to carrying out this task.

Table 9. Nutrient concentration in soybean leaves adopted in the interpretation of foliar diagnosis results classified as low, intermediate or high (EMBRAPA, 2013)

Level	Element					
	K	Ca	Mn	Fe	Cu	Zn
	g kg ⁻¹		mg kg ⁻¹			
Low	< 17	< 6.8	< 28	< 59	< 6	< 31
Adequate	17-26	6.8-11.8	28-75	59-120	6-11	31-58
High	> 26	> 11.8	> 75	> 120	> 11	> 58

Finally, the overall sample preparation and instrumental time required to access the concentration of K, Ca, Mn, Fe, Cu, and Zn in one plant by pXRF were approximately 3 h and 51 h for fresh and dried leaves, respectively. The time spent in the procedure for ICP OES was about 51 h. The relative short analysis time offered by pXRF represents a step forward to its use in agriculture. However, both time of analysis, LOD and correlation with established techniques must be improved to allow boarding pXRF equipment in agricultural machinery. Additionally, complementary pXRF strategies must be developed to quantify P and S, this issue might be overcome using fundamental parameters or external calibration curves and will be tested in a further study.

References

ABEROUMAND, A. Nutritional evaluation of edible *Portulaca oleracea* as plant food. **Food Analytical Methods**, v. 2, p. 204-207, 2009. DOI 10.1007/s12161-008-9049-9

AWASTHI, S. et al. **Multivariate methods for analysis of environmental reference materials using laser-induced breakdown spectroscopy**. *Analytical Chemistry Research*, v. 12, p. 10–16, 2017.

BACHIEGA, P. et al. Benchtop and handheld energy-dispersive x-ray fluorescence (EDXRF) as alternative for selenium concentration measurement in biofortified broccoli seedling. **Food Analytical Methods**, v. 12, p. 1-8, 2019.

BLONSKI, M. S. et al. Elementary chemical analysis in leaves infected by fumagina by X-ray fluorescence technique. **Brazilian Archives of Biology and Technology**, v. 50, p. 851–860, 2007.

CAMPOS, N. V. et al. Accumulation and spatial distribution of arsenic and phosphorus in the fern *Pityrogramma calomelanos* evaluated by micro X-ray fluorescence spectrometry. *Journal of Analytical Atomic Spectrometry*, v. 30, p. 2375–2383, 2015.

CARVALHO, G. G. A. et al. Direct determination of the nutrient profile in plant materials by femtosecond laser-induced breakdown spectroscopy. *Analytica Chimica Acta*, v. 876, p. 26–38, 2015b.

CARVALHO, G. G. A. et al. Influence of particle size distribution on the analysis of pellets of plant materials by laser-induced breakdown spectroscopy. *Spectrochimica Acta. Part B*, v. 105, p. 130–135, 2015a.

CHUPARINA, E. V.; AISUEVA, T. S. Determination of heavy metal levels in medicinal plant *Hemerocallis minor* Miller by X-ray fluorescence spectrometry. **Environmental Chemistry Letters**, v. 9, p. 19–23, 2011.

CURRIE, L. A. Limits for Qualitative Detection and Quantitative Determination: application to radiochemistry. **Analytical Chemistry**, v. 40, p. 586–593, 1968.

DALY, K.; FENELON, A. Application of energy dispersive X-ray fluorescence spectrometry to the determination of copper, manganese, zinc, and sulfur in grass (*Lolium perenne*) in grazed agricultural systems. **Applied Spectroscopy**, v. 72, p. 1661-1673, 2018.

DEMIR, K. et al. Essential and non-essential element composition of tomato plants fertilized with poultry manure. **Scientia Horticulturae**, v. 127, p. 16–22, 2010.

DURAN, N. M. et al. X-ray spectroscopy uncovering the effects of Cu based nanoparticle concentration and structure on *Phaseolus vulgaris* germination and seedling development. **Journal of Agricultural and Food Chemistry**, v. 65, p. 7874-7884, 2017.

EL-DEFTAR, M. M. et al. Evaluation of elemental profiling methods, including laser-induced breakdown spectroscopy (LIBS), for the differentiation of Cannabis plant material grown in different nutrient solutions. **Forensic Science International**, v. 251, p. 95–106, 2015.

EMBRAPA. **Tecnologias de produção de soja**. Região central do Brasil. Londrina: Embrapa Soja, 2013. 226 p. (Sistemas de Produção, 16).

GEBBERS, R.; SCHIRRMANN, M. Potential of using portable x-ray fluorescence spectroscopy for rapid soil analysis. In: STAFFORD, J.(Ed.). **Precision agriculture '15**. Wageningen: Wageningen Academic Publishers, 2015. p. 27-33. Papers presented at the 10th European Conference on Precision Agriculture; 10th European Conference on Precision Agriculture.

GOMES, M. S. et al. A novel strategy for preparing calibration standards for the analysis of plant materials by laser-induced breakdown spectroscopy: a case study with pellets of sugar cane leaves **Spectrochimica Acta. Part B**, v. 86, p. 137–141, 2013.

GONDAL, M. A. et al. Direct spectral analysis of tea samples using 266nm UV pulsed laser-induced breakdown spectroscopy and cross validation of LIBS results with ICP-MS. **Talanta**, v. 152, p. 341–352, 2016.

GUERRA, M. B. B. et al. Evaluation of micro-energy dispersive X-ray fluorescence spectrometry for the analysis of plant materials. **Journal of Analytical Atomic Spectrometry**, v. 28, p. 1096–1101, 2013.

GUERRA, M. B. B. et al. Comparison of analytical performance of benchtop and handheld energy dispersive X-ray fluorescence systems for the direct analysis of plant materials. **Journal of Analytical Atomic Spectrometry**, v. 29, p. 1667–1674, 2014.

GUERRA, M. B. B. et al. Direct analysis of plant leaves by EDXRF and LIBS: microsampling strategies and cross-validation. **Journal of Analytical Atomic Spectrometry**, v. 30, p. 1646-1654, 2015.

GUERRA, M. B. B. et al. In situ determination of K, Ca, S and Si in fresh sugar cane leaves by handheld energy dispersive x-ray fluorescence spectrometry. **Journal of Brazilian Chemical Society**, v. 29, p. 1086-1093, 2018.

HOAGLAND, D. R.; ARNON, D. I. **The water-culture method for growing plants without soil**. Berkeley: California Agricultural Experiment Station, 1950. 32 p. (California Agricultural Experiment Station. Circular, 347).

JENKINS, R. **X-ray fluorescence spectrometry**. 2.ed. New York: Wiley, 1999.

KHRAMOVA, E. P. et al. SR XRF analysis for studying plants in an area of geological heterogeneity. **Surf Investig X-ray, Synchrotron Neutron Techniques**, v. 6, p. 454–457, 2012.

KHUDER, A. et al. Determination of trace elements in Syrian medicinal plants and their infusions by energy dispersive X-ray fluorescence and total reflection X-ray fluorescence spectrometry. **Spectrochimica Acta. Part B**, v. 64, p. 721–725, 2009.

LEROUX, J.; MAHMUD, M. X-ray quantitative analysis by an emission-transmission method. **Analytical Chemistry**, v. 38, p. 76-82, 1966.

LUNDEGARDH, H. Leaf analysis as a guide to soil fertility. **Nature**, v. 151, p. 310–311, 1943.

MCLAREN, T. I. et al. Rapid, nondestructive total elemental analysis of vertisol soils using portable x-ray fluorescence. **Soil Science Society of America Journal**, v. 76, p. 1436-1445, 2012.

MCLAREN, T. I.; GUPPY, C. N.; TIGHE, M. K. A rapid and nondestructive plant nutrient analysis using portable x-ray fluorescence. **Soil Science Society of America Journal**, v. 76, p. 1446–1453, 2012.

MELQUIADES, F. L. et al. Direct determination of sugar cane quality parameters by x-ray spectrometry and multivariate analysis. **Journal of Agricultural and Food Chemistry**, v. 60, p. 10755-10761, 2012.

NAYAK, P. et al. ED-XRF spectrometry-based comparative inorganic profile of leaf-derived in vitro calli and in vivo leaf samples of *Phyllanthus amarus* Schum. & Thonn. - a hepatoprotective herb. **Applied Radiation Isotopes**, v. 69, p. 567–573, 2011.

OLIVEIRA, S. R.; RAPOSO, J. L.; GOMES NETO, J. A. Fast sequential multi-element determination of Ca, Mg, K, Cu, Fe, Mn and Zn for foliar diagnosis using high-resolution continuum source flame atomic absorption spectrometry: feasibility of secondary lines, side pixel registration and least-squares background. **Spectrochimica Acta. Part B**, v. 64, p. 593–596, 2009.

SANTOS JUNIOR, D. et al. Laser-induced breakdown spectroscopy for analysis of plant materials: a review. **Spectrochimica Acta. Part B**, v. 71-72, p. 3-13, 2012.

SOUZA, P. F. et al. Determination of silicon in plant materials by laser-induced breakdown spectroscopy. **Spectrochimica Acta. Part B**, v. 83, p. 61–65, 2013.

THOMAS, W. Foliar diagnosis: principles and practice. **Plant Physiology**, v. 12, p. 571–599, 1937.

TOWETT, E. K.; SHEPHERD, K. D.; LEE, D. B. Plant elemental composition and portable x-ray fluorescence (pXRF) spectroscopy: quantification under different analytical parameters. **X-Ray Spectrometry**, v. 45, p. 117–124, 2016.

WEST, M. T. et al. 2017 atomic spectrometry update – a review of advances in X-ray fluorescence spectrometry and its special applications. **Journal of Analytical Atomic Spectrometry**, v. 32, p. 1629-1649, 2017.

3 FOLIAR UPTAKE OF NANO COPPER OXIDE IN SOYBEAN PLANTS

Abstract

Copper (Cu) is an essential element for soybean development. Among the different sources of copper supplementation, the Cu nanoparticles seem to be an innovative approach with a wide range of plant benefits that varies from plant defense until lignin development. Herein, we did a chemical, physiological and morphological study in order to evaluate if Cu nanoparticles can present an improvement in copper uptake compared to a soluble source, such as CuSO_4 . At first, we characterized the Cu nanoparticles that showed spherical and irregular forms. Nano CuO is absorbed by soybean leaves and redistributed to other leaves, although, how the particles penetrate the cells is still unknown. Shoot dry matter of plants was positively affected by the treatments, especially by the 40 nm nCuO. The copper speciation showed that the CuO applied is transformed from Cu^{1+} to Cu^{2+} 14 days after application. When deposited on the soybean trefoil limbo it was observed that the soluble sources can promote damage to the leaf surface. On the other hand, Cu NPs, can cause epicuticular wax dissolution.

Keywords: nanomaterials, copper oxide, mineral nutrition, foliar uptake, epicuticular wax.

3.1 Introduction

Fertilizers correspond to approximately 28% of the total cost production of soybean culture in Brazil (CONAB, 2016). In 2016, it is estimated that the fertilizer industry profited US\$ 1.5 billion, corresponding to 0.4% of Brazilian agribusiness. Foliar fertilizers correspond to 70% of this total amount (ABISOLO, 2017).

Of the total copper applied to the plants 10 g ton^{-1} are exported to the grains (EMBRAPA, 2013). Copper content in soybean leaves ranges from 10 to 30 mg kg^{-1} (VITTI; TREVISAN, 2000).

Copper plays important roles in higher plants. It participates in the structure of proteins, constituent of enzymes, participates in physiological processes such as electron flux in the light phase and the activation of ribulose diphosphate carboxylase in the dark phase of photosynthesis, respiration, hormonal regulation, indirect effect of biological nitrogen fixation and metabolism of secondary compounds. Besides these functions, copper has an important role in disease resistance, pollen grain structure and uniform grain maturation (MALAVOLTA, 2006; BROADLEY et al., 2011).

Usually, the main sources of micronutrients are made from inorganic products (oxides, carbonates and metallic salts as sulphates, chlorides and nitrates), chelates, fritted trace elements (FTE) and organic complexes (MORTVEDT, 2001; LOPES, 1999). According to Malavolta et al. (2000), the most common fertilizers containing copper are copper sulphate (13% of copper), copper dichloride (16%), cupric oxide (75%), cuprous oxide (89%), ammonia cupric phosphate (32%), copper nitrate (22%) and copper carbonate (48%). For foliar application, copper sulphate, Na₂Cu EDTA and NaCu HEDTA are the most used (VITTI; TREVIZAN, 2000).

The adoption of nanomaterials in agricultural science has been increasing with the constantly growing population and the demand for higher agricultural yields is needed (IAVICOLI et al., 2017). At the same time, the use of nanotechnology in agriculture and other areas continue to raise doubts and concern over possible human and environmental health problems (KAH, 2015). As possible beneficial uses can be highlighted nanofertilizers, nanopesticides, sensing devices, water and soil remediation and crop coating (IAVICOLI et al., 2017). On the contrary, nanoparticles impact organisms because of their potential to transfer across environmental species and bioaccumulate in species at the top of food chains (NASROLLAHZADEH; SAJADI, 2019).

According to Wang et al. (2016) nanoparticles entrance in plant tissues occurs through either the root tissues or the aboveground organs and tissues (e.g., cuticles, trichomes, stomata, stigma, and hydathodes), including through wounds and root junctions. Even with the occurrence size exclusion limits of a series of barriers (e.g. cell walls, Casparian strip, plasmodesmata), the entrance of nanoparticles in cells is effective. A possible explanation is that size exclusion limits seem to be dynamic and influenced by calcium, silicon, proteins, virus, environmental stresses and by the nanoparticles themselves.

The use of copper nanoparticles in plants has already been reported for seeds (ADHKARI et al., 2012; ATHA et al., 2012; DURAN et al., 2017; DA COSTA; SHARMA, 2016; NAIR; CHUNG, 2014a; 2014b; 2015; PERREAULT; POPOVIC; DEWEZ, 2014; RAJPUT et al., 2018) and roots (EBBS et al., 2016). Giannousi, Avramidis and Dendrinou-Samara (2013) has applied nano CuO in leaves of tomatoes but testing it as an agrochemical against *Phytophthora infestans*.

Adhkari et al. (2012) relate that with increasing concentration of NPs, the elongation of the roots was severely inhibited as compared to that in control and in many cases root necrosis occurred. Duran et al. (2017) state that the nanoparticles did not affect seed germination, but seedling weight gain was promoted by 100 mg Cu L⁻¹ and inhibited by 1,000 mg Cu L⁻¹

of 25 nm CuO and CuSO₄. Similar results were obtained by Nair and Chung (2014a) and the authors report that application of 500 mg L⁻¹ of CuO NPs significantly reduced the shoot growth, weight, and total chlorophyll content. However, the root length and fresh weights were significantly reduced at all concentrations of CuO NPs application on soybean.

Alike the cited authors, Rajput et al. (2018) concluded that the CuO NPs inhibited barley growth by affecting the germination rate, root and shoot lengths, affected stomatal aperture and root morphology. Furthermore, the Cu content of roots and leaves of CuO NPs treated plants was 5.7 and 6.4-folds higher than the control (without CuO NPs), respectively. In contrast, Giannousi, Avramidis and Dendrinou-Samara (2013) concluded that CuO NPs are more effective than the trade agrochemicals. Moreover, assessments regarding phytotoxicity indicated that they can be used without any deleterious effect on plants.

In view of all the discussion and uncertainties regarding the use of nano CuO as fertilizers, the aim of this study is to demonstrate the possible benefits of copper nanomaterials as foliar fertilizer.

3.2 Materials and Methods

3.2.1 Nanomaterials characterization. Purity. 25 and 40 nm CuO nanoparticles were acquired from US Nanomaterials Research Inc (USA). The powder samples (200 mg) were weighted in a 6.3 mm aperture X-ray sample cup (no. 3577 - Spex Ind. Inc., USA) and sealed with a 5 µm thick polypropylene film (no. 3520 - Spex Ind. Inc., USA). The analysis were conducted under vacuum, in triplicate, using a rhodium (Rh) X-ray tube at 50 kV and auto-tunable current adjusted for a detector deadtime below 30% and a 3-mm collimator. The X-ray spectrum of the sample was acquired utilizing a Si (Li) detector for 300 s and through the fundamental parameters method it was possible to determinate contaminants content present in these nanomaterials.

3.2.2 Structural characterization. X-ray diffraction (XRD) was used to confirm the majority composition of the CuO nanoparticles. The X-ray diffraction measurements were obtained in a Bruker D2 Phaser instrument, operating with Cu K α ($\lambda=1.5418$ Å) radiation, 30 kV, 10 mA, sample holder rotation of 15 rpm and Lynxeye[®] energy dispersive one-dimensional detector with 192 channels. The diffractograms were acquired under the following conditions: continuous scanning mode in the 2 θ range from 10 to 90°, step = 0.02° and acquisition time = 0.5 s, obtained from the sample powders.

Through the diffractograms it was possible to estimate the crystallite sizes using the Scherrer equation (Equation 1) for different planes.

$$D(hkl) = K\lambda / \beta \cos\theta \quad (\text{Equation 1})$$

where:

K: Scherrer's constant (0.94 for spherical crystals);

λ : wavelength referring to the X-ray source (0.154184 nm for Cu);

β : Full width at half maximum of the peak;

θ : measured angle in degree.

3.2.3 Physicochemical features of dispersions. Dispersions in distilled water of the nanomaterials (100 mg L^{-1}) were prepared to determine the aggregates' sizes by dynamic light scattering (DLS) and its charge by zeta potential using a Zetasizer equipment (Malvern, UK). The pH/conductivity of the dispersions were determined by a handheld pH meter, model SevenGo Duo SG23 (Mettler Toledo, USA).

3.2.4 Nano CuO morphology. CuO nanoparticles with different sizes were used. The nanoparticles dispersions were prepared using 5 mg of the nanoparticles diluted in deionized water. Then, the nanoparticles dispersions were sonicated (Fisher Scientific). After the sonication, 20 μl of the dispersion were deposited on the Parafilm[®] film and the copper grids (300 mesh) carbon-coated were deposited on the CuO nanoparticle dispersion for five minutes. The excess of the dispersion was removed with a filter paper. The morphology of the nanoparticles was evaluated by transmission electron microscopy (JEM 1011, JEOL, Japan) in dispersions of 100 mg L^{-1} . The images were analysed by the software ImageJ[®]. Approximately 60-70 particles were measured and a histogram of distribution was created in the software Origin[®].

3.2.5 Soybean cultivation. The experiment was conducted in a greenhouse of the Soil Science Department at Luiz de Queiroz Superior School of Agriculture (ESALQ/USP). The soil used in the experiment was a sandy soil, with low content of Cu (0.2 mg dm^{-3}). The base saturation (BS) was raised for 60% through liming according to the base saturation method. The soil was collected in the municipality of São Pedro/SP, analysed before and after the experiment, and its physicochemical properties are shown in Table 1.

Table 1. Physicochemical properties of the soil collected in the municipality of São Pedro/SP, before and after the assembly of the experiment

Determination	Unit	Before	After
		Value	
Sand		858	858
Silt	g kg^{-1}	17	17
Clay		125	125
pH CaCl_2		4.1	5.4
O.M. - Walkley	g dm^{-3}	10	< 5.0
H + Al		18	12
K	$\text{mmol}_c \text{ dm}^{-3}$	0.2	1.7
Ca		1	9
Mg		1	5
P		2	18
B		0.07	< 0.15
Cu	mg dm^{-3}	0.2	< 0.1
Fe		8	6
Mn		1.3	1.4
Zn		0.3	0.3
SB	$\text{mmol}_c \text{ dm}^{-3}$	2.2	15.7
CEC		20.2	27.7
BS	%	11	59

SB: sum of bases; CEC: cation-exchange capacity; BS: base saturation.

Four seeds of soybean, cultivar KWS RK 7214 IPRO, were sown per pot. The exceeding seedlings were removed, leaving two plants per pot. Each pot of 2.5 L was filled with two kg of soil, daily irrigated with enough deionized water to keep the soil close to its field capacity.

3.2.6 Copper solutions. Copper sulphate solutions, in the same concentrations of the nanomaterials were used for comparison. The experiment was assembled under a completely randomized design with three repetitions. Control treatments consisted of three pots with two plants in each, that only deionized water was applied to the leaves, and three pots with two plants in each, that a solution of deionized water + dispersant (5%) was applied to the leaves.

The application of all treatments was made in the first 3 trefoils through aspersion when the plants were in V3 stage. Before application, the soil was covered in order to not be contaminated by droplets of the spray. The dispersant used was the polyethylene glycol (PEG) with a molecular weight = 15,000 – 20,000 g mol⁻¹ from Sigma-Aldrich®. The nanoparticles were dispersed in deionized water and in aqueous dispersions containing the dispersant (5%). The factors and levels of the treatments are shown in Table 2.

Table 2. Factors and levels of the treatments applied

Factors	Levels			
Particle size	25 nm nCuO	40 nm nCuO	Micrometric CuO	CuSO ₄ ·5H ₂ O
Dispersant (PEG)	With	Without		
Dose	0 mg plant ⁻¹	0.75 mg plant ⁻¹	7.50 mg plant ⁻¹	

In total there were 54 pots, which come from the following combination of factors and levels:

- 4 (particle size) x 2 (dispersant) x 2 (dose) x 3 (repetitions) + 6 (control)

The doses were chosen based on the commercial recommended dose (0.75 mg plant⁻¹) and 10 times higher (7.5 mg plant⁻¹), plus control (0 mg plant⁻¹).

For the analysis, one plant was collected 21 days (V7/V8 stage) after the application of the treatments and the other plant, 45 days (R4/R5 stage) after the application. The responses studied were: shoot dry mass (trefoils which have not received the treatments), copper concentration and accumulation.

After harvesting, the plants were divided in sets of leaves (until the third trefoil and the fourth trefoil onwards), the material was identified, placed in paper bags and oven-dried at 65° C for 72 hours. Afterwards, each set of leaves was weighed and the samples grinded in Willey type knife mill (1 mm mesh).

3.2.7 ICP OES analysis. After grinding, the plant material was weighed (*ca.* 200 mg) and subsequently digested by microwave-assisted acid digestion in closed TFM[®] vessels (Provecto Analytica DGT 100 plus), containing 6.0 mL of 20% v v⁻¹ HNO₃ and 2.0 mL of 30% w w⁻¹ H₂O₂. The following microwave heating program was selected: a) 7 minutes at 400 W; b) 15 minutes at 850 W; c) 7 minutes at 320 W and; d) 2 minutes at 0 W. The digested material was diluted to 25 ml and analysed using the ICP OES spectrometer (iCap 7400 Duo optical emission spectrometer, Thermo Scientific, Waltham, MA, USA). The analysis conditions of the ICP OES are presented in Table 3. For trueness checking, the standard reference material NIST 1547 Peach leaves was analysed.

Table 3. Characteristics and operational conditions of the analysis carried out in ICP OES (iCap 7400 Duo optical emission spectrometer, Thermo Scientific, Waltham, MA, USA)

Characteristics	Operational Conditions
View	Radial
Detector	Wavelength range: 166-847 nm
<i>Operational parameters</i>	
Exposure time	10 s
RF power	1.2kW
Plasma gas-flow rate	12 L min ⁻¹
Auxiliary gas-flow rate	0.5 L min ⁻¹
Nebulizer gas-flow rate	0.6 L min ⁻¹
Emission line	Cu 324.754 nm

3.2.8 Chemical speciation analysis. Another set of vases containing two plants in each vase were cultivated to receive the following particle sizes: 25nm nCuO, micrometric CuO and copper sulphate. The dispersions and solution of these particles' sizes were prepared in the highest concentration (7.50 mg plant⁻¹) and without dispersant. Each treatment was applied using 2 repetitions and the dispersions were sprayed on the leaves 1 and 14 days before analysis.

The analyses for determining copper speciation were accomplished using microprobe X-ray absorption near-edge structure (μ -XANES) at the D09B-XRF beamline at the Brazilian Synchrotron Light Laboratory (LNLS, Campinas, Brazil). At XRF beamline, synchrotron radiation was generated by a bending-magnet and collimated by slits. The monochromatic beam was produced by a Si (111) crystal and a KB mirror system was used to focus it to the 20 μm diameter spot size. The μ -XANES was recorded in fluorescence mode using a silicon drift detector (SDD; AXAS-A, KETEK GmbH, Germany). The energy was calibrated utilizing a reference Cu foil.

3.2.9 Scanning electron microscopy (SEM). Soybean leaves were sprayed with different treatments and harvested after 14 days. Then, pictures of the leaves' surfaces were taken using a Hirox digital (Hirox, Japan) microscope. Three samples of each treatment were fixed in a Karnovsky solution adjusted to pH 7.2, using phosphate buffer (KARNOVSKY, 1965), dehydrated using a graded cetonic series (10, 30, 50, 70, 90, and 100%), critical point-dried using CO_2 (HORRIDGE; TAMM, 1969), mounted on aluminum stubs using double-sided carbon tape and coated with a 30–40 nm gold film and examined with a scanning electron microscope (Jeol - JSM IT 300) at 15 kV and digitally recorded at a working distance of 15 mm.

3.2.10 Experimental design and statistical analysis. The greenhouse experiment was set under a totally randomized design in a 4 x 2 x 3 + 1 factorial scheme (4 particle sizes, 2 dispersant and 3 concentrations), plus a universal control treatment.

All the experimental analyses were conducted at SAS 9.4. Prior to ANOVA the data was tested to check the variance homogeneity (Levene's test) and normality of residues (Shapiro-Wilk test).

For the ANOVA, the data was analyzed by a factorial scheme 5 x 2, being five sources of copper (control, copper sulphate, 25nm, 40 nm and micrometric copper oxide) and with or without dispersant. Least squares means comparison test adopted for the effects was the Tukey-Kramer Test, with 5% significance.

3.3 Results and Discussion

3.3.1 Nanomaterials characterization. Purity of the nanomaterials is shown in Table 4. Even though 40 nm nCuO presents chromium in its composition (less than 0.05%), both nanomaterials present high purity.

Table 4. Purity and contaminant on the nanomaterials used in the experiment

Nanomaterial	Manufacturer	Purity (%)	Contaminant (mg kg ⁻¹)
			Cr
25 nm nCuO	US Nanomaterials Research Inc.	100%	-
40 nm nCuO	US Nanomaterials Research Inc.	99.958%	418

The XRD diffractograms are shown in Figure 1 and one can observe that the diffraction pattern is different in some peaks for 25 and 40 nm and this characteristic is emphasized by the estimated values (Table 5) for the crystallite sizes of three different planes: 25 nm nCuO (-111, 200/111 e -202) and 40 nm nCuO (110, 002 e 200). For both sizes of the nCuO, different values were estimated in the three planes, indicating that these materials may have different shapes and composition. Data indicates that 40 nm nanoparticles are CuO while 25 nm nanoparticles are a mix of CuO and metallic Cu.

Figure 1. XRD diffractograms of 25 and 40 nm nCuO

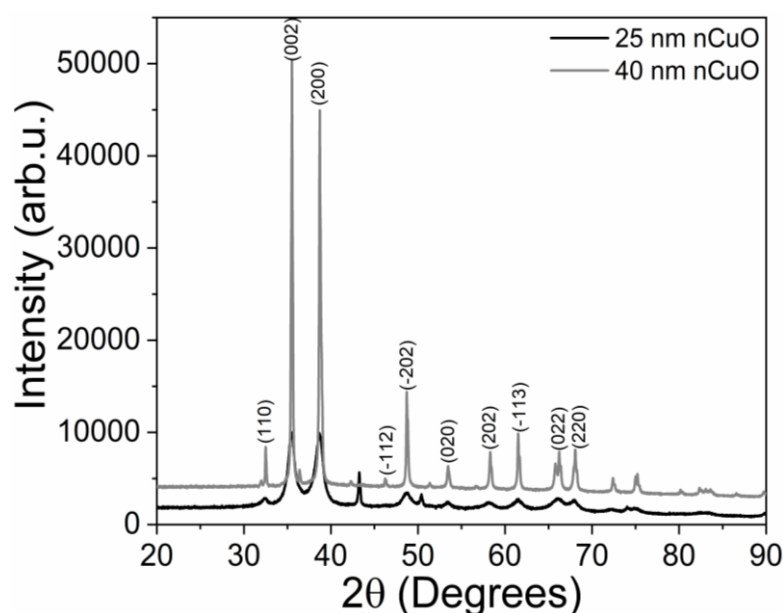
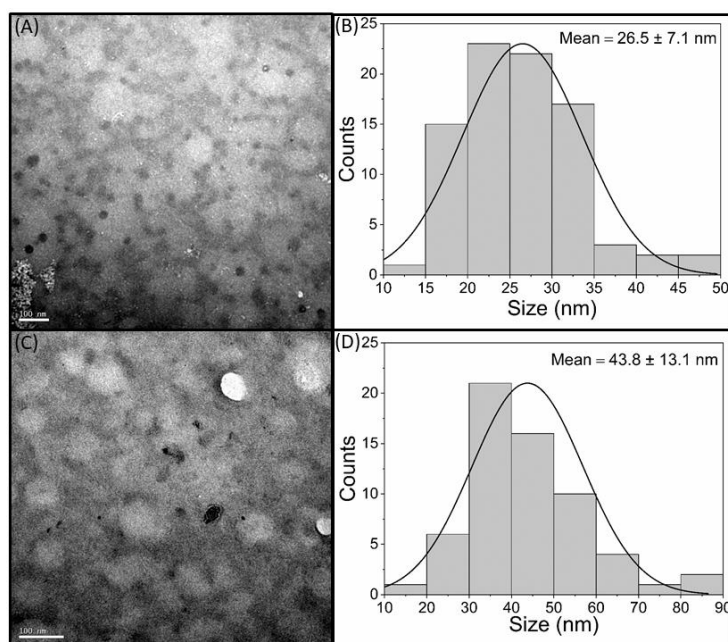


Table 5. Estimated crystallite sizes by Scherrer's equation for nano CuO (25 and 40nm) in different planes

Plane	$D_{(hkl)}$ (nm)	
	25nm nCuO	40nm nCuO
-111	6.0	-----
200/111	5.9	-----
-202	5.0	-----
110	-----	46.0
002	-----	55.4
200	-----	36.6

This information about the nanomaterials' shapes could be confirmed by the images (Figure 2) obtained by transmission electron microscopy (TEM). For 25nm nCuO (Figure 2A) is observed a spherical aspect, while for the 40nm nCuO (Figure 2C) a more elongated aspect is seen. One can notice that both particles present a normal size distribution, as shown in the histograms for 25 nm nCuO (Figure 2B) and 40 nm nCuO (Figure 2D).

Figure 2. TEM images of (A) 25nm nCuO and (C) 40nm nCuO and their respective histograms (B and D). Scale bar: 100 nm



Regarding the DLS values and Zeta potential (Table 6), 25 nm nCuO presents 2 peaks, with a main aggregates' size of 428 nm and positive charge while the 40 nm nCuO presents aggregates of 180 nm and negative charge.

Table 6. Zeta potential and Dynamic Light Scattering of CuO nanoparticles

Nanomaterial	Zeta Potential (mV)	Dynamic Light Scattering (Cluster diameter – nm)	
		Peak 1	Peak 2
25nm nCuO	75.6 ± 5.14	428 (98 %)	5477 (2%)
40 nm nCuO	-7.07 ± 6.22	180 (100 %)	-----

The pH values and conductivity of the dispersions used in the experiment are presented in Table 7. For pH, the data ranged from acid values (4.56) to alkaline values (7.50). Except to the copper sulphate, the treatments in which the dispersant was applied presented a higher value of pH when compared to the ones without dispersant. The same situation is observed for the conductivity. Treatments with dispersant had higher values than treatments without dispersant, in exception to the solutions of copper sulphate.

Table 7. Ph and conductivity of the treatments used in the experiment

Particle Size	Dispersant	Concentration (mg plant ⁻¹)	pH	Conductivity ($\mu\text{S cm}^{-1}$)
25 nm	With	0.75	7.31	95.3
	With	7.5	7.50	93.6
	Without	0.75	6.59	27.8
	Without	7.5	6.54	31.0
40 nm	With	0.75	7.20	88.3
	With	7.5	7.16	89.5
	Without	0.75	6.59	30.8
	Without	7.5	6.47	26.3
Micrometric CuO	With	0.75	7.20	88.4
	With	7.5	7.17	91.1
	Without	0.75	6.45	30.4
	Without	7.5	6.51	18.23
Copper sulphate	With	0.75	5.20	173.0
	With	7.5	4.56	102.1
	Without	0.75	5.61	163.1
	Without	7.5	5.18	1155
Control	With	0	7.22	85.0
	Without	0	6.94	18.82

3.3.2 Effect of CuO nanoparticles on the soybean leaf. Figure 3 shows the digital microscopy analysis of the control leaf (Figures 3A and 3B) and the foliar injuries caused by the application of 25 nm nCuO (Figures 3C and 3D), micrometric CuO (Figures 3E and 3F), copper sulphate (Figures 3G and 3H). Comparing the treatments, we observed that all of them accumulate mainly on the vein surface (Figure 3 C-F and 3G). The nCuO forms a dark precipitate (Figure 3C), while the micrometric CuO does not show any color difference (Figure 3E) and in the CuSO₄ treated leaves it was possible to observe that the veins are black and, in some regions, there is whitish appearance (arrows in Figure 3G). Leaves treated with CuSO₄ presented curly symptom, that differs from the other treatments (Figure 3H) and can present whitish appearance between the leaf veins (arrow in 3H).

Figure 3. Digital microscopy photos of *Glycine max* (L.) Merrill plants exposed to different CuO dispersions and CuSO₄: A, C, E, G: 2D images. B, D, F, H: 3D images. Injuries caused by foliar application of 25 nm nCuO (C and D), micrometric CuO (E and F), copper sulphate (G and H), against the control leaf (A and B) seen on a Hirox KH-8700 model digital microscope. Photos taken 14 days after foliar application.

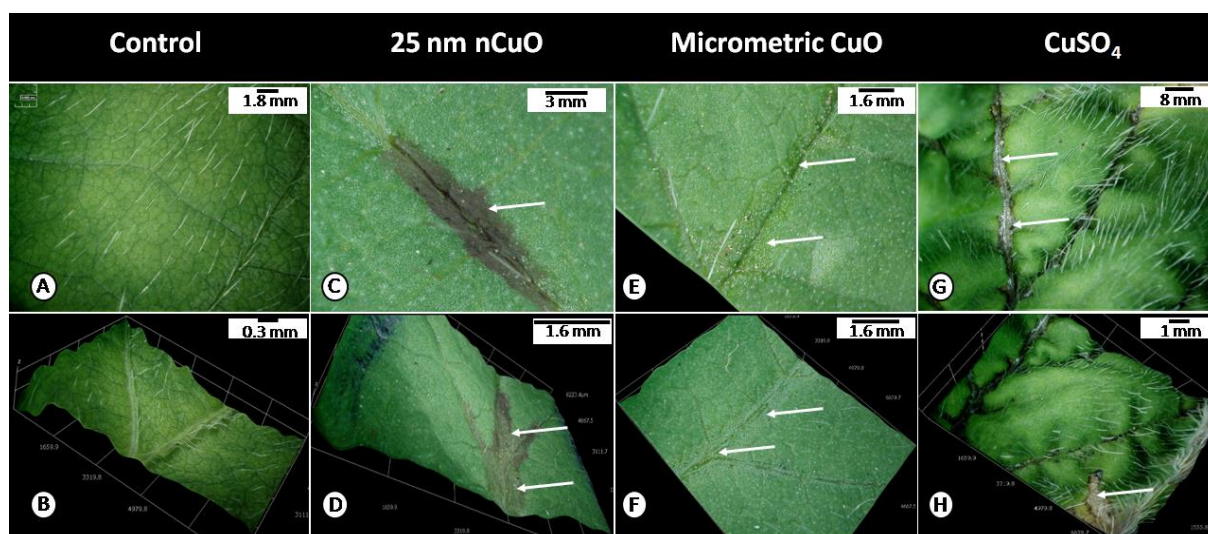
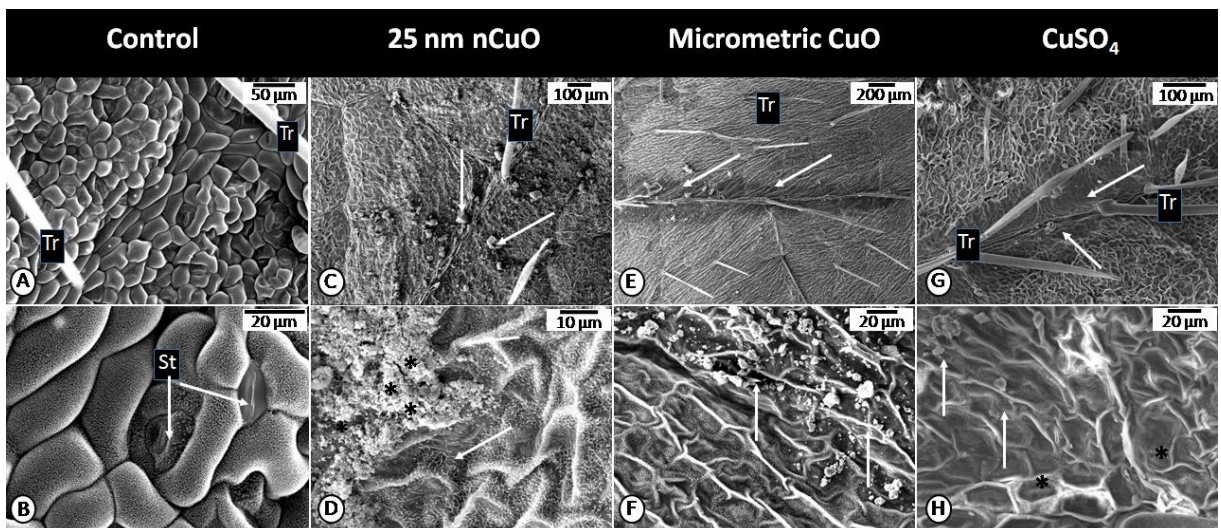


Figure 4 shows the ultrastructural details of the leaves presented in Figure 3. In the control plants, the soybean leaf epidermis is composed by turgid cells covered by epicuticular wax platelets (Figure 4A and 4B). This cuticle pattern agrees with previous works (FENGSHAN et al., 2004; HAGEDORN et al., 2017). Under the scanning electron microscopy, we observed that CuO nanoparticles can form aggregates (Figure 4C and 4D).

On the other hand, no aggregate was observed with micrometric CuO (Figure 4E and 4F) and CuSO₄ (Figure 4G and 4H) treatments. When observed in detail, we noticed that all treatments showed absence or scarce presence of platelets crystals in the region in contact with the CuO nano- and microparticles. It seems that the wax crystals melt down when in contact with Cu NPs.

Figure 4. Scanning electron micrographies of *Glycine max* (L.) Merrill plants exposed to different CuO dispersions and CuSO₄. A, C, E, G: Overview. B, D, F, H: 3D details. A/B: Control. C/D: Lesions induced by 25 nm nCuO dispersion. Note the deposition of nCuO(*) and the absence of epicuticular wax crystals (arrows). E: Changes on the vein region (arrows). F: CuO crystals (arrows). G/H: CuSO₄ induces severe damage on the vein (arrows in G) and the absence of epicuticular wax (*). Tr: Trichomes; St: Stomata. Images taken 14 days after foliar application.



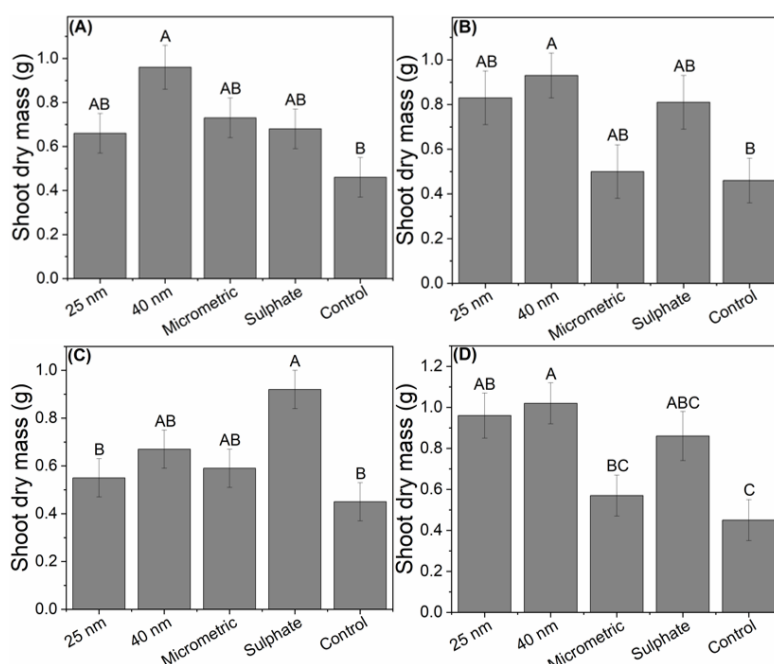
Dappe et al. (2019) have reported the effects of CuO NPs in cabbage. Seeds were germinated in trays and kept in greenhouse for 2 months. One mg of CuO NPs per plant was deposited on the adaxial surface of the 3 higher leaves and plants were harvested 5, 10 and 15 days after application. Dappe et al. (2019), Rajput et al. (2018) and Xiong et al. (2017) results agree to our study. Alike what was observed and shown in Figure 4, the authors report that the nanoparticles cause structural changes in the stomata and reduction of the epicuticular waxes.

3.3.3 Effects of nCuO on plant biometrics and Cu translocation. Washing the leaves is a common practice prior to quantification of nutrient absorption or chemical speciation (XIE et al., 2019; LARUE et al., 2014a). This procedure aims at removing the target nanoparticles, or fertilizers, from the leaf surface leaving only the nutrients that were absorbed. However, XRF images (LARUE et al., 2014a) and SEM (LARUE et al., 2014b) showed that even after washing, TiO₂ and Ag nanoparticles remained on top of the epidermis of lettuce. Hence, in the present study, we decided to determine the copper content in the leaves that appeared after the spraying.

The dispersant did not affect the biomass production at 21 days. However, for treatments applied at 7.5 mg plant⁻¹, the dispersant increased biomass production at 45 days. This suggests that the dispersant eased the copper uptake.

As presented in Figure 5, the copper increased biomass production at 21 and 45 days.

Figure 5. Shoot dry mass of soybean plants treated with 0.75 (A/C) and 7.5 mg Cu plant⁻¹ (B/D). The plants were harvested 21 (A/B) and 45 days (C/D) after application.



*Means with the same letter within each figure do not differ statistically.

At 21 days, for treatments applied at 0.75 mg plant⁻¹, the 40 nm CuO yielded the highest biomass production (0.96 g), while the other copper sources were statically equal and the negative control presented the lowest biomass (0.46 g). However, at 45 days copper sulphate presented the highest biomass yield (0.93 g) followed by 40 nm nCuO = micrometric > 25 nm nCuO = negative control.

For treatments applied at $7.5 \text{ mg plant}^{-1}$ all sources influenced biomass production at 21 and 45 days. In both periods 40 nm nCuO resulted in higher biomass, 0.93 g and 1.02 g for 21 and 45 days, respectively. For the negative control the biomass values were 0.46 g and 0.45 g for 21 and 45 days, respectively. Copper sulphate and micrometric CuO, which are usually employed as fertilizers, produced 0.86 g and 0.57 g at 45 days, respectively.

Some studies agree to the results presented here. Even using lower doses, in 2016, Juarez-Maldonado et al., verified that tomato nCu-chitosan hidrogels-treated presented an improve in height, stem diameter and dry weight of the shoots treated at 15, 30, 60 and 150 mg L^{-1} .

In the same sense, Cu nanoparticles were able to increase root and shoot biomass when the seeds were primed with CuO NPs at 60 mg L^{-1} and 100 mg L^{-1} (ADHIKARI et al., 2012).

There are few studies in which the nanoparticles were foliar sprayed. Hong et al. (2016) have tested the effects of foliar application of CuO NPs in cucumber and similar to our study the authors have tested the effects of nano application over different harvest times. Plants were grown in containers and they were 3 weeks-old (two true leaves) they were sprayed with nano and bulk CuO at 50, 100 and 200 mg L^{-1} . Two weeks after treatment one plant was harvested and the other was kept for more 48 days, receiving 250 ml of dispersions every three days. At the highest concentration nano CuO impacted cucumber photosynthetic parameters and reduced fruit firmness, along with the 50 mg L^{-1} treatment. In this study the nanoparticles have caused negative effects for the plants.

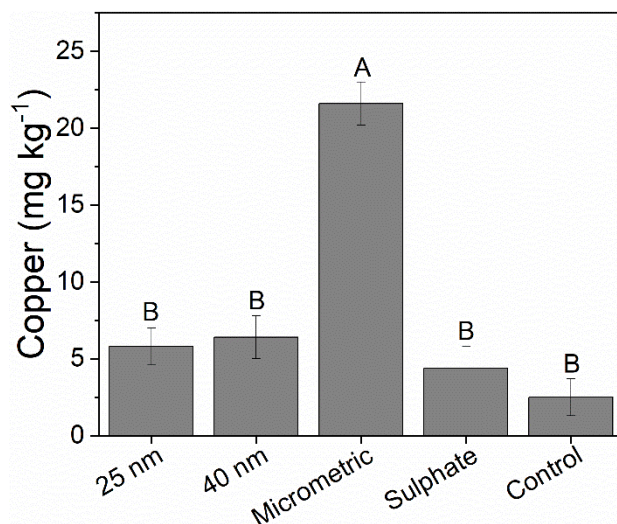
The impacts of CuO NPs in lettuce and cabbage were investigated by Xiong et al. (2017). Dry CuO NPs were deposited on the leaves of three weeks-old plants at 0, 10 and $250 \text{ mg plant}^{-1}$. The plants were analysed 5, 10 and 15 days after application. A high uptake occurred after 15-days application, along with a decrease in plant weight, photosynthesis level, water content and the appearance of necrotic areas near the stomata. Differently from the present study, the authors have applied the nanoparticles using a high concentration, which probably impacted negatively the parameters studied.

At 21 days after application, the dispersant increased copper concentration in plant tissues of plants treated with 0.75 and $7.5 \text{ mg plant}^{-1}$. On the other hand, at 45 days the dispersant decreased copper concentration in plants treated with $0.75 \text{ mg plant}^{-1}$ and did not affect the copper concentration in plants treated with $7.5 \text{ mg plant}^{-1}$.

The sources of copper did not affect the copper concentration in the tissue of plants treated with $0.75 \text{ mg plant}^{-1}$. The concentration of copper found was equal to the negative control. Conversely, the highest copper concentration in tissues was found for plants treated

with $7.5 \text{ mg plant}^{-1}$ of the micrometric source ($21.6 \pm 1.4 \text{ mg kg}^{-1}$). All other sources were statistically equal to the negative control (Figure 6).

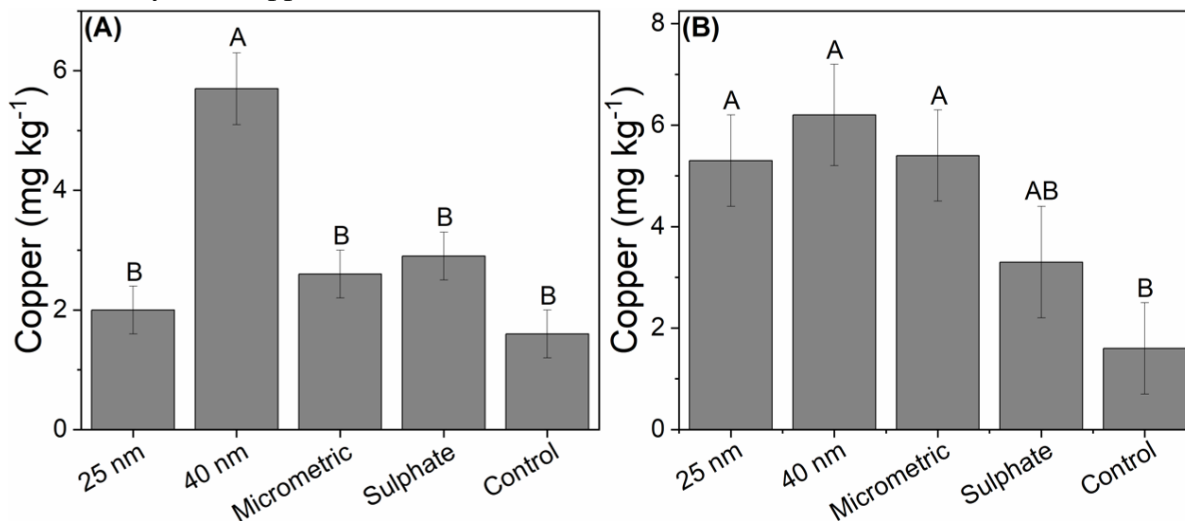
Figure 6. Copper concentration in soybean plants treated with $7.5 \text{ mg Cu plant}^{-1}$ at 21 days after application.



*Means with the same letter do not differ statistically.

Figure 7A shows that at 45 days the plants treated with 40 nm at $0.75 \text{ mg plant}^{-1}$ presented the highest concentration of copper in the tissues ($5.7 \pm 0.6 \text{ mg kg}^{-1}$) and the other sources did not present statistical difference among themselves. The concentration of copper in the tissues of plants treated with $7.5 \text{ mg plant}^{-1}$ (Figure 7B) depended on the source and it varied accordingly $40 \text{ nm} = \text{micrometric} = 25 \text{ nm} > \text{sulphate} > \text{control}$.

Figure 7. Copper concentration in soybean plants treated with 0.75 (A) and $7.5 \text{ mg Cu plant}^{-1}$ (B) at 45 days after application.

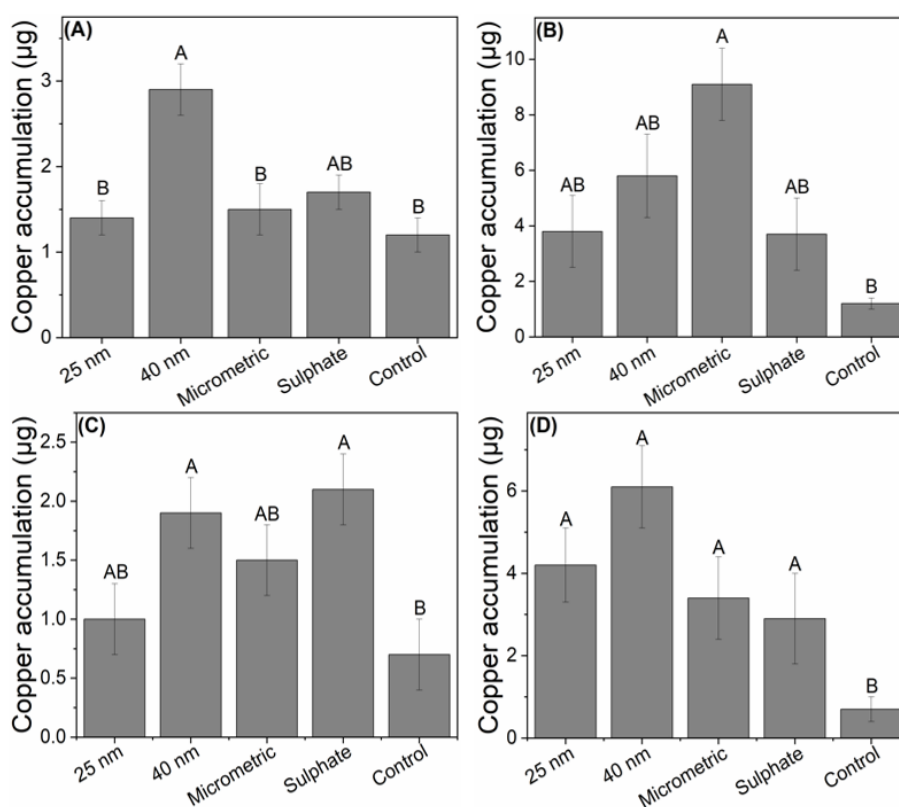


*Means with the same letter within each figure do not differ statistically.

The data regarding copper accumulation in the leaves is presented in Figure 8. Figure 8A shows that the copper accumulation at 21 days plants treated with 0.75 mg plant⁻¹ followed the order 40 nm (2.9 µg) > sulphate (1.7 µg) > micrometric (1.5 µg) = 25 nm (1.4 µg) = negative control (1.2 µg). At 21 days the highest copper accumulation (9.1 ± 1.3 µg) was found in plants treated with micrometric CuO at 7.5 mg plant⁻¹ (Figure 8B). The other sources were statistically equal among themselves but superior to the control. We have to highlight that plants treated with 40 nm nCuO contained 5.8 ± 1.5 µg of copper, while the negative control presented the lowest value (1.20 ± 0.2 µg).

The sources sulphate and 40 nm nCuO at 0.75 mg plant⁻¹ presented the highest accumulation, 2.1 and 1.9 µg, respectively, at 45 days (Figure 8C). However, at 7.5 mg plant⁻¹, copper accumulation was positively affected by all sources (Figure 8D).

Figure 8. Copper accumulation in soybean plants treated with 0.75 (A/C) and 7.5 mg Cu plant⁻¹ (B/D). The plants were harvested 21 (A/B) and 45 days (C/D) after application



*Means with the same letter within each figure do not differ statistically.

Laughton et al. (2019) have applied nano CuO and Cu(OH)₂ at a copper concentration of 790 mg L⁻¹ in leaves of lettuce. The plants were harvested in a 9-days period after application. The authors report that the total copper mass concentration remained the same over the period, however, the time between application and harvest was too short to the plant show any difference. They also report that some leaves were washed and it resulted in the removal of total copper content. Again, in such short time, the products applied did not have enough to penetrate the cuticle of leaves. The results obtained in this study differ from the ones of our study. Plants harvested 21 days after application already showed different values for copper mass concentration (Figure 6), indicating that there was copper penetration and redistribution after this period. Considering what is related by Laughton et al. (2019), the penetration of copper nanoparticles occurs between 9 and 21-days period after application.

The effect of copper foliar application is clearly shown by the treatments supplied at 7.5 mg plant⁻¹. At 21-days the 40 nm CuO source produced the highest biomass. It is worth note that the high copper concentration found for micrometric source was a consequence of the low biomass production of this source.

Plants that received copper foliar application at 7.5 mg plant⁻¹ produced more biomass (Figure 5B and 5D) and accumulated more copper in tissues (Figure 8B and 8D).

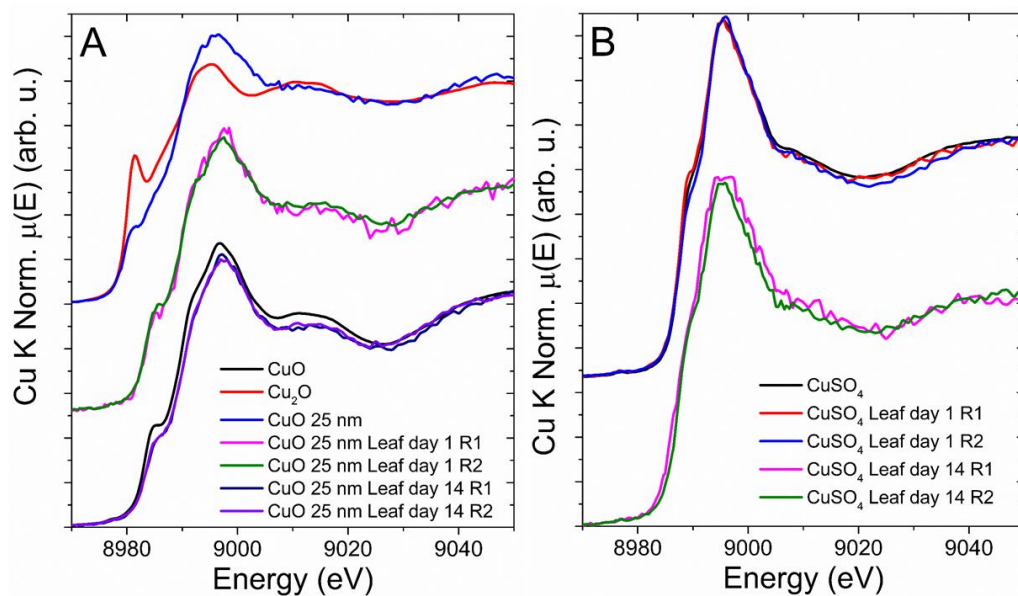
We noticed that past 45 days of treatments application, the copper concentration in the tissues were lower than at 21 days. We believe that it might be related to exportation of copper to grains.

3.3.4 Characterization of CuO NPs deposited on the leaf surface. Figure 9 presents the Cu-K edge XANES spectra recorded for leaves exposed to 25 nm CuO and CuSO₄ (aq) applied to leaves as well as pristine materials. In agreement to XRD patterns (Figure 1), XANES spectra for pristine 25 nm CuO suggests that it is a mixed oxide, it showed a small shoulder at 8983 eV which corresponds to 1s to 4p transition in Cu¹⁺. After one and 14 days of application, the Cu¹⁺ fraction was converted to Cu²⁺. However, it is not possible to state whether this took place inside or outside the leaves.

Since we could not guarantee that copper would be completely removed from the leaf surface, we decided to investigate whether it would undergo transformation regardless being inside or outside the leaf. The presence of Cu²⁺ in plants treated with 25 nm CuO and CuSO₄ is consistent with previous reports (SHI et al., 2008). The authors reported the presence of Cu²⁺ within *Elsholtzia splendens* bound to cell wall and organic species such as histidine,

oxalate, and glutathione. On the other hand, Polette et al. (2000) reported that *Larrea tridentata* accumulated copper as a mixture of Cu^{1+} and Cu^{2+} .

Figure 9. Cu–K edge XANES spectra recorded in soybean leaves treated with 630 mg Cu L^{-1} dispersions. Spectra recorded of the 25 nm nCuO treatment (A) and spectra recorded of the CuSO_4 treatment (B). R1 stands for repetition 1 and R2 stands for repetition 2



3.4 Conclusions

Nanometric copper oxides are capable of supplying this nutrient to plants through foliar spraying. Leaves which were not sprayed with nano CuO presented the nutrient 21 days application application.

The deposition of copper sources on leaves be it copper sulphate or nano CuO, caused damages. All treatments showed an absence or a scarce presence of platelets crystals in the region in contact with the CuO nano- and microparticles.

Shoot dry mass of plants was positively affected by the treatments, especially by the 40 nm nCuO.

Of all the sources studied, the 40 nm nCuO was the one which presented better results of the parameters studied.

The copper speciation showed that the CuO applied is transformed from Cu¹⁺ to Cu²⁺ 14 days after application.

The use of nanoparticles as fertilizers is possible but plant responses to the application vary according to the size of the nanoparticles itself and dose. The use or not of dispersant interfere in the plant responses.

References

ABISOLO. **Anuário brasileiro de tecnologia em nutrição vegetal**. São Paulo, 2017.

ADHIKARI, T. et al. Effect of copper oxide nano particle on seed germination of selected crops. **Journal of Agricultural Science and Technology A**, v. 2, p. 815-823, 2012.

ATHA, D. H. et al. Copper oxide nanoparticle mediated dna damage in terrestrial plant models. **Environmental Science and Technology**, v. 46, 1819–1827, 2012. doi: 10.1021/es202660k.

BROADLEY, M. et al. Function of nutrients: Micronutrients. In: MARSCHNER, P. (Ed.). **Marschner's Mineral Nutrition of Higher Plants**. 3.ed. New York: Academic Press, 2011a. p. 206–211.

COMPANHIA NACIONAL DE ABASTECIMENTO - CONAB. **Compêndio de Estudos Conab** - v. 1. Brasília, DF, 2016.

DA COSTA, M. V. J.; SHARMA, P. K. Effect of copper oxide nanoparticles on growth, morphology, photosynthesis, and antioxidant response in *Oryza sativa*. **Photosynthetica**, v. 54, n. 1, p. 110-119, 2016. doi: 10.1007/s11099-015-0167-5.

DAPPE, V. et al. The role of epicuticular waxes on foliar metal transfer and phytotoxicity in edible vegetables: case of Brassica oleracea species exposed to manufactured particles. **Environmental Science and Pollution Research**, v. 26, p. 20092–20106, 2019.

DURAN, N. M. et al. X-ray spectroscopy uncovering the effects of Cu based nanoparticle concentration and structure on *Phaseolus vulgaris* germination and seedling development. **Journal of Agricultural and Food Chemistry**, v. 65, p. 7874-7884, 2017.

EBBS, S. D. et al. Accumulation of zinc, copper, or cerium in carrot (*Daucus carota*) exposed to metal oxide nanoparticles and metal íons. **Environmental Science. Nano**, v. 3, p. 114–126, 2016.

EMBRAPA. **Tecnologias de produção de soja**. Região central do Brasil. Londrina: Embrapa Soja, 2013. 226 p. (Sistemas de Produção, 16).

GIANNOUSI, K.; AVRAMIDIS, I.; DENDRINOUSAMARA, C. Synthesis, characterization and evaluation of copper based nanoparticles as agrochemicals against *Phytophthora infestans*. **RSC Advances**, v. 3, p. 21743–21752, 2013. doi:10.1039/C3RA42118J.

HONG, J. Foliar applied nanoscale and microscale CeO₂ and CuO alter cucumber (*Cucumis sativus*) fruit quality. **Science of the Total Environment**, v. 563–564, p. 904–911, 2016.

HORRIDGE, G. A.; TAMM, S. L. Critical point drying for scanning electron microscopy study of cilial motion. *Science*, v. 13, p. 871–818, 1969.

IAVICOLI, I. et al. Nanotechnology in agriculture: Opportunities, toxicological implications, and occupational risks. **Toxicology and Applied Pharmacology**, v. 329, p. 96–111, 2017.

KAH, M. Nanopesticides and nanofertilizers: emerging contaminants or opportunities for risk mitigation? **Frontiers in Chemistry**, v. 3, p. 1–6, 2015.

KARNOVSKY, M. J. A formaldehyde–glutaraldehyde fixative of high osmolality for use in electron microscopy. **Journal of Cell Biology**, v. 27, p. 137–138, 1965.

LARUE, C. et al. Fate of pristine TiO₂ nanoparticles and aged paint-containing TiO₂ nanoparticles in lettuce crop after foliar exposure. **Journal of Hazardous Materials**, v. 273, p. 17–26, 2014a.

LARUE, C. et al. Foliar exposure of the crop *Lactuca sativa* to silver nanoparticles: Evidence for internalization and changes in Ag speciation. **Journal of Hazardous Materials**, v. 264, p. 98–106, 2014b.

LAUGHTON, S. et al. Persistence of copper-based nanoparticle-containing foliar sprays in *Lactuca sativa* (lettuce) characterized by spICP-MS. **Journal of Nanoparticle Research**, v. 21, p. 174–197, 2019.

MALAVOLTA, E. Funções dos macro e micronutrientes. In: MALAVOLTA, E. (Ed.). **Manual de nutrição mineral de plantas**. São Paulo: Agronômica Ceres, 2006. p. 336–347.

MALAVOLTA, E.; GOMES, F. P.; ALCARDE, J. C. **Adubos e adubações**. São Paulo: Nobel, 2000. 200 p.

MALDONADO, A. J. et al. Cu Nanoparticles absorbed on chitosan hydrogels positively alter morphological, production, and quality characteristics of tomato. **Journal of Applied Botany and Food Quality**, v. 89, p. 183–189, 2016.

NAIR, P. M. G.; CHUNG, I. M. A mechanistic study on the toxic effect of copper oxide nanoparticles in soybean (*Glycine max* L.) root development and lignification of root cells. **Biological Trace Element Research**, v. 162, p. 342–352, 2014a. doi: 10.1007/s12011-014-0106-5.

NAIR, P. M. G.; CHUNG, I. M. Impact of copper oxide nanoparticles exposure on *Arabidopsis thaliana* growth, root system development, root lignification, and molecular level changes. **Environmental Science and Pollution Research**, v. 21, p. 12709–12722, 2014b. doi: 10.1007/s11356-014-3210-3.

NAIR, P. M. G.; CHUNG, I. M. Study on the correlation between copper oxide nanoparticles induced growth suppression and enhanced lignification in Indian mustard (*Brassica juncea* L.). **Ecotoxicology and Environmental Safety**, v. 113, p. 302–313, 2015. doi: 10.1016/j.ecoenv.2014.12.013.

NASROLLAHZADEH, M.; SAJADI, S. M. Risks of nanotechnology to human life. In: NASROLLAHZADEH, M. (Ed.). **An introduction to green nanotechnology**. Amsterdam: Elsevier, 2019. Chap. 7, p. 323–336. (Interface Science and Technology, 28).

PERREAULT, F.; POPOVIC, R.; DEWEZ, D. Different toxicity mechanisms between bare and polymer-coated copper oxide nanoparticles in *Lemna gibba*. **Environmental Pollution**, v. 185, p. 219–227, 2014.

POLETTE, L. A. et al. XAS and microscopy studies of the uptake and bio-transformation of copper in *Larrea tridentata* (creosote bush). **Microchemical Journal**, v. 65, p. 227–236, 2000.

RAJPUT, V. et al. Toxicity of copper oxide nanoparticles on spring barley (*Hordeum sativum* distichum). **Science of the Total Environment**, v. 645, p. 1103–1113, 2018.

SHI, J. et al. An X-ray absorption spectroscopy investigation of speciation and biotransformation of copper in *Elsholtzia splendens*. **Plant and Soil**, v. 302, p. 163–174, 2008.

TAN, W. et al. Foliar exposure of $\text{Cu}(\text{OH})_2$ Nanopesticide to Basil (*Ocimum basilicum*): variety-dependent copper translocation and biochemical responses. **Journal of Agricultural and Food Chemistry**, v. 66, n. 13, p. 3358–3366, 2018.

VITTI, G. C.; TREVISAN, W. **Manejo de macro e micronutrientes para alta produtividade de soja**. Piracicaba: POTAFOS, 2000. 16 p. (Informações Agronômicas. Encarte Técnico, 90).

WANG, P. et al. Nanotechnology: a new opportunity in plant sciences. **Trends in Plant Science**, v. 21, n. 8, p. 699–712, 2016.

XIE, C. et al. Effects of foliar applications of ceria nanoparticles and CeCl_3 on common bean (*Phaseolus vulgaris*). **Environmental Pollution**, v. 250, p. 530–536, 2019.

XIONG, T. T. et al. Copper oxide nanoparticle foliar uptake, phytotoxicity, and consequences for sustainable urban agriculture. **Environmental Science and Technology**, v. 51, p. 5242–5251, 2017.

4 FOLIAR UPTAKE OF NANO CERIUM OXIDE IN SOYBEAN PLANTS

Abstract

The application of the rare earth element cerium in plants has emerged few years ago, although its possible beneficial effects are still controversive. Some studies have shown that in a proper concentration Ce can improve plant growth and development, increase yields and alleviate environmental stresses, while others debate the potential toxicity of these nanoparticles. This study has applied two sizes of cerium oxide nanoparticles, its bulk form and cerium nitrate on soybean plants to try to elucidate whether this element brings beneficial effects. The plants were foliar sprayed with dispersions of the abovementioned particles, using a dispersant or not, in two doses, and harvested 21 and 45 days after application. Both nanomaterials (25 and 70 nm) are similar and show characteristic diffractions for cerium oxide. Nanoparticles of cerium oxide were absorbed by soybean leaves and redistributed to other leaves. The use of cerium nanoparticles, did not interfere in agronomic parameters such as biomass production and the number of pods. Cerium concentration and accumulation presented different values depending on the source and the dose. Among the sources, cerium nitrate was the one which yielded the highest values of both parameters and the dose 10 mg plant⁻¹ presented higher values than the dose 0.1 mg plant⁻¹ and the control, which were statistically equal. More detailed studies on physiological and biochemical effects of this rare earth element on crop plants should be carried out for a better understanding of how the interaction Ce-plant occurs.

Keywords: nanomaterials, cerium oxide, rare earth element, mineral nutrition, foliar spraying, ICP-MS.

4.1 Introduction

Cerium (Ce) is one of the 15 members of the lanthanide series, which along with scandium and yttrium comprise the rare earth elements (REE). Cerium is the most abundant REE in the earth's crust (66 µg g⁻¹) and its abundance is not that different compared with Zn and Cu, which are much more involved in environmental investigations than Ce (TYLER, 2004). With a market at US \$ 9 billions (GANGULI; COOK, 2018), it is estimated that the global REE mine production increased from 132,000 metric tons in 2017 to 170,000 in 2018, with ~70% of this value produced by China. Although Ce is not considered

essential to plants, some studies have shown that in a proper concentration Ce can improve plant growth and development, increase yields and alleviate environmental stresses (SALGADO et al., 2019; VILELA et al., 2018; HU et al., 2004; CHAO et al., 2009).

Much attention is being paid to the use of Ce as nano-fertilizers in the agriculture. The majority of Ce is found in the trivalent (Ce^{3+}) and tetravalent (Ce^{4+}) states, thus CeO_2 is the most common form (CASSEE et al., 2011). In commercial micro-fertilizers, Ce is mostly found as chloride and nitrate forms (SHYAM; AERY, 2012). Different solubility (MUDUNKOTUWA et al., 2011), surface charges (EL BADAWY et al., 2011), chemical reactivity (DREIZIN, 2009) and many other features that can be interesting to the development of new products, including foliar fertilizers.

Cerium nanoparticles are predominantly found as CeO_2 and they have been used in many engineering and biological applications such as catalytic materials (TROVARELLI, 1996), medicines (CELARDO et al., 2011), solar cells (CORMA et al., 2004), gas sensors (JASINSKI; SUZUKI, T.; ANDERSON, 2003) and solid oxide fuel cells (ESPOSITO; TRAVERSA, 2008). CeO_2 nanoparticle is one of the most explored nanomaterial due to its unique property to store and release oxygen (HAILSTONE et al., 2009), and though it is predominantly explored in innovative technologies, the use of Ce and other REE nanoparticles in the agriculture as plant stimulator has recently drawn attention of the research community.

On the other hand, the broadening use of Ce nanoparticles in industrial products have raised concerns about its final disposal in the environment and its potentially toxic interactions with living systems, once Ce nanoparticles can be easily up taken, translocated, accumulated and biotransformed in plant tissues and consequently migrate into the food chains (HUSSAIN et al., 2019; ZHANG et al., 2012). This is a matter of intense debate in the recent literature and the potential toxicity of these nanoparticles and the mechanisms behind it still needs to be deeply investigated.

The Ce impact on plants varies according to the plant species, applied concentration, tested material, particle size and time of exposure. It is compiled in Table 1 a set of studies concerning the effects of foliar application of Ce on plants. In general, the effects occur in a dose-dependent manner. Some of them reported increase in plant height (JAHANI et al., 2019; XIE et al., 2015) and weight (XIE et al., 2019; MA; REN; YAN, 2014) by applying a dose bellow 100 mg L^{-1} , whereas above this concentration these parameters and photosynthesis rate decreased (JAHANI et al., 2019; HONG et al., 2016). Cerium was also beneficial to inhibit the absorption and accumulation of heavy metals (LI et al., 2013), increase seed yield in drought-stressed plants (DJANAGUIRAMAN et al., 2018), improve photosynthetic parameters and

alleviate UV-B radiation induced stress (LIANG et al., 2006; LIANG; HUANG; ZHOU, 2006). Other effects are associated with enzyme activity and plant mineral, sugar and protein content (LI et al., 2013; XIE et al., 2015; 2019).

Aiming at contributing to the knowledge of how Ce interacts with plants this study investigated the effects of CeO₂ nanoparticles in two different sizes (25 and 70 nm), as well as bulk CeO₂ and Ce(NO₃)₃ applied as foliar fertilizer in soybean (*Glycine max* (L.) Merrill) plants.

Table 1. Bibliographical survey on the foliar application Ce and their effects on plants. All biometric data presented statistical difference

Plant species	Type and concentration (mg L ⁻¹)	Application method	Nanoparticle size (nm)	Time of exposure	Main effects	Ref.
<i>Phaseolus vulgaris</i> L.	CeO ₂ ; 250, 500, 1000 and 2000	Three-weeks-old plants were sprayed with 200 mL NPs suspension per treatment (n=3) every 48 h during two weeks	10-30	30 days	Most of the applied concentrations decreased stomatal density, anthocyanin, relative water and chlorophyll content, while stomatal length, catalase and electrolyte leakage were increased. Proline and peroxidase were both increased and decreased by the treatments, but most of other the responses were dose-dependent. Aerial height and root length only decreased at 2000 mg L ⁻¹ . NP application caused membrane damage and induced oxidative stress	SALEHI et al., 2018
<i>Spinacia oleracea</i>	CeO ₂ ; 10 and 100	Four-week-old plants were sprayed with NPs suspension twice per week for three weeks	~ 4	3 weeks	Both concentrations decreased Ca content in the roots and Zn content in the leaves. 10 mg L ⁻¹ induced more metabolic changes in leaves, while 100 mg L ⁻¹ induced more metabolic changes in roots	ZHANG et al., 2019
<i>Cucumis sativus</i>	CeO ₂ ; 50, 100 and 200	Three-weeks-old plants were sprayed with 250 mL NPs suspension per treatment (n=4). The total volume was split in three applications, every four hours	8 ± 1	15 days	Decreased photosynthesis rate at 100 and 200 mg L ⁻¹ , transpiration rate at 100 mg L ⁻¹ , and increased stomatal conductance at 50 mg L ⁻¹	HONG et al., 2016
<i>Cucumis sativus</i>	CeO ₂ ; 40, 80, 160 and 320	Fifteen-days-old hydroponically grown plants were sprayed with a total volume of 100 mL per treatment that was split in three applications, every four hours	8 ± 1	15 days	Some treatments altered dehydroascorbate reductase (DHAR), catalase (CAT) and ascorbate peroxidase (APX) activities in leaves, stems and roots	HONG et al., 2014
<i>Sorghum bicolor</i> (L.) Moench	CeO ₂ ; 10	60 days after sowing, each pot was foliar-sprayed with 600 mL, that is, 6 mg of nanoceria for three plants ⁻¹ . After that, water was withheld for 21 days	15 ± 5 nm	21 days	Reduced leaf superoxide radical and hydrogen peroxide levels and decreased cell membrane lipid peroxidation under drought. Increased leaf carbon assimilation rates, pollen germination and seed yield in drought-stressed plants	DJANAGUIRAMAN et al., 2018
<i>Lactuca sativa</i>	CeO ₂ ; 50, 100 and 200	Plants were foliar-sprayed once after every other week, in total 3 times	micrometric	30 days	Treatments increased vitamin C and soluble sugar, reduced nitrite content, enhanced activities of superoxide dismutase and peroxidase dismutase, inhibited the absorption of Cd/Pb and decreased content and accumulation of Cd/Pb in shoots and roots	LI et al., 2013

<i>Cyclocarya paliurus</i>	Ce(NO ₃) ₃ ; 17, 86 and 434	Each plant was foliar-sprayed twice with 300 mL of solution, once every 15 days. Drops of Tween20 were added to the solution as a surfactant.	micrometric	30 days	Some treatments increased: seedling height; leaf proteins and sugars; K, P, Mg, Mn, Fe and Cu concentration; concentration of triterpenoids, quercetin and kaempferol; activities of SOD, peroxidase (POX) and phenylalanine ammonia-lyase (PAL) in the leaves. 434 mg L ⁻¹ was only harmful to sugar content	XIE et al., 2015
<i>Calendula officinalis</i> L.	CeO ₂ ; 50, 100, 200, 400, 800, 1600 and 3200	Two-week-old seedlings were sprayed with NPs suspension five times during five weeks	10-30	50 days	At 50 and 100 mg L ⁻¹ shoot length, fresh weight and chlorophyll content were increased, while from 200 mg L ⁻¹ these parameters were decreased. By applying more than 200 mg L ⁻¹ the soluble sugar content of leaves and proline were increased. Hydrogen peroxide and membrane electrolyte leakage were respectively increased after 100 and 200 mg L ⁻¹ . The activities of some antioxidant enzymes were induced by high concentrations	JAHANI et al., 2019
<i>Phaseolus vulgaris</i> L.	CeCl ₃ (micrometric) and CeO ₂ NPs; 40, 80 and 160	100 mL of suspensions and solutions were sprayed at 15 days after transplanting (plants were transplanted 16 days after sowing). The treatments were sprayed on the leaves every other day during 17 days	CeO ₂ NPs: 6.9 ± 0.4	64 days	Only CeO ₂ at 40 mg L ⁻¹ increased dry weight (51.8% relative to the control). Plants exposed to 80 and 160 mg L ⁻¹ CeCl ₃ increased SOD activity and malondialdehyde (MDA) content. Some treatments interfered S, Mn, Mo and Zn content of pods. Chemical speciation analysis pointed out that Ce in treated leaves remained as its pristine form for both CeCl ₃ and CeO ₂ NPs treatments	XIE et al., 2019
<i>Brassica chinensis</i> L.	CeCl ₄ ; 100	Twenty days old plants were foliar fertilized daily during 8 days	micrometric	8 days	Increased plot yield, fresh and dry weight and soluble sugar content. Decreased the titratable acid, vitamin C, Cu, Cd, Ni and Pb contents	MA; REN; YAN, 2014
<i>Brassica juncea</i> L.	CeCl ₃ ; 12	Five-week-old seedlings were foliar sprayed once on the leaves until drops began to fall	micrometric	8 days	Mitigated the harmful effect caused by UV-B exposure during the growth of seedlings and increased photosynthetic parameters	LIANG et al., 2006a
<i>Glycine max</i> L.	CeCl ₃ ; 20	Seedlings with the third leaf completely developed were foliar sprayed once on the leaves until drops began to fall	micrometric	7 days	Increased photosynthetic parameters and alleviated the inhibition of UV-B radiation on the photosynthesis	LIANG et al., 2006b

4.2 Materials and Methods

4.2.1 Nanomaterials characterization. Purity. 25 and 70 nm CeO₂ nanoparticles were acquired from MK Impex Corp. (Canada). The nanomaterials were analyzed by an energy dispersive X-ray fluorescence spectrometer (EDX 720, Shimadzu, Kyoto, Japan). The powder samples (200 mg) were weighted in a 6.3 mm aperture X-ray sample cup (no. 3577 - Spex Ind. Inc., USA) and sealed with a 5 µm thick polypropylene film (no. 3520 - Spex Ind. Inc., USA). The analysis were conducted under vacuum, in triplicate, using a rhodium (Rh) X-ray tube at 50 kV and auto-tunable current adjusted for a detector deadtime below 30% and a 3-mm collimator. The X-ray spectrum of the sample was acquired utilizing a Si (Li) detector for 300 s and through the fundamental parameters method it was possible to determinate contaminants content present in these nanomaterials.

4.2.2 Structural characterization. X-ray diffraction (XRD) was used to confirm the majority composition of the CeO₂ nanoparticles. The X-ray diffraction measurements were obtained in a Bruker D2 Phaser instrument, operating with Cu K α ($\lambda=1.5418 \text{ \AA}$) radiation, 30 kV, 10 mA, sample holder rotation of 15 rpm and Lynxeye[®] energy dispersive one-dimensional detector with 192 channels. The diffractograms were acquired under the following conditions: continuous scanning mode in the 2θ range from 10 to 90°, step = 0.02° and acquisition time = 0.5 s, obtained from the sample powders.

4.2.3 Physicochemical features of dispersions. Dispersions in distilled water of the nanomaterials (100 mg L⁻¹) were prepared to determinate the aggregates' sizes by dynamic light scattering (DLS) and its charge (Zeta potential) using a Zetasizer equipment (Malvern, UK).

4.2.4 Nano CeO₂ morphology. The morphology of the nanoparticles was evaluated by transmission electron microscopy (JEM 1011, JEOL, Japan) in dispersions of 100 mg L⁻¹.

4.2.5 Soybean cultivation. The experiment was conducted in a greenhouse of the Soil Science Department at Luiz de Queiroz Superior School of Agriculture (ESALQ/USP). The soil used in the experiment was a sandy soil, the base saturation (BS) was raised for 60% through liming according to the base saturation method. Four seeds of soybean, cultivar KWS RK 7214 IPRO, were sown per pot. The exceeding seedlings were removed, leaving 2 plants per pot. Each pot of 2.5 L was filled with 2 kg of soil, daily irrigated with enough deionized water to keep the soil close to its field capacity.

4.2.6 Cerium solutions. Cerium based solutions, in the same concentrations of the nanomaterials were used for comparison. The experiment was assembled under a completely randomized design with three repetitions. Control treatments consisted of three pots with two plants in each, that only deionized water was applied to the leaves, and three pots with two plants in each, that a solution of deionized water + dispersant (5 wt.%) was applied to the leaves.

The application of all treatments was made in the first 3 trefoils through aspersion when the plants were in V3 stage. The dispersant used was the polyethylene glycol (PEG) with a molecular weight = 15,000 – 20,000 g mol⁻¹ from Sigma-Aldrich®. The nanoparticles were dispersed in deionized water and in aqueous dispersions containing the dispersant (5 wt. %). The factors and levels of the treatments are shown in Table 2.

Table 2. Factors and levels of the treatments applied

Factors	Levels			
Particle size	25 nm nCeO ₂	70 nm nCeO ₂	Micrometric CeO ₂	Ce(NO ₃) ₃ ·6H ₂ O
Dispersant (PEG)	With	Without		
Dose	0.1 mg plant ⁻¹	10 mg plant ⁻¹		

The doses were selected based on a previous cerium effect on plants study of our research group. In total there were 54 pots, which come from the following combination of factors and levels:

- 4 (particle size) x 2 (dispersant) x 2 (dose) x 3 (repetitions) + 6 (control)

For the analysis, one plant was collected 21 days (V7/V8 stage) after the application of the treatments and the other plant, 45 days (R4/R5 stage) after the application. The responses studied were: shoot dry mass, number of pods, cerium concentration and accumulation.

In the days to collect the materials, the plants were divided in sets of leaves, the material identified, placed in paper bags and oven-dried at 65° C for 72 hours. Afterwards, the set of leaves that have not received the treatment was weighed and the samples grinded in Willey type knife mill (1 mm mesh).

4.2.7 Analytical blank test. As the contents of cerium to be analysed in the samples were low, a preliminar blank test was performed in order to assure that there was no contamination in the digestion process. Five analytical blanks were prepared in two different laboratories, using the reagents, tubes and microwave ovens of each laboratory.

4.2.8 ICP-MS analysis. Samples and standard reference materials were microwave-assisted acid digested in triplicate. A closed vessel microwave oven (ETHOS 1600, Milestone, Italy) was used according to the following procedure: 200 mg of ground material was accurately weighed in the TFM[®] vessels and 5.0 mL of 20% v v⁻¹ sub-boiled HNO₃ and 2.0 mL of 30% w w⁻¹ H₂O₂ were added. The microwave heating program consisted of the following steps: (1): ramp from room temperature to 120 °C in 5 min; (2): keeping at 120 °C for 2 min; (3): ramp from 120 °C to 160 °C in 3 min; (4): keeping at 160 °C for 2 min; (5): ramp from 160 °C to 220 °C in 5 min; (6): keeping at 220 °C for 20 min; (7): cooling for 20 min. After cooling, the final solutions were transferred to volumetric flasks and diluted up to 20 mL with high-purity de-ionized water (resistivity > 18.2 MΩ cm). The solutions were analysed by ICP-MS spectrometer (X-Series 2, Thermo Scientific, Germany). For trueness checking, the standard reference materials NIST 1547 (Peach leaves), NIST 1573a (Tomato leaves) and NIST 1515 (Apple leaves) were analysed.

4.2.9 Experimental Design and statistical analysis. The greenhouse experiment was set under a totally randomized design in a 4 x 2 x 3 + 1 factorial scheme (4 particle sizes, 2 dispersant and 3 concentrations), plus a universal control treatment.

All the experimental analyses were conducted at R. environment version 3.6. Prior to ANOVA the data was tested to check the normality (Shapiro-Wilk test). Logarithmic transformation was used for the data regarding cerium concentration and accumulation for both dates of analysis (21 and 45 days after treatment application).

For the ANOVA, Tukey Test with 5% significance was adopted for means comparison of the effects.

4.3 Results and Discussion

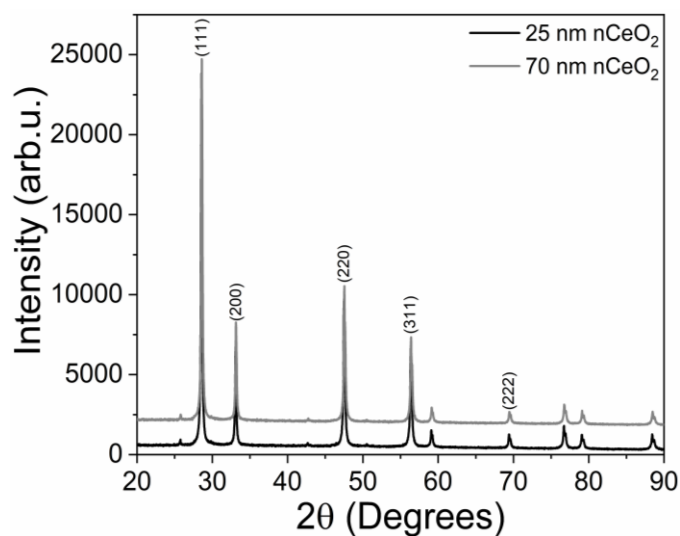
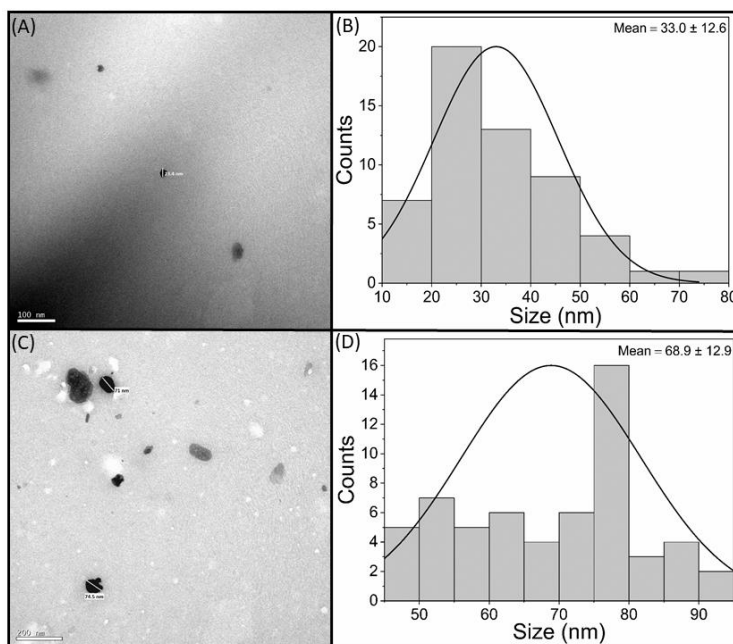
4.3.1 Nanomaterials characterization. Purity and contaminants of the nanomaterials used in the experiment are shown in Table 3.

Table 3. Purity and contaminant on the nanomaterials used in the experiment

Nanomaterial	Manufacturer	Purity (%)	Contaminant (mg kg ⁻¹)		
			Zn	Ni	Zr
25 nm nCeO ₂	MK Impex Corp.	99.88%	474	460	281
70 nm nCeO ₂	MK Impex Corp.	99.87%	674	354	262

The XRD diffractograms are shown in Figure 1. Diffractograms for both nanomaterials (25 and 70 nm) are similar and show characteristic diffractions for cerium oxide, as also described by Masui et al. (2003).

The shape of the nanomaterials could be confirmed by the images (Figure 2) obtained by transmission electron microscopy (TEM). For 25nm nCeO₂ (Figure 2A) is observed a spherical aspect, while for the 70nm nCeO₂ (Figure 2C) a more elongated aspect is seen. The particles present a normal size distribution, as shown in the histograms for 25 nm nCeO₂ (Figure 2B) and 70 nm nCeO₂ (Figure 2D).

Figure 1. XRD diffractograms of 25 and 70 nm nCeO₂Figure 2. TEM images of (A) 25nm nCeO₂ and (C) 70nm nCeO₂ and their respective histograms (B and D). Scale bar: 100 nm

Regarding the dynamic light scattering and zeta potential values (Table 4), both particles present 2 peaks, with a main aggregates' size (more than 98%) of 237 nm (25 nm nCeO₂) and 297 nm (70 nm nCeO₂). The aggregates have a negative charge ranging from -8.9 to 15.7 mV.

Table 4. Zeta potential and Dynamic Light Scattering of CeO₂ nanoparticles

Nanomaterial	Zeta Potential (mV)	Dynamic Light Scattering (Cluster diameter – nm)	
		Peak 1	Peak 2
25nm nCeO ₂	-15.7 ± 6.6	237 (98.4 %)	5284 (1.6%)
70 nm nCeO ₂	-8.9 ± 4.6	297 (98.1 %)	5560 (1.1%)

Although the putative individual particle size of the nanoparticles is 25 and 70 nm, in aqueous dispersion the nanoparticles were aggregated. This occurs due to the Van der Waals forces and was also reported by Marucci et al. (2019).

4.3.2 Analytical blank test. As shown in Table 5, the five blanks prepared in Laboratory 2 presented cerium contamination during the process. This contamination came from the tubes used in the digestion process. Previously to this analysis, another set of digestions were carried out but the tubes were not properly decontaminated.

Table 5. Cerium content ($\mu\text{g L}^{-1}$) in analytical blank determined by ICP-MS prepared in different laboratories

Laboratory	Reagents	Blank 1	Blank 2	Blank 3	Blank 4	Blank 5
1	HNO ₃ 20%	0.006	< LOD	< LOD	< LOD	< LOD
	HNO ₃ 20% + H ₂ O ₂ 30%	< LOD	0.009	< LOD	< LOD	< LOD
2	HNO ₃ 20%	7.232	6.308	6.73	0.229	0.214
	HNO ₃ 20% + H ₂ O ₂ 30%	28.64	471.8	17.4	19.87	19.73

*LOD= 0.006151 $\mu\text{g L}^{-1}$

4.3.3 Effects of nCeO₂ on plant biometrics and Ce translocation. The dispersant by itself did not affect any of the parameters studied (biomass production, number of pods, cerium concentration and accumulation). In the same sense, the source or dose by themselves did not affect the biomass (21 or 45 days after treatment application) and the number of pods.

In literature few studies report effects of foliar-spraying cerium NPs on agronomic characteristics of crop plants. Rodrigues et al. (2019) have also tested the effects of bulk cerium on soybean and the authors report that the treatments did not affect plant biometrics such as plant height, number of leaves and number of pods.

No differences in aerial part of bean (*Phaseolus vulgaris* L.) were observed by Salehi et al. (2018) but the authors report that spraying lowered stomatal density, increased stomatal length and altered photosynthesis. They also report that spraying have caused damage to the leaves, which was also visually observed during the experiment. Most part of leaves that have received the treatments fell before the end of the experiment.

According to Xie et al. (2019) none of the treatments significantly affected plant biometrics (height, number of leaves, leaf length, and dry matter percentage) compared to the control.

Differently from our results, in which particle size did not affect agronomic parameters, different cerium particle sizes impacted cucumber fruit firmness (HONG et al., 2016). Different sizes are likely to cause different responses, including oxidative stress (MATTIELLO et al., 2015) due to their size feature and surface area (HUSSAIN et al., 2009).

Shoot dry mass at 45 days after treatment application was affected by the interaction source x dose (Table 6). The highest biomass production was obtained with the treatment 70 nm CuO in the dose 0.1 mg plant⁻¹ (1.10 ± 0.24 g), followed by micrometric CuO in the dose 10 mg plant⁻¹ (0.87 ± 0.26 g) = 25 nm CuO in the dose 0.1 mg plant⁻¹ (0.78 ± 0.30 g) = nitrate in the dose 0.1 mg plant⁻¹ (0.68 ± 0.27 g). The remaining treatments produced less biomass than the treatments above mentioned and were statistically equal between themselves and to the control.

Table 6. Shoot dry mass (g) of soybean plants harvested 45 days after treatment application

Source	Dose (mg plant ⁻¹)	Shoot dry mass (g)
25 nm CuO	0.1	0.78 ± 0.30 ab
	10	0.65 ± 0.18 b
70 nm CuO	0.1	1.10 ± 0.24 a
	10	0.63 ± 0.23 b
Micrometric CuO	0.1	0.62 ± 0.18 b
	10	0.87 ± 0.26 ab
Nitrate	0.1	0.68 ± 0.27 ab
	10	0.57 ± 0.24 b
Control	0	0.65 ± 0.18 b

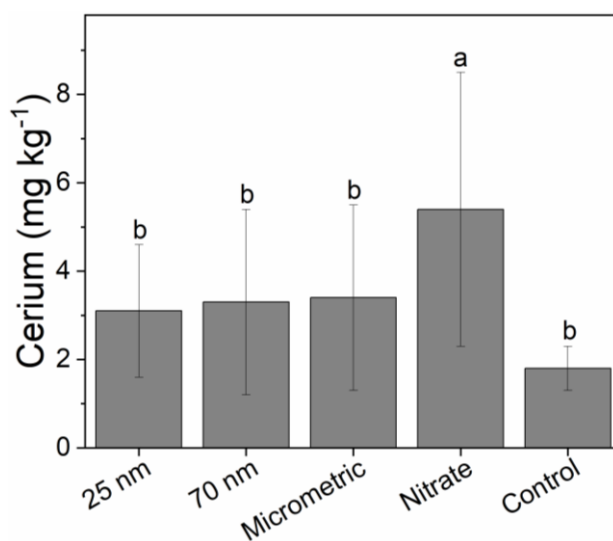
*Means with the same letter do not differ statistically.

The results for cerium concentration and accumulation in leaves are presented below. Cerium was determined 21 and 45 days after the application of treatments. It is important to highlight that the analyzed tissues did not receive the treatments themselves, thus, in principle, the data show cerium translocation.

The external surface of leaves of higher plants comprises a cuticular layer covered by waxy deposits. Even though the wax contains a wide range of organic compounds that can trap theNPs, cerium was absorbed and redistributed to other leaves as demonstrated next.

Figure 3 shows the cerium concentration in plants 21 days after treatment application. The source cerium nitrate presented the highest concentration ($5.4 \pm 3.1 \text{ mg kg}^{-1}$). All the other sources did not differ from the control. The source by itself presented no statistical difference for cerium concentration at 45 days after treatment application. Thus, the result observed at 21 days is due to the solubility of the nitrate and the assimilation of the element by the leaves is faster than the other sources.

Figure 3. Cerium concentration as function of sources in soybean plants harvested 21 days after treatment application as function of source



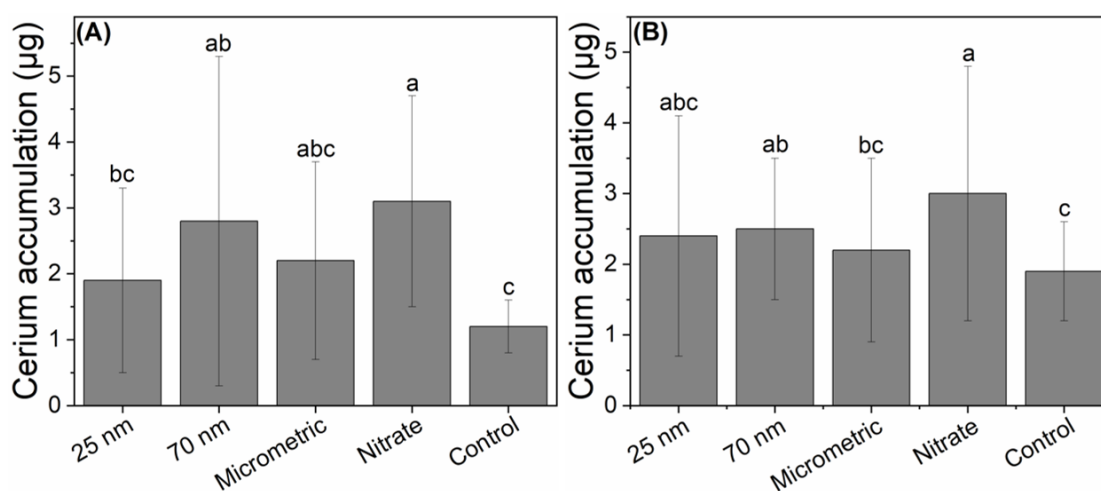
*Means with the same letter do not differ statistically.

At both 21 and 45 days after treatment application, even control plants present cerium, when it should not. We hypothesize that contamination might have occurred during the grinding process.

Cerium accumulation in leaves is presented in Figure 4. At 21 days after treatment application (Figure 4A), the nitrate presented the highest value ($3.1 \pm 1.6 \mu\text{g}$), followed by 70 nm CuO ($2.8 \pm 2.5 \mu\text{g}$), micrometric CuO ($2.2 \pm 1.5 \mu\text{g}$) and 25 nm CuO ($1.9 \pm 1.4 \mu\text{g}$). All the sources statistically accumulated more cerium than the control ($1.2 \pm 0.4 \mu\text{g}$).

Similar results were observed at 45 days after treatment application (Figure 4B). The nitrate presented the highest value for cerium accumulation ($3.0 \pm 1.8 \mu\text{g}$), followed by 70 nm CuO ($2.5 \pm 1.0 \mu\text{g}$), 25 nm CuO ($2.4 \pm 1.7 \mu\text{g}$), micrometric CuO ($2.2 \pm 1.3 \mu\text{g}$). The control presented the value $1.9 \pm 0.7 \mu\text{g}$, statistically less than all the sources.

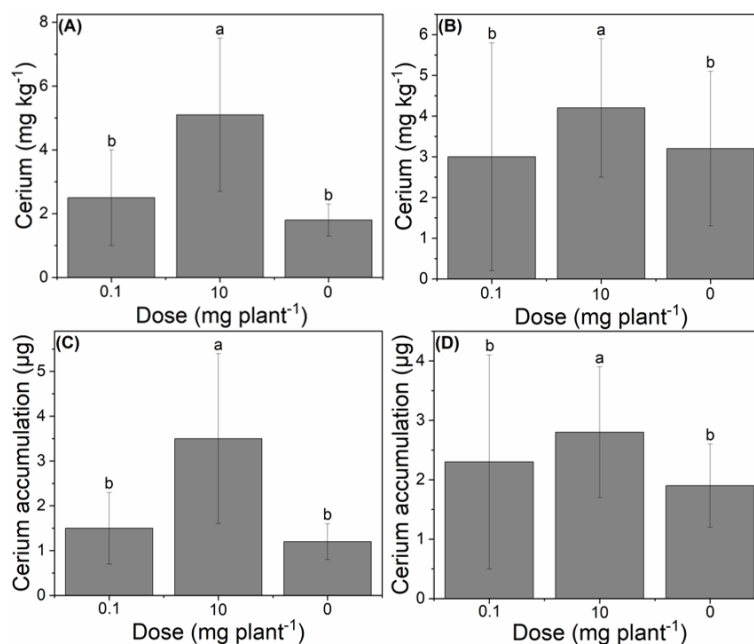
Figure 4. Cerium accumulation as function of sources in soybean plants harvested 21 (A) and 45 (B) days after treatment application



*Means with the same letter do not differ statistically.

The effects of doses on cerium concentration and accumulation are shown in Figure 5. The results were similar for both parameters at 21 and 45 days after treatment application. The dose 10 mg plant^{-1} presented higher values than the dose $0.1 \text{ mg plant}^{-1}$ and the control, which were statistically equal.

Figure 5. Cerium concentration (A/B) and accumulation (C/D) as function of doses in soybean plants harvested 21 (A/C) and 45 (B/D) days after treatment application



*Means with the same letter do not differ statistically.

Salehi et al. (2018) declare that Ce concentration in the leaves showed a dose dependent absorption, uptake and translocation of Ce, like the results obtained in our experiment. In their study, cerium uptake occurred by roots or through leaves. When applied through leaves, the element concentration was much higher than soil application. For the authors, this difference could be related to bioavailability, as a result of adsorption-desorption and mobility processes, as well as to limited root uptake.

Hong et al. (2014) have found similar results for cerium concentration and different harvesting time. In their study, Ce concentration in leaves treated with higher concentration was significantly higher than the concentration found in leaves treated with the lower concentration. And alike in this study, the uptake did not increase with time. For them, this happened because the number of NPs on the surface saturated the routes of entrance through the leaves avoiding penetration.

A difference from their study and ours is that they have tested foliar application of NPs as powder and dispersion, and both ways promoted cerium redistribution in the plants.

The effects of the interaction between source x dispersant on cerium concentration and accumulation are presented on Table 7. Cerium concentration at 45 days after treatment application was not statistically significant.

At 21 days after treatment application, the treatments that have presented the highest values of concentration (mg kg^{-1}) follow the order: nitrate without dispersant (6.8 ± 3.5) > micrometric CuO with dispersant (4.6 ± 2.2) = nitrate with dispersant (4.1 ± 2.3) = 70 nm CuO with dispersant (3.9 ± 2.9). All the sources, with or without dispersant, presented higher values of concentration than the control treatment.

Results for cerium accumulation at 21 days after treatment application followed a similar order as the concentration, with nitrate without dispersant presenting the highest value ($3.90 \pm 1.51 \mu\text{g}$), followed by 70 nm CuO with dispersant ($3.85 \pm 3.26 \mu\text{g}$). The control without dispersant produced the least accumulation value ($1.07 \pm 0.06 \mu\text{g}$).

The results of cerium accumulation at 45 days after treatment application did not range as much as at 21 days but once again nitrate without dispersant presented the highest value ($3.80 \pm 2.31 \mu\text{g}$). Micrometric CuO without dispersant ($3.80 \pm 2.31 \mu\text{g}$) = 25 nm CuO with dispersant ($1.47 \pm 1.06 \mu\text{g}$) = Control with dispersant ($1.33 \pm 0.46 \mu\text{g}$) were statistically equal and presented the least accumulation values.

Table 7. Cerium concentration (mg kg^{-1}) and accumulation (μg) of soybean plants harvested 21 and 45 days after treatment application

Source	Dispersant	21 DAA		45 DAA
		Concentration (mg kg^{-1})	Accumulation (μg)	Accumulation (μg)
25 nm CuO	With	2.9 ± 1.4 b	1.38 ± 0.78 bc	1.47 ± 1.06 bc
	Without	3.2 ± 1.6 b	2.40 ± 1.70 abc	3.30 ± 1.77 ab
70 nm CuO	With	3.9 ± 2.9 ab	3.85 ± 3.26 ab	2.70 ± 1.35 ab
	Without	2.8 ± 0.9 b	1.82 ± 0.48 abc	2.25 ± 0.68 ab
Micrometric CuO	With	4.6 ± 2.2 ab	2.77 ± 1.56 abc	2.35 ± 0.68 ab
	Without	2.2 ± 1.0 b	1.70 ± 1.34 bc	2.08 ± 1.77 bc
Nitrate	With	4.1 ± 2.3 ab	2.32 ± 1.33 abc	2.13 ± 0.45 ab
	Without	6.8 ± 3.5 a	3.90 ± 1.51 a	3.80 ± 2.31 a
Control	With	1.7 ± 0.4 bc	1.30 ± 0.56 bc	1.33 ± 0.46 bc
	Without	1.9 ± 0.7 bc	1.07 ± 0.06 c	2.50 ± 0.27 ab

*Means with the same letter do not differ statistically.

**DAA = days after application

The foliar uptake of cerium is also reported in literature (SALEHI et al., 2018; HONG et al., 2014; XIE et al., 2019), however, differently from nutrients such as potassium and magnesium, which are redistributed by the floem, the redistribution of cerium is still unknown.

Cerium speciation was not performed in this experiment but it is reported in literature that plants treated with CeO_2 nanoparticles remain in the same form (WANG; TARAFDAR; PRATIM, 2013; HERNANDEZ-VIEZCAS et al., 2013).

4.3 Conclusions

Nanoparticles of cerium oxide were absorbed by soybean leaves and redistributed to other leaves. Biomass production and the number of pods were not influenced by cerium application.

Cerium nitrate, due to its soluble form, presented the highest values of cerium concentration and accumulation at 21 and 45 days. Both parameters were also dose-dependent.

Cerium can not be considered a benefic element because its effects in plants are still controversial, depending on particle size, dose and application way (soil or spraying). On the other hand, we did not observe toxic effects such as reported by several studies in the literature.

There are few studies regarding foliar application of nano cerium. For a better understanding of the influence of Ce NPs after foliar application, detailed studies on physiological and biochemical effects of this rare earth element on crop plants should be carried out.

References

CASSEE, F. R. et al. Exposure, health and ecological effects review of engineered nanoscale cerium and cerium oxide associated with its use as a fuel additive. **Critical Reviews in Toxicology**, v. 41, n. 3, p. 213–229, 2011.

CELARDO, I. et al. Pharmacological potential of cerium oxide nanoparticles. **Nanoscale**, v. 3, n. 4, p. 1411-1420, 2011.

CHAO, L. et al. Cerium under calcium deficiency—influence on the antioxidative defense system in spinach plants. **Plant and Soil**, v. 323, n. 1-2, p. 285–294, 2009.

CORMA, A. et al. Hierarchically mesostructured doped CeO₂ with potential for solar-cell use. **Nature Materials**, v. 3, n. 6, p. 394-397, 2004.

DJANAGUIRAMAN, M. et al. Cerium oxide nanoparticles decrease drought-induced oxidative damage in sorghum leading to higher photosynthesis and grain yield. **ACS Omega**, v. 3, n. 10, p. 14406-14416, 2018.

DREIZIN, E. L. Metal-based reactive nanomaterials. **Progress in Energy and Combustion Science**, v. 35, n. 2, p. 141–167, 2009.

DURAN, N. M. et al. X-ray spectroscopy uncovering the effects of Cu based nanoparticle concentration and structure on *Phaseolus vulgaris* germination and seedling development. **Journal of Agricultural and Food Chemistry**, v. 65, p. 7874-7884, 2017.

EL BADAWY, A. M. et al. Surface charge-dependent toxicity of silver nanoparticles. **Environmental Science and Technology**, v. 45, n. 1, p. 283–287, 2011.

ESPOSITO, V.; TRAVERSA, E. Design of electroceramics for solid oxides fuel cell applications: playing with ceria. **Journal of the American Ceramic Society**, v. 91, n. 4, p. 1037–1051, 2008.

GANGULI, R.; COOK, D. R. Rare earths: A review of the landscape. **Energy & Sustainability**, v. 5, E9, 2018. doi: 10.1557/mre.2018.7.

HAILSTONE, R. K. et al. A study of lattice expansion in CeO₂ nanoparticles by transmission electron microscopy. **The Journal of Physical Chemistry C**, v. 113, n. 34, p. 15155–15159, 2009.

HERNANDEZ-VIEZCAS, J. A. et al. In situ synchrotron X-ray fluorescence mapping and speciation of CeO₂ and ZnO nanoparticles in soil cultivated soybean (*Glycine max*). **ACS Nano**, v. 7, n. 2, p. 1415–1423, 2013.

HONG, J. et al. Evidence of Translocation and Physiological Impacts of Foliar Applied CeO₂ Nanoparticles on Cucumber (*Cucumis sativus*) Plants. **Environmental Science and Technology**, v. 48, n. 8, p. 4376–4385, 2014.

HONG, J. Foliar applied nanoscale and microscale CeO₂ and CuO alter cucumber (*Cucumis sativus*) fruit quality. **Science of the Total Environment**, v. 563–564, p. 904–911, 2016.

HU, Z. et al. Physiological and Biochemical Effects of Rare Earth Elements on Plants and Their Agricultural Significance: A Review. **Journal of Plant Nutrition**, v. 27, n. 1, p. 183–220, 2004.

HUSSAIN, I. et al. Plant-nanoceria interaction: Toxicity, accumulation, translocation and biotransformation. **South African Journal of Botany**, v. 121, p. 239–247, 2019.

HUSSAIN, S. et al. Oxidative stress and proinflammatory effects of carbon black and titanium dioxide nanoparticles: role of particle surface area and internalized amount. **Toxicology**, v. 260, p. 142–149, 2009.

JAHANI, S. et al. Effect of foliar application of cerium oxide nanoparticles on growth, photosynthetic pigments, electrolyte leakage, compatible osmolytes and antioxidant enzymes activities of *Calendula officinalis* L. **Biologia**, v. 74, n. 9, p. 1063–1075, 2019. doi: 10.2478/s11756-019-00239-6.

JASINSKI, P.; SUZUKI, T.; ANDERSON, H. U. Nanocrystalline undoped ceria oxygen sensor. **Sensors and Actuators B: Chemical**, v. 95, n. 1–3, p. 73–77, 2003.

LI, S. et al. Spraying Silicon and/or Cerium Sols Favorably Mediated Enhancement of Cd/Pb Tolerance in Lettuce Grown in Combined Cd/Pb Contaminated Soil. **Procedia Environmental Sciences**, v. 18, p. 68–77, 2013.

LIANG, C. J. et al. Effects of cerium on growth and physiological mechanism in plants under enhanced ultraviolet-B radiation. **Journal of Environmental Sciences**, v. 18, n. 1, p. 125–129, 2006.

- LIANG, C.; HUANG, X.; ZHOU, Q. Effect of cerium on photosynthetic characteristics of soybean seedling exposed to supplementary ultraviolet-B radiation. **Journal of Environmental Sciences**, v. 18, n. 6, p. 1147-1151, 2006.
- MA, J. J.; REN, Y. J.; YAN, L. Y. Effects of spray application of lanthanum and cerium on yield and quality of chinese cabbage (*Brassica chinensis* L) based on different seasons. **Biological Trace Element Research**, v. 160, n. 3, p. 427-432, 2014.
- MARUCCI, R. C. et al. Are Cerium Oxide Nanoparticles Transferred from Plants to the Aphid *Myzus persicae* (Hemiptera: Aphididae)? **Florida Entomologist**, v. 102, n. 3, p. 555-561, 2019.
- MASUI, T. et al. Synthesis and characterization of cerium oxide nanoparticles coated with turbostratic boron nitride. **Journal of Materials Chemistry**, v. 13, p. 622–627, 2003.
- MATTIELLO, A. et al. Evidence of phytotoxicity and genotoxicity in *Hordeum vulgare* L. exposed to CeO₂ and TiO₂ nanoparticles. **Frontiers in Plant Science**, v. 6, p. 1–13, 2015.
- MUDUNKOTUWA, I. A. et al. Dissolution of ZnO Nanoparticles at Circumneutral pH: A Study of Size Effects in the Presence and Absence of Citric Acid. **Langmuir**, v. 28, n. 1, p. 396–403, 2011.
- RODRIGUES, E. S. et al. Foliar application of rare earth elements on soybean (*Glycine max* (L)): Effects on biometrics and characterization of phytotoxicity. **Journal of Rare Earths**, 2019. doi: 10.1016/j.jre.2019.09.004.
- SALEHI, H. et al. Morphological, proteomic and metabolomic insight into the effect of cerium dioxide nanoparticles to *Phaseolus vulgaris* L. under soil or foliar application. **Science of the Total Environment**, v. 616-617, p. 1540–1551, 2018.
- SALGADO, O. G. G. et al. Cerium alleviates drought-induced stress in *Phaseolus vulgaris*. **Journal of Rare Earths**, 2019. doi.org/10.1016/j.jre.2019.07.014.
- SHYAM, R.; AERY, N. Effect of cerium on growth, dry matter production, biochemical constituents and enzymatic activities of cowpea plants [*Vigna unguiculata* (L.) Walp.]. **Journal of Soil Science and Plant Nutrition**, v. 12, n. 1, p. 1–14, 2012.
- TROVARELLI, A. Catalytic Properties of Ceria and CeO₂-Containing Materials. **Catalysis Reviews**, v. 38, n. 4, p. 439–520, 1996.
- TYLER, G. Rare earth elements in soil and plant systems – A review. **Plant and Soil**, v. 267, p. 191–206, 2004.
- VILELA, L. A. F. et al. Cerium (Ce) and lanthanum (La) promoted plant growth and mycorrhizal colonization of maize in tropical soil. **Australian Journal of Crop Science**, v. 12, n. 05, p. 704 – 710, 2018.
- WANG, W.; TARAFDAR, J.; PRATIM, B. Nanoparticle synthesis and delivery by an aerosol route for watermelon plant foliar uptake. **Journal of Nanoparticle Research**, v. 15, p. 1417–1418, 2013.

XIE, C. et al. Effects of foliar applications of ceria nanoparticles and CeCl₃ on common bean (*Phaseolus vulgaris*). **Environmental Pollution**, v. 250, p. 530-536, 2019.

XIE, Y. et al. Effects of cerium nitrate on the growth and physiological characteristics in *Cyclocaryapaliurus* seedlings. **Journal of Rare Earths**, v. 33, n. 8, p. 898-904, 2015.

ZHANG, H. et al. Metabolomics Reveal the “Invisible” Responses of Spinach Plants Exposed to CeO₂ Nanoparticles. **Environmental Science and Technology**, v. 53, n. 10, p. 6007-6017, 2019.

ZHANG, P. Biotransformation of Ceria Nanoparticles in Cucumber Plants. **ACS Nano**, v. 6, n. 11, p. 9943-9950, 2012.

5 GENERAL CONCLUSIONS

Agriculture preceded the industrial revolution by many centuries, but research in nanotechnology for industrial application started many years ago, while for agriculture purposes, research is something very recent and challenging. The number of scientific publications in this area really increased in the last decade.

Methods for direct and *in vivo* analyses of plants, such as X-ray fluorescence spectroscopy (XRF), are extremely important in order to reduce time of diagnosis, costs, and diminish the number of steps in the analytical sequence and, then, reduce the generation of chemical waste. Our attempt to create a method like this was not successful to determine copper content due to its low concentration in plants, which is lower than the limit of detection of the equipment, but it was possible to access the nutritional status of other nutrients.

Regarding the established hypothesis, this thesis showed that nanoparticles of different sizes are absorbed by leaves and are redistributed to different parts of the plant, even in low concentrations. The use of nanomaterials has affected agronomic parameters such as shoots dry mass but hasn't influenced the number of pods. Copper and cerium content in the leaves were altered by particles' size, use of dispersant and dose.

Concerning the nanoparticles characteristics, despite their nominal size indicated by the manufacturers, when in contact with a solvent, agglomerates are formed, greatly increasing particle size. This happens due to Van der Waals forces and it was observed through dynamic light scattering analyses. Particles with a nominal size of 25-70 nm can form aggregates of hundreds of nanometers. Purity tests have shown that there is a minimal contamination in the nanoparticles (less than 1%), that may not interfere in the use of these nanomaterials.

Transmission electron microscopy (TEM) images have shown that the nanoparticles present a spherical or a more elongated shape and their estimated size is very to the one informed by the manufacturer.

X-ray diffraction data indicates that nano CuO 40 nm is copper oxide while 25 nm nanoparticles are a mix of CuO and metallic Cu. Both nano CeO₂ are constituted of cerium dioxide.

Digital microscopy analysis on the deposition of nano CuO on the leaves indicated that all of them accumulate mainly on the vein surface. The nCuO formed a dark precipitate, while the micrometric CuO did not show any color difference and in the CuSO₄ treated leaves it was possible to observe that the veins were black and, in some regions, there was whitish appearance, which differed from the other treatments.

X-ray absorption near edge structure (XANES) spectra for pristine 25 nm CuO suggested that it is a mixed oxide corresponding to 1s to 4p transition in Cu¹⁺ and after 14 days of application, the Cu¹⁺ fraction was converted to Cu²⁺.

Nano copper oxide dispersions can be used as sources of the element but plant responses are different according to the particle size and concentration.

Nanoparticles of cerium oxide were absorbed by soybean leaves and redistributed to other leaves. The use of cerium nanoparticles did not interfere in the agronomic parameters such as biomass production and number of pods.

Cerium concentration and accumulation on the leaves that haven't received foliar spray presented different values depending on the source and dose.

No toxic effects on plants were observed in both studies. This probably happened due to the low doses applied to the plants. Our idea from the beginning was to provide to the plants doses that were environmentally relevant.

Lastly, further studies are required to integrate the results here presented. The possible use of nanoparticles in agriculture is tremendous and research in this field is less than a decade old. The adoption of new technologies is paramount to achieve higher productivity and sustentable agriculture and food industry.

ANNEX

Annex A – Permission to reuse in Thesis

06/02/2020

RightsLink - Your Account

JOHN WILEY AND SONS LICENSE TERMS AND CONDITIONS

Feb 06, 2020

This Agreement between Geovani T Costa Junior ("You") and John Wiley and Sons ("John Wiley and Sons") consists of your license details and the terms and conditions provided by John Wiley and Sons and Copyright Clearance Center.

License Number	4743830400169
License date	Jan 07, 2020
Licensed Content Publisher	John Wiley and Sons
Licensed Content Publication	X-Ray Spectrometry
Licensed Content Title	Direct determination of mineral nutrients in soybean leaves under vivo conditions by portable X-ray fluorescence spectroscopy
Licensed Content Author	Hudson Wallace Pereira de Carvalho, Eduardo Almeida, Marcos Henrique Feresin Gomes, et al
Licensed Content Date	Sep 4, 2019
Licensed Content Volume	0
Licensed Content Issue	0
Licensed Content Pages	10
Type of Use	Dissertation/Thesis
Requestor type	Author of this Wiley article
Format	Print and electronic
Portion	Full article
Will you be translating?	No
Title of your thesis / dissertation	Foliar uptake of CuO and CeO ₂ nanoparticles by soybean (<i>Glycine max</i> L.)
Expected completion date	Mar 2020
Expected size (number of pages)	120
Requestor Location	Rua Sylvio Gumiere, 103* Rua Sylvio Gumiere Piracicaba, SP 13412-409 Brazil Attn: Rua Sylvio Gumiere, 103*
Publisher Tax ID	EU826007151
Total	0.00 USD
Terms and Conditions	

TERMS AND CONDITIONS

This copyrighted material is owned by or exclusively licensed to John Wiley & Sons, Inc. or one of its group companies (each a "Wiley Company") or handled on behalf of a society with which a Wiley Company has exclusive publishing rights in relation to a particular work (collectively "WILEY"). By clicking "accept" in connection with completing this licensing transaction, you agree that the following terms and conditions apply to this transaction (along with the billing and payment terms and conditions established by the Copyright Clearance Center Inc., ("CCC's Billing and Payment terms and conditions"), at the time that you opened your RightsLink account (these are available at any time at <http://myaccount.copyright.com>).

Terms and Conditions

- The materials you have requested permission to reproduce or reuse (the "Wiley Materials") are protected by copyright.
- You are hereby granted a personal, non-exclusive, non-sub licensable (on a stand-alone basis), non-transferable, worldwide, limited license to reproduce the Wiley Materials for the purpose specified in the licensing process. This license, and any CONTENT (PDF or image file) purchased as part of your order, is for a one-time use only and

06/02/2020

RightsLink - Your Account

limited to any maximum distribution number specified in the license. The first instance of republication or reuse granted by this license must be completed within two years of the date of the grant of this license (although copies prepared before the end date may be distributed thereafter). The Wiley Materials shall not be used in any other manner or for any other purpose, beyond what is granted in the license. Permission is granted subject to an appropriate acknowledgement given to the author, title of the material/book/journal and the publisher. You shall also duplicate the copyright notice that appears in the Wiley publication in your use of the Wiley Material. Permission is also granted on the understanding that nowhere in the text is a previously published source acknowledged for all or part of this Wiley Material. Any third party content is expressly excluded from this permission.

- With respect to the Wiley Materials, all rights are reserved. Except as expressly granted by the terms of the license, no part of the Wiley Materials may be copied, modified, adapted (except for minor reformatting required by the new Publication), translated, reproduced, transferred or distributed, in any form or by any means, and no derivative works may be made based on the Wiley Materials without the prior permission of the respective copyright owner. For STM Signatory Publishers clearing permission under the terms of the [STM Permissions Guidelines](#) only, the terms of the license are extended to include subsequent editions and for editions in other languages, provided such editions are for the work as a whole in situ and does not involve the separate exploitation of the permitted figures or extracts. You may not alter, remove or suppress in any manner any copyright, trademark or other notices displayed by the Wiley Materials. You may not license, rent, sell, loan, lease, pledge, offer as security, transfer or assign the Wiley Materials on a stand-alone basis, or any of the rights granted to you hereunder to any other person.
- The Wiley Materials and all of the intellectual property rights therein shall at all times remain the exclusive property of John Wiley & Sons Inc, the Wiley Companies, or their respective licensors, and your interest therein is only that of having possession of and the right to reproduce the Wiley Materials pursuant to Section 2 herein during the continuance of this Agreement. You agree that you own no right, title or interest in or to the Wiley Materials or any of the intellectual property rights therein. You shall have no rights hereunder other than the license as provided for above in Section 2. No right, license or interest to any trademark, trade name, service mark or other branding ("Marks") of WILEY or its licensors is granted hereunder, and you agree that you shall not assert any such right, license or interest with respect thereto
- NEITHER WILEY NOR ITS LICENSORS MAKES ANY WARRANTY OR REPRESENTATION OF ANY KIND TO YOU OR ANY THIRD PARTY, EXPRESS, IMPLIED OR STATUTORY, WITH RESPECT TO THE MATERIALS OR THE ACCURACY OF ANY INFORMATION CONTAINED IN THE MATERIALS, INCLUDING, WITHOUT LIMITATION, ANY IMPLIED WARRANTY OF MERCHANTABILITY, ACCURACY, SATISFACTORY QUALITY, FITNESS FOR A PARTICULAR PURPOSE, USABILITY, INTEGRATION OR NON-INFRINGEMENT AND ALL SUCH WARRANTIES ARE HEREBY EXCLUDED BY WILEY AND ITS LICENSORS AND WAIVED BY YOU.
- WILEY shall have the right to terminate this Agreement immediately upon breach of this Agreement by you.
- You shall indemnify, defend and hold harmless WILEY, its Licensors and their respective directors, officers, agents and employees, from and against any actual or threatened claims, demands, causes of action or proceedings arising from any breach of this Agreement by you.
- IN NO EVENT SHALL WILEY OR ITS LICENSORS BE LIABLE TO YOU OR ANY OTHER PARTY OR ANY OTHER PERSON OR ENTITY FOR ANY SPECIAL, CONSEQUENTIAL, INCIDENTAL, INDIRECT, EXEMPLARY OR PUNITIVE DAMAGES, HOWEVER CAUSED, ARISING OUT OF OR IN CONNECTION WITH THE DOWNLOADING, PROVISIONING, VIEWING OR USE OF THE MATERIALS REGARDLESS OF THE FORM OF ACTION, WHETHER FOR BREACH OF CONTRACT, BREACH OF WARRANTY, TORT, NEGLIGENCE, INFRINGEMENT OR OTHERWISE (INCLUDING, WITHOUT LIMITATION, DAMAGES BASED ON LOSS OF PROFITS, DATA, FILES, USE, BUSINESS OPPORTUNITY OR CLAIMS OF THIRD PARTIES), AND WHETHER OR NOT THE PARTY HAS BEEN ADVISED OF THE POSSIBILITY OF SUCH DAMAGES. THIS LIMITATION SHALL APPLY NOTWITHSTANDING ANY FAILURE OF ESSENTIAL PURPOSE OF ANY LIMITED REMEDY PROVIDED HEREIN.
- Should any provision of this Agreement be held by a court of competent jurisdiction to be illegal, invalid, or unenforceable, that provision shall be deemed amended to achieve as nearly as possible the same economic effect as the original provision, and the legality, validity and enforceability of the remaining provisions of this Agreement shall not be affected or impaired thereby.
- The failure of either party to enforce any term or condition of this Agreement shall not constitute a waiver of either party's right to enforce each and every term and condition of this Agreement. No breach under this agreement shall be deemed waived or excused by either party unless such waiver or consent is in writing signed by the party granting such waiver or consent. The waiver by or consent of a party to a breach of any provision of this Agreement shall not operate or be construed as a waiver of or consent to any other or subsequent breach by such other party.
- This Agreement may not be assigned (including by operation of law or otherwise) by you without WILEY's prior written consent.

06/02/2020

RightsLink - Your Account

- Any fee required for this permission shall be non-refundable after thirty (30) days from receipt by the CCC.
- These terms and conditions together with CCC's Billing and Payment terms and conditions (which are incorporated herein) form the entire agreement between you and WILEY concerning this licensing transaction and (in the absence of fraud) supersedes all prior agreements and representations of the parties, oral or written. This Agreement may not be amended except in writing signed by both parties. This Agreement shall be binding upon and inure to the benefit of the parties' successors, legal representatives, and authorized assigns.
- In the event of any conflict between your obligations established by these terms and conditions and those established by CCC's Billing and Payment terms and conditions, these terms and conditions shall prevail.
- WILEY expressly reserves all rights not specifically granted in the combination of (i) the license details provided by you and accepted in the course of this licensing transaction, (ii) these terms and conditions and (iii) CCC's Billing and Payment terms and conditions.
- This Agreement will be void if the Type of Use, Format, Circulation, or Requestor Type was misrepresented during the licensing process.
- This Agreement shall be governed by and construed in accordance with the laws of the State of New York, USA, without regards to such state's conflict of law rules. Any legal action, suit or proceeding arising out of or relating to these Terms and Conditions or the breach thereof shall be instituted in a court of competent jurisdiction in New York County in the State of New York in the United States of America and each party hereby consents and submits to the personal jurisdiction of such court, waives any objection to venue in such court and consents to service of process by registered or certified mail, return receipt requested, at the last known address of such party.

WILEY OPEN ACCESS TERMS AND CONDITIONS

Wiley Publishes Open Access Articles in fully Open Access Journals and in Subscription journals offering Online Open. Although most of the fully Open Access journals publish open access articles under the terms of the Creative Commons Attribution (CC BY) License only, the subscription journals and a few of the Open Access Journals offer a choice of Creative Commons Licenses. The license type is clearly identified on the article.

The Creative Commons Attribution License

The [Creative Commons Attribution License \(CC-BY\)](#) allows users to copy, distribute and transmit an article, adapt the article and make commercial use of the article. The CC-BY license permits commercial and non-

Creative Commons Attribution Non-Commercial License

The [Creative Commons Attribution Non-Commercial \(CC-BY-NC\) license](#) permits use, distribution and reproduction in any medium, provided the original work is properly cited and is not used for commercial purposes.(see below)

Creative Commons Attribution-Non-Commercial-NoDerivs License

The [Creative Commons Attribution Non-Commercial-NoDerivs License \(CC-BY-NC-ND\)](#) permits use, distribution and reproduction in any medium, provided the original work is properly cited, is not used for commercial purposes and no modifications or adaptations are made. (see below)

Use by commercial "for-profit" organizations

Use of Wiley Open Access articles for commercial, promotional, or marketing purposes requires further explicit permission from Wiley and will be subject to a fee.

Further details can be found on Wiley Online Library <http://olabout.wiley.com/WileyCDA/Section/id-410885.html>

Other Terms and Conditions:

v1.10 Last updated September 2015

Questions? customer-care@copyright.com or +1-855-239-3415 (toll free in the US) or +1-978-646-2777.